SEMMELWEIS EGYETEM

DOKTORI ISKOLA

Ph.D. értekezések

3351.

KOVÁCS TAMÁS

Embriológia, őssejt és fejlődésbiológia

című program

Programvezető: Dr. Nagy Nándor, egyetemi tanár

Témavezető: Dr. Nagy Nándor, egyetemi tanár

DEVELOPMENTAL ROLE OF EMBRYONIC CECA IN HINDGUT ENTERIC NERVOUS SYSTEM FORMATION

PhD Thesis

Tamás Kovács

Semmelweis University Doctoral School

Molecular Medicine Division

Supervisor: Nándor Nagy, D.Sc.

Official reviewers: Ágota Apáti, D.Sc.
Mária Sótiné Bagyánszki, Ph.D.

Head of the Complex Examination Committee: Edit Buzás, D.Sc.

Members of the Complex Examination Committee: Attila Mócsai, D.Sc.
Elen Gócza, D.Sc.

Budapest
2026.

Table of Contents

List of abbreviations .....

1. INTRODUCTION 8

1.1. Anatomy of the enteric nervous system 8

1.2. The neural crest cells and development of the enteric nervous system 9

1.3. Hirschsprung's disease 15

1.3.1. Anatomic pathology of HSCR 17

1.3.2. Epidemiology and variants of HSCR 17

1.3.3. Genetics of HSCR and related animal models 18

1.4. The avian embryo as a model system for developmental studies *24*

1.5. The role of embryonic ceca in the formation of ENS in the hindgut *25*

1.6. Pleiotropic effects of the bone morphogenetic proteins (BMPs) on the development of the ENS *26*

2. OBJECTIVES 28

3. METHODS 29

3.1. Animals / Embryos 29

3.2. Histological methods 29

3.2.1. Preparation of samples 29

3.2.2. Immunohistochemistry 30

3.2.3. Immunofluorescence 30

3.2.4. Whole-mount immunostaining 34

3.3. In situ hybridization 34

3.3.1. Whole-mount in situ hybridization 34

3.3.2. In Situ Hybridization on FFPE sections and on primary cell cultures 34

3.4. Embryo manipulation techniques and ex vivo experiments 35

3.4.1. Collagen gel culture 35

3.4.2. Intestinal organ culture assay 35

3.4.3. Chorioallantoic membrane (CAM) transplantation 35

3.4.4. Viral overexpression 36

3.4.5. Ceca ablation and recombination chimera 36

3.4.6. Vital dye labeling 36

3.5. Primary cell culture and in vitro experiments 37
3.5.1. Cell migration assay 37
3.5.2. Cell proliferation, EdU labeling 37
3.6. Microscopic images 38
3.7. RNA-Seq analysis 38
3.8. Statistics 39

4. RESULTS 40

4.1. Avian ceca are required for normal enteric nervous system development 40
4.1.1. Characterization of ENCDC migration across the cecal and hindgut regions in chick embryo *40*
4.1.2. Embryonic cecal buds are required for normal ENS development *42*
4.2. Identifying ceca derived factors as new important signaling cues in ENS formation of avian hindgut 46
4.2.1. Role of WNT-related genes 46
4.2.1.1. Validation of Wnt pathway genes expression in the ceca 48
4.2.1.2. WNT11 inhibits neuronal differentiation 49
4.2.2. The role of BMP4 in hindgut ENS development *53*
4.2.2.1. Expression of BMP4 signaling components implies a contribution to hindgut ENS development 53
4.2.2.2. Blocking of BMP4 signaling results in hindgut hypoganglionosis 56
4.2.2.3. The overexpression of BMP4 via retrovirus leads to extensive gangliogenesis 58
4.2.2.4. GDNF suppresses the aggregation of ENCDC induced by BMP4 59

5. DISCUSSION 62

5.1. Ceca-specific non-canonical WNT11 signaling balances ENCDC migration and differentiation in the developing hindgut 63
5.2. BMP4 promotes enteric gangliogenesis following GDNF dependent ENCDC migration in the ceca 65
5.3. Cecal regulation of ENCDCs: a model of progenitor expansion and migration via balanced BMP4, GDNF, and WNT11 signaling 67
5.4. Future perspectives 68

6. CONCLUSIONS 70

7. SUMMARY 71

8. REFERENCES 72

9. BIBLIOGRAPHY OF THE CANDIDATE'S PUBLICATIONS 109

9.1. List of own publications related to the PhD thesis 109

9.2. List of own publications not related to the PhD thesis 110

10. ACKNOWLEDGEMENTS 116

List of Abbreviations

ABC ..... avidin-biotin complex
ACVR ..... activin receptor
ANOVA ..... analysis of variance
Ao / a ..... aorta
ATM ..... artemin
BAC ..... benzalkonium chloride
BFABP ..... brain fatty acid binding protein
BMP ..... bone morphogenetic factor
BMPR ..... bone morphogenetic factor receptor
BSA ..... bovine serum albumin
CAM ..... chorioallantoic membrane
ChAT ..... choline acetyl transferase
CM-DiI ..... 1,1'-dioctadecyl-3,3,3',3'-tetramethylindocarbocyanine perchlorate
CN 4-chloro-1-naphthol
DAPI ..... 4,6-diamino-2-phenylindole dihydrochloride
DEG ..... differentially expressed genes
dist ..... distal
DMEM ..... Dulbecco's Modified Eagle Medium
DMSO ..... dimethyl sulfoxide
DNA ..... deoxyribonucleic acid
E or ED ..... embryonic day
ECE ..... endothelin converting enzyme
EDN3 ..... endothelin B
EDNRB ..... endothelin receptor type B
EdU ..... 5-ethynyl-2'-deoxyuridine

ELAVL4 ..... Embryonic Lethal Abnormal Vision (Drosophila)-Like (Neuron Specific Binding Protein) 4
EMT ..... epithelial-mesenchymal transition
ENCDC ..... enteric neural crest derived cell
ENS ..... enteric nervous system
ENSCs ..... enteric neuronal stem cells
ep ..... epithelium
ERCC1 ..... excision repair cross complementation group 1
Fam162b ..... family with sequence similarity 162 Member B
FGF ..... fibroblast growth factor
FZD ..... Frizzled
gag ..... group specific antigen
GDNF ..... glial cell-line derived neurotrophic factor
GFP ..... green fluorescent protein
GFRα ..... GDNF family receptor alpha
Gli ..... glioma-associated oncogene homolog
HAEC ..... Hirschsprung-associated enterocolitis
hg ..... hindgut
HH ..... Hamburger-Hamilton stage
HNK1 ..... human natural killer-1
HOX ..... homeobox
hpf ..... hours post fertilization
HSCR ..... Hirschsprung disease
ic ..... interceca
IHH ..... Indian hedgehog
KIAA1279 ..... kinesin family (KIF) binding protein
MEN ..... multiple endocrine neoplasia
mes ..... mesonephros
mg ..... midgut

mp ..... myenteric plexus
NC ..... neural crest
NCAM ..... neural cell adhesion molecule
NCC ..... neural crest cell
nNOS ..... neuronal nitric oxide synthase
NoR ..... nerve of Remak
not ..... notochord
NPY ..... neuropeptide-Y
NRG ..... neuregulin
NT ..... neural tube
NTN ..... neurturin
NT-3 ..... neurotrophin 3
PAX3 ..... paired box gene 3
PBS ..... phosphate buffered saline
PenStrep ..... penicillin-streptomycin
PFA ..... paraformaldehyde
PHOX2B ..... paired-like homeobox 2b
PPI ..... protein-protein interaction
prox ..... proximal
pSMAD ..... mothers against decapentaplegic homolog (phosphorylated form)
PGP9.5 ..... Protein gene product 9.5
PSP ..... persephin
$p75^{NTR}$ ..... neurotrophin receptor
RA ..... retinoic acid
RCAS ..... replication-competent avian retrovirus
RET ..... rearranged during transfection
RNA ..... ribonucleic acid
RPKM ..... reads per kilobase per million mapped reads
SEMA ..... semaphorin
Sfrp1 ..... Secreted frizzled-related protein 1

SHH ..... Sonic hedgehog
SIP1 ..... Siah-interacting protein
SMA ..... smooth muscle actin
smp ..... submucosal plexus
SOX10 ..... Sry (sex determining region Y)-related HMG (high mobility group) box 10
TBS ..... Tris buffered saline
TBX ..... T-box transcription factor
TCF4 ..... Transcription factor 4
TLX2 ..... T cell leukemia homeobox 2
TrkC ..... Tropomyosin receptor kinase C
VIP ..... vasoactive intestinal peptide
WNT ..... Wingless-related integration site
ZEB2 ..... Zinc finger E-box binding homeobox 2

1. Introduction

1.1. Anatomy of the enteric nervous system

The enteric nervous system (ENS) is the largest part of the peripheral nervous system. This extensive and complex autonomic network is responsible for numerous functions in the gastrointestinal tract, such as intestinal motility, control of local blood flow, mucosal transport and secretion, maintaining barrier functions, preservation of normal gut flora, and regulation of immune- and endocrine functions **(1)**. The ENS contains more neurons than the spinal cord and can mediate reflex action independently of the central nervous system. It contains about 80-100 million enteric neurons that can be classified into functionally distinct subpopulations, including intrinsic primary neurons, interneurons, motor neurons, secretomotor-, and vasomotor neurons **(2)**.

The ENS, which ranges from the esophagus to the rectum, can be divided into intrinsic and extrinsic compartments. The neuronal and glial elements of the intrinsic ENS are arranged in two concentric ganglionated plexuses **(Figure 1)**, which are also interconnected through intraganglionic nerve fibers **(3)**. The myenteric plexus, also known as Auerbach's plexus, is located within the intestinal wall, between the circular and longitudinal smooth muscle layers along the entire gut length. The submucosal plexus, which is absent in the esophagus, consists of an outside (mucosal) part called Schabadash's plexus and an inner (submucosal) network called Meissner's plexus **(4)**. Given the extensive connection between the two submucosal ganglion systems and the lack of their functional differences, they are often referred to as single plexus.

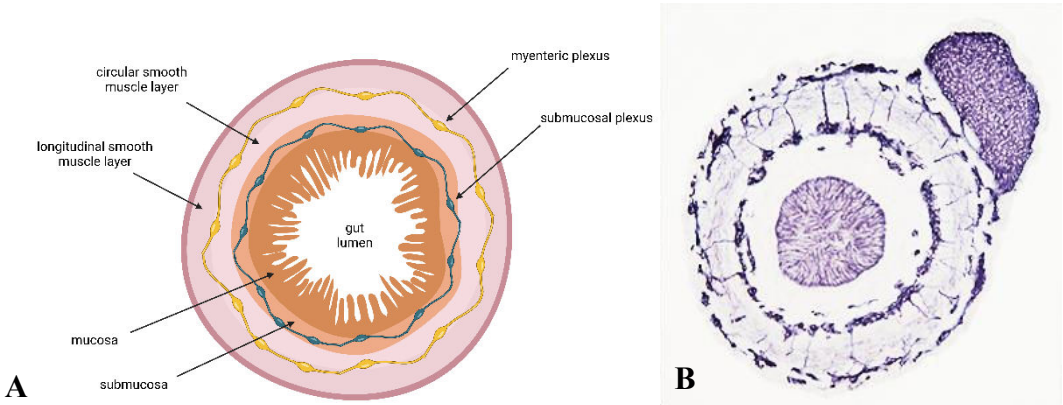

Figure 1. Structure of the ENS. Schematic representation (A) of the gut cross section with the two concentric ganglionated plexuses. 9ED chick embryo hindgut cross section stained with Tuj1 neural marker (B) delineating the enteric plexuses and the interconnecting nerve fibers. The schematic figure was created with BioRender.com. The microscopic photo is my own work.

Our recent research in avian and mammalian species has identified ramified myeloid cells within these ganglia **(5)**. This finding suggests the existence of a third cell type in the intestinal ganglia, intermingled with neurons and glial cells. These cells, termed "intraganglionic macrophages", are situated within the connective tissue capsule surrounding the enteric ganglia **(6)** and express cell surface markers characteristic of microglia **(5)**.

The ENS — through the local reflex circuits involving sensory, motor- and interneurons—regulates most functions of the gut and plays a crucial role maintaining normal gastrointestinal motility. Therefore, its essential function is undeniable, and not surprisingly, all acquired or inherited abnormalities of ENS can lead to serious health consequences. Insights into the development of the gastrointestinal tract and the "second brain," as it is often referred to **(7)**, are relevant for understanding the pathophysiology and treatment of newborns and children with motility disorders. A deeper understanding of ENS development may help improve stem cell therapy options to meet the increasing demand for medical care for affected patients.

1.2. The neural crest cells and development of the enteric nervous system

Gastrulation is a critical stage in the development of all vertebrate embryos, leading to the formation of three distinct germ layers: endoderm, mesoderm, and ectoderm. The endoderm gives rise to the epithelial lining of the gastrointestinal tube, as well as the parenchymal cells of the liver and pancreas. The mesoderm forms mesenchymal components such as the smooth muscle and stromal cells of the lamina propria and submucosa. The ectoderm is further divided into three types of cells: the outer ectoderm, neural tube, and neural crest (NC). The neural crest, commonly called the fourth germ layer, originates from the dorsal neural tube (NT) to specific inductive signals. The components of bone morphogenetic protein (BMP) signaling are directly involved in the neural crest induction **(8)**. The coordinated activity of Noggin and BMP-4 in the dorsal neural tube initiates the delamination of Slug-expressing neural crest cells **(9)**. The expression of the BMP inhibitor Noggin exhibits a gradient, with minimal levels in the rostral area and maximal levels in the caudal part of the neural tube. This results in a region of elevated BMP-4 activity (consistent BMP-4 levels and reduced Noggin concentration) at the site of compartmentalized somites, where neural crest delamination

occurs. After the induction, epithelial-mesenchymal transition (EMT) enables neural crest cells (NCCs) to detach from the NT (**Figure 2**), migrate along specific paths to distinct tissues, and undergo differentiation into diverse cell types. BMP-dependent Wnt signaling is essential for the epithelial-mesenchymal transition (EMT) of neural crest cells: blockage of the canonical route obstructed neural crest delamination, but the overexpression of β-catenin restored neural crest delamination in the Noggin-inhibited neural primordia **(10)**.

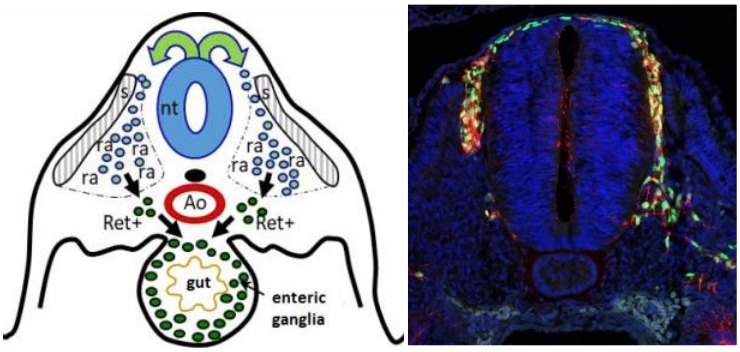

Figure 2. Neural crest cells (NCCs) originate from the dorsal neural tube (nt) as shown in both the schematic figure (A) and chicken embryo cross section (B) stained with SOX10 (green) and HNK1 (red). The microscopic picture is my own work.

The neural crest cells are highly invasive, multipotent stem cell populations which give rise to various tissue and cell types all over the body (summarized in **Table 1**). They can be subdivided into four distinct populations based on their cranio-caudal positions according to the somites: cranial, cervical, truncal and sacral, all of which have their own migration pathway, gene expression profile, and differentiation potential. They are responsible for the development of pigmentary cells, the adrenal medulla, craniofacial structures, the dentine of teeth, conotruncal cardiac structures, and the sympathetic and parasympathetic divisions of the peripheral nervous system. In the context of ENS development, the neural crest population which emerges from the cervical region of the NT at the level of the 1st-7th pair of somites is of the utmost importance. Neural crest ablation studies on chicken embryos confirmed first the neural crest origin of the intrinsic ENS **(11)**. Chicken-quail and chicken-GFP (green fluorescent protein)-expressing transgenic chicken chimeras further confirmed the cervical neural crest origin of the vast majority of ENS precursor cells **(12)**. The NCCs emerging from the cervical region of the

NT can be divided into populations originating from the somite levels 1st to 3rd and 4th to 7th. The former one is made up of two populations with a dorsolateral and a ventral migration pathway. In chicken embryos at the stage of 2nd embryonic day (E2, or 10th Hamburger-Hamilton stage [HH10]) and in 8.5-embryonic-day-old mouse embryos, NCCs that follow the dorsolateral route reach the developing heart and contribute to the formation of the aorto-pulmonary septum, parasympathetic cardiac neurons, glial cells, and myocytes. **(13,14)**. These are called cardiac NCCs. The other population migrates ventrally at HH13 from the dorsal part of NT, forming the ganglia of the wall of esophagus and stomach and the ENS of the foregut **(15,16)**. They got the name of vagal neural crest because this population colonizes the parasympathetic ganglia of the vagus nerve as Schwann-cell precursors **(17)**. The NCCs from the caudal segment of the cervical population (from 4-7th somites) which migrate ventrally join the population colonizing the foregut (from 1-3rd somites) and create the intrinsic part of the ENS all along the whole gastrointestinal tract. The NCCs emigrating from the 7th somite level are both differentiating to melanocytes and forming the dorsal root ganglia (**18**). The truncal neural crest cells (between 8-28th somite) do not correspond to the intrinsic plexuses of ENS, but form the para- and prevertebral sympathetic ganglia, celiac ganglia, inferior mesenteric ganglia, and the chromaffin cells of the adrenal medulla. The cervical population and the sacral cells originating caudally to the 28th somite form together the sympathetic chain around dorsal aorta, the superior cervical ganglion, pelvic plexus, and Remak-ganglion specific to the avian species (**19**). Studies in the avian system provided strong evidence for the contribution of the sacral NC (caudally to the 28th somite) to the hindgut ENS (**20–23**). These cells invade the mesenchyme around the cloaca, where they form the ganglia of pelvic plexus and later continue their rostro-caudal migration (**24,25**) and provide the main source of extrinsic innervation of the distal bowel **(12,20,21)**. Whether the sacral NC contributes to the ENS in the mammalian hindgut remained unclear until the latest results with genetically engineered mouse embryos; they do not contribute to murine ENS (**26–29**). Recently, some alternative pathways of neuronal cell population in the gut have been described, such as the migration of Schwann cell precursors along extrinsic nerves (**30**) or trans-mesenteric migration which comprises another pathway for enteric nervous precursor cells to reach the colon, as some of the cells from the midgut bypass the mouse ceca and migrate directly through the mesentery into the wall of the adjacent hindgut (**31**).

Table 1. Origin, populations and derivatives of neural crest cells
The migration routes are shown on a schematic representation of a 4-week-old human embryo. The figure was created with BioRender.com and modified based on Rothstein et al., 2018. (**32**)

<table>
<tr><th rowspan="5"></th><th>Origin</th><th colspan="2">Population</th><th>Derivatives</th></tr>
<tr><td></td><td colspan="2">Cranial (cephalic)</td><td>cranial ganglia, connective tissues of the face, odontoblasts, parafollicular cells of thyroid</td></tr>
<tr><td rowspan="2">S1-7</td><td rowspan="2">Cervical</td><td>Cardiac</td><td>cardiac neurons and glial cells, aorticopulmonary septum, myocytes</td></tr>
<tr><td>Vagal</td><td>Schwann-cell precursors, intrinsic ENS</td></tr>
<tr><td>S8-27</td><td colspan="2">Truncal</td><td>dorsal root ganglia, sympathetic ganglia, chromaffin cells of adrenal medulla, melanocytes</td></tr>
<tr><td>S28-</td><td colspan="2">Sacral</td><td>sympathetic ganglia, extrinsic ENS, Schwann-cell precursors, Nerve of Remak (NoR)</td></tr>
</table>

The enteric neural and glial cells are derived from the NC (**11,33**). Two groups of undifferentiated cells, derived from neural crests, colonize the gut wall and migrate both in a craniocaudal direction (forming the intrinsic) and in a caudocranial direction (forming the extrinsic innervation). After delamination, the vagal neural crest cells (originating from the 1-7th somite level) with ventral migration pathway are colonizing the proximal foregut **(15)**. In human fetus, these neural crest cells (NCCs) initially enter the developing esophagus (named enteric neural crest-derived cells, ENCDCs from this point) during the third week of gestation and subsequently, during the fourth and seventh week of gestation, and move in the craniocaudal direction towards the anal canal **(Table 2) (16)**. Neural crest-derived cells originating from 4-7th somite level migrate also ventrally, join the migration wavefront of cells mentioned above, and colonize the whole gastrointestinal tract.

Table 2. Comparing the development of the ENS across various species based on the timing of the emergence of cells originating from the vagal neural crest.
Based on Nagy and Goldstein, 2017. **(16)**

	Proximal foregut	**Stomach**	**Cecal region**	**The distal end of the hindgut**
Zebrafish	32 hpf	-	-	66 hpf
Quail	E2.5	E4	E5	E7
Chick	E2.5	E4.5	E5.5	E8
Mouse	E9.5	E10.5	E11.5	E14.5
Human	Week 3	Week 4	Week 6	Week 7

The neural crest derived cells are constantly and simultaneously proliferating, migrating and the rearwards cells are differentiating. The undifferentiated neural crest cells have characteristic markers (**Table 3**), such as SOX10 (SRY-related HMG-box 10), PHOX2B (paired-like homeobox 2B) transcription factors and G-protein coupled endothelin receptor B (EDNRB), $p75^{NTR}$ neurotrophin receptor and tyrosine kinase receptor (RET). During the colonization process, the cells migrate collectively in groups: the cells in the leading front are undifferentiated, and the cells behind the "wave- front" are in the different stages of differentiation. The neural lineage commitments start shortly after the neural crest cells have entered the developing foregut. The glial differentiation is a later process. In these neural crest derived neurons, the expression level of SOX10 and p75 is lowered, but they are still RET^+ and $PHOX2B^+$. The neural cells are still in the precursor state but have already started to produce PGP9.5 (protein gene product 9.5), type III β-tubulin (TUJ1), ELAV-like RNA Binding Protein 4 (ELAVL4, Hu C/D) (**Table 3**), showing mitotic activity **(16)**. They are considered differentiated neurons when they have started to produce neurotransmitters, like neural nitric oxide synthase (nNOS), vasoactive intestinal peptide (VIP), neuropeptide Y (NPY), substance P, and choline acetyl transferase (ChAT). In mice the definitive neurons of the myenteric plexus appear first in the 11st – 13rd embryonic days, but neurotransmitter producing submucosal neurons only differentiate after birth **(34,35)**. The glial precursor cells maintain their SOX and P75 markers, but the expression of RET is lowered. They start to express the glia-specific markers, such as brain fatty acid-binding protein (BFABP), the calcium binding domain of intestinal calcium-binding protein (ICaBP type calcium binding domain; S100), and lastly the glial fibrillary acidic protein; GFAP) (**Table 3**) **(36)**. Interestingly,

the enteric glial cells maintain their neurogenic potential, and they are capable of dedifferentiating to progenitor-like state and differentiate into neurons due to injury **(37,38)**.

Table 3. Differentiation of enteric neurons and glia with corresponding markers based on Nagy and Goldstein, 2017 **(16)**

Neural crest cells (NCCs)	**Vagal NCC-derived cells**	**Enteric neural crest derived cells (ENCDCs)**	**Enteric neuron**
			HuC/D, Tuj1, Phox2b, Ret, PGP9.5, TMEM100, L1CAM, N-cadherin, NCAM, neurofilament, peripherin
Wnt1, FoxD3, Sox10	Sox2/10, Ednrb, nestin, p75, HNK1	Sox2/10, Ednrb, Ret, Phox2b, nestin, p75, HNK1, L1CAM, N-cadherin, HAND2, Hoxb5, Ascl1/Mash1, ErbB3	**Enteric glia**
			Bfabp, PLP1, GFAP, S100β, Sox2/10, nestin, p75, CD49b, ErbB3

The final step in the development of the ENS is the formation of ganglia. After NCCs have reached the gut and migrate through the mesenchyme of foregut and midgut, they are uniformly dispersed (except in the ceca where they tend to congregate) and randomly start to form primitive ganglia. In this stage the smooth muscle layers are not differentiated yet, therefore the neural crest cells are settled in the outer mesenchymal layer of the gut wall **(39,40)**. With the increase in the level of muscle structuring, the neural crest cells are pushed to the outer side forming the circular smooth muscle layer. In contrast, in chicken embryo, the differentiation of smooth muscle layers is already finished before the arrival of neural crest cells, and they are colonizing first the submucosal region and later forming the myenteric plexus. In avian embryos, the laminin expressing endothelial cells form two concentric capillary networks prior to the entrance of neural crest-derived cells. These structures pre-determine the position of future plexuses **(41)**. In mouse embryos, the submucosal plexus is only formed postnatally **(42)**. The myenteric plexus is formed in humans at the 12th week of gestation. Once the craniocaudal migration is complete, the neuroblasts migrate from the myenteric plexus through the circular muscle layer in a radial direction into the submucosal layer, forming the submucosal plexus and the characteristic cross-sectional pattern **(43)**. This migration occurs in a craniocaudal direction between the 12th and 16th weeks of gestation **(44)**. The timing of avian ENS development more closely resembles human development, which makes it a better choice for disease modeling.

1.3. Hirschsprung's disease

Abnormalities in the development of cells derived from the neural crest are called congenital neurocristopathies **(45–47)**. These can be categorized into two primary groups, one of which includes abnormalities resulting from the migration or morphogenesis of cells originating from the neural crest, such as Hirschsprung's disease (HSCR), aorticopulmonary septal defect, and DiGeorge syndrome. The other major category comprises tumors and proliferative diseases, like neurofibromatosis, pheochromocytoma, neuroblastoma and ganglioneuromatosis. Neurointestinal disorders may arise from either congenital or acquired causes. The root causes of neurointestinal diseases may include genetic, inflammatory, degenerative, and paraneoplastic mechanisms **(48)**. Developmental abnormalities of the ENS can be classified based on variations in the number of neurons: hyperganglionosis refers to ganglioneuromatosis or ganglioneuroma, whereas hypoganglionosis is connected to the intestinal pseudo-obstruction, and aganglionosis **(49)**.

Neonatal intestinal obstruction can be caused by a rare condition known as HSCR. In 1886, Dr. Harald Hirschsprung, a Danish physician, provided a clear and succinct description of the condition known as "congenital megacolon." His treatise was entitled „Constipation in newborns due to dilation and hypertrophy of the colon" **(Figure 3) (50)**. A method of treatment was not offered by him, nor was the etiology proposed for this condition. At the time, he was unaware of the previous reports **(51)** concerning the subject for instance provided by Frederik Ruysch (1691) **(52)**, who mentioned the first case of megacolon in his chirurgical anatomy book.

Initially – in the 1900s – it was proposed that this disorder has a neurogenic cause. However, four decades later, Ehrenpreis still believed that the loss of ganglion cells, as observed by others, was a consequence of continuous colonic dilatation and stasis rather than the primary cause **(50,53)**. In 1948, Whitehouse discovered that aganglionosis is a congenital abnormality **(54)**. While early studies identified familial instances of HSCR **(55)**, the unraveling of the human genome provided insight into the genetic origins of the disease. The discoveries were made through collaboration among basic scientists, medical geneticists, and pediatric surgeons: mutations were identified in 50% of the patients from families with HSCR, mainly affecting the tyrosine kinase domain of RET proto-oncogene **(56)**. Further studies have confirmed genetic linkages involved in the

development of the ENS. Most of them belong to the RET **(57)** and endothelin signaling pathways **(58,59)**. Recent advances in genetic technologies, including next-generation sequencing provide more insight into the development and complexity of the ENS and reveal new HSCR-related genes **(60–62)**.

Figure 3. Historical overview of the discovery of Hirschsprung's disease (HSCR). A.) The title page of Frederik Ruysch's book on surgical anatomy, published in 1691, in which he first mentions megacolon. B) Portrait of Harald Hirschsprung and headline of a publication describing congenital megacolon in detail. C-D) The primary defect in HSCR is the lack of innervation of the distal colorectum. Intestinal peristalsis is absent in the affected segment; the bowel contents are stagnant. The proximal segment with normal innervation and the abdomen is markedly distended (C-D images of the courtesy of Dr. Allan M. Goldstein).

Currently the only available treatment option is the surgical resection of the aganglionic segment and reconnection of the healthy colon with the rectum. Among these laparoscopic, transanal pull-through procedures are the Duhamel-, Swenson- and Soave-procedures. After surgical procedures the recovery is often not complete, due to the occurrence of Hirschsprung-associated enterocolitis (HAEC) **(63)** and recurring passage issues.

Researchers are working to develop novel stem cell therapies, whereby stem cells could be transplanted into the aganglionic segment of the bowel to replace the missing ENS **(64,65)**. Furthermore, there is a need for a more precise understanding of the appropriate therapeutic strategies for several patients with different variations of HSCR. Further research on the ENS and the molecular genetics of these diseases may offer additional insights into these concerns and enhance our understanding of how to manage affected infants in the future.

1.3.1. Anatomic pathology of HSCR

The fundamental pathophysiologic characteristic of HSCR is identified as a functional obstruction, which is attributed to a narrowed distal aganglionic segment that inhibits the propagation of peristaltic waves.

The condition of HSCR is defined by fundamental defects of the ENS, accompanied by secondary effects in the gut emerging from the physiological consequences of aganglionosis. The most apparent and diagnostically significant feature of HSCR is recognized as congenital aganglionosis of the distal rectum and a variable length of the adjacent proximal bowel. In around 80% of the cases, short-segment HSCR (ssHSCR) develop where aganglionosis is localized to the rectosigmoid colon. The gut segment situated directly adjacent to the aganglionic segment called transition zone denotes ganglionic yet neuroanatomically anomalous bowel. This should be distinguished from the funnel-shaped gross anatomical transition zone, typically located at or near the proximal end of the aganglionic segment **(66)**. The predominant neuropathological characteristics observed in the transition zone include partial circumferential aganglionosis, myenteric hypoganglionosis, and submucosal nerve hypertrophy **(66)**.

1.3.2. Epidemiology and variants of HSCR

The prevalence of HSCR is estimated to be 1 in 5000 live births **(67,68)**, showing some geographic heterogeneity with an incidence of 1 in 10000 births in Europe **(67)** and 1 in 5000 in Japan **(69)**.

Classical segment HSCR refers to patients (80%) whose aganglionic segment does not extend beyond the upper sigmoid. On the other hand, long-segment HSCR (10%) is characterized by aganglionosis that extends to the splenic flexure or transverse colon. Total colonic aganglionosis (5-8%), as the name suggests, occurs when the aganglionic segment extends to the entire colon and a short segment of the terminal ileum. The rarest and most severe form of HSCR is the total intestinal aganglionosis **(70)**, where there is an absence of ganglion cells from the duodenum to the rectum. This condition occurs in less than 1% of patients **(71,72)**. The absence of ganglion cells in HSCR has been attributed to a failure of migration of the NCCs. The earlier the arrest of migration, the longer the aganglionic segment is.

Studies have shown that there is a higher prevalence of males being affected compared to females, with a ratio of 4 males to every 1 female **(68,73)**. In long-segment HSCR, the ratio of males to females is 1:1-2:1, showing a less pronounced male dominance **(73)** and it is even reversed in total colonic aganglionosis, where the male-to-female ratio is 0.8:1 **(74)**. The cause of these imbalanced ratios is uncertain; no X-linked genetic regions have been identified in HSCR. The majority of HSCR cases are sporadic and are thought to be caused by many factors and genetic influences.

1.3.3. Genetics of HSCR and related animal models

The pathological mechanism resulting in the distinctive histological features of aganglionosis and enlarged nerve trunks in HSCR remains inadequately elucidated. The inability of ENCDCs to reach their normal distal intestinal location, proliferate, develop, or survive is considered the key commencing factor in the pathogenesis of HSCR **(75)**. The normal process of development necessitates the intricate interplay of genes that encode transcription factors, signaling molecules and their receptors (**Table 4**) which regulate the morphogenesis and differentiation of the ENS. Alterations in gene function, anomalies in NCC or alterations in the gut microenvironment may result in irregular development of the ENS (**Table 4**) **(76–80)**.

Non-syndromic HSCR, which refers to the occurrence of HSCR without any other defects, has been connected to pathogenic variations in several genes. HSCR has been linked to high levels of expression in at least 11 neuro-developmental genes, specifically RET, GDNF, NTN, SOX10, EDNRB, EDN3, ECE1, ZFHX1B (ZEB2), PHOX2B, KIAA1279, and TCF4. Non-syndromic HSCR is influenced by genes that fall into four primary groups. The first group includes RET and its ligands GDNF and NTN. The second group consists of EDNRB and the associated genes EDN3 and ECE1. The third group involves the NRG signaling pathway, specifically NRG1 and NRG3. Lastly, the fourth group encompasses the SEMA signaling pathway, which includes SEMA3C and SEMA3D. **(81,82)**

Table 4. The most important genes involved in the morphogenesis and differentiation of the ENS and the mouse models of intestinal aganglionosis with their corresponding phenotype.

Genes	Function	Mouse model	Mouse phenotype
RET	Tyrosine kinase receptor	Ret$^{-/-}$	total intestinal aganglionosis
GDNF	Glial cell-derived neurotrophic factor	Gdnf$^{-/-}$	total intestinal aganglionosis
NTN	Neurturin, RET ligand	Ntn$^{-/-}$	hypoganglionosis
GFRα	GDNF family receptor alpha 1	GFRα1$^{-/-}$	total intestinal aganglionosis
		GFRα2$^{-/-}$	hypoganglionosis
EDNRB	Endothelin B receptor	Ednrb$^{-/-}$	aganglionosis of distal hindgut
EDN-3	Endothelin B	Etr3$^{-/-}$	aganglionosis of distal hindgut
SOX10	Sry/HMG box transcription factor	DOM	total intestinal aganglionosis
PHOX2B	Paired-like homeobox 2b	Phox2b$^{-/-}$	total intestinal aganglionosis
IHH	Indian hedgehog	Ihh$^{-/-}$	segmental aganglionosis
SHH	Sonic hedgehog	Shh$^{-/-}$	ectopic neurons

The significance of the RET/GDNF/GFRα1 signaling pathway lies in its ability to support the survival of neurons, promote mitosis of neuronal progenitor cells, facilitate neuronal differentiation, and support neurite extension. These effects have been demonstrated through both *in vitro* and *in vivo* assays, highlighting the importance of this pathway for various subpopulations of peripheral and central neurons **(83–88)**. The RET receptor is the signaling component of receptor complexes including four ligands, glial-derived neurotrophic factor (GDNF), neurturin (NTN), artemin (ATM) and persephin (PSP) **(89)**. GDNF acts as a chemo-attractive agent and upon binding to its co-receptor GFRα1, it activates the RET receptor, promoting the migration of NCCs **(90)** and stimulates the proliferation and survival of NC-derived precursor cells in the embryonic gut **(91–94)**. The generation of RET knockout mice has further illustrated the importance of RET in mammalian organogenesis **(95)**. Apoptosis of enteric NCC in the foregut has

been observed in RET-deficient mice, resulting in intestinal aganglionosis **(86)**. It is worth noting that there is evidence suggesting that the proliferation and survival of enteric NCCs and the length of the aganglionic segment is altered by the dosage of RET **(96)**. Homozygous mice deficient in RET develop near-total aganglionosis, whereas heterozygous mice exhibit a normal ENS **(97)**. Mice with a homozygous null mutation in GDNF have been created, and these mice exhibit the absence of kidneys and ENS, so affirming the essential function of GDNF in the development of ENS **(97,98)**. RET signaling also influences neuron survival and ENS development following complete colonization **(96)**. It has been demonstrated that the RET proto-oncogene also plays a major role in the development of human HSCR **(56,99,100)**. RET mutations are responsible for 50% of familial cases and 15-20% of sporadic cases of HSCR **(101–103)**. The lack of GDNF/GFRα1-mediated signaling leads to the failure of ENS development, and they exhibit comparable phenotypes as Ret-/- animals with the disruption of ENS beyond the esophagus and the absence of kidneys **(97,98,104–107)**. The $Gdnf^{+/-}$ mice display hypoganglionosis, characterized by a 50% decrease in enteric neurons **(108,109)**. The absence of NTN/GFRα2-mediated signaling leads to less severe defects in ENS development. The Ntn-deficient mice exhibit diminished nerve fiber density in the ENS and abnormalities in neurotransmitter release and gastrointestinal motility **(110)**. It is not assumed that the Ntn mutation alone leads to HSCR, but it may play a role in the severity of the disease **(111)**.

The endothelins (EDN1, EDN2 and EDN3) are intercellular messengers that act via cell surface receptors, such as EDNRA and EDNRB. EDN3 and EDNRB play a crucial role in the migration and development of the ENS **(112–114)**. In two naturally occurring mice strains, the piebald spotting (s^l) and the lethal spotting (*ls*) mice **(115)**, both the endothelin-3 (Edn3) and endothelin-receptor B (Ednrb) genes are affected **(112,113)**. Additionally, there are several reports indicating that the downregulation of EDN3 expression might be involved in the development of HSCR in sporadic cases **(59,116–121)**. Alongside its role in promoting the proliferation of enteric NCCs, EDNRB also hinders the differentiation of neuronal precursor cells. When this function is disrupted, the population of precursor cells is unable to continue dividing or migrating, resulting in an inability to fully colonize the gut **(122)** which could result in HSCR **(123,124)**. Patients with Waardenburg syndrome who have a mutation in endothelin-3

(EDN3) **(125,126)** or its receptor, endothelin receptor type B (EDNRB) **(116,117,124,127,128)**, also have HSCR as a component of their condition (type 4 Waardenburg syndrome or Shah-Waardenburg syndrome). Deletion of the endothelin-converting enzyme (ECE), which is responsible for the production of biologically active EDN **(79,81,129)**, leads to colorectal aganglionosis **(112,113)**. In addition to colonic aganglionosis, craniofacial and cardiac abnormalities are observed in the ECE1 knockout mice **(130)**.

The SOX10, also known as the sex determination region Y-box gene, is expressed in neural crest cells (NCCs) that play an instrumental part in the development of the peripheral nervous system in embryos **(131,132)**. SOX10 is necessary for the survival of the enteric neural crest cells (NCCs), ensuring that they remain undifferentiated and able to proliferate **(133–136)**. SOX10 mutations have been found as a causal factor for the elongated hypoganglionic transition zone and aganglionosis in the distal colon in the naturally occurring dominant megacolon (DOM) mice **(132,137)**. The malfunction of the SOX10 gene leads to the early death of neural crest cells **(132,138)**. In humans, Sox10 mutations were detected in patients with Waardenburg-Shah syndrome, which includes defects in the ENS and pigmentation abnormalities **(139,140)**.

The Phox2b gene, coding a transcription factor containing a homeodomain, plays a crucial role in neurogenesis and controls the expression of RET in mice. It plays a role in the formation of enteric ganglia by promoting the proliferation and survival of NCCs **(90)**. When this gene is disrupted, it leads to a phenotype similar to HSCR **(90,141)** with a total disappearance of the ENS. In humans it is involved in the syndromic form of HSCR in conjunction with the congenital hypoventilation syndrome **(142,143)**.

Homeobox genes (*Hox*) are highly conserved genes of the network of transcription factors which turn on cascades of other genes **(144)**. The enteric Hox code plays a crucial role in ensuring proper morphogenesis and determining the distinct Hox expression patterns in the gut, both in terms of their spatial, temporal, and combinatorial aspects **(145)**. Studies in both mice and humans have revealed the significant role they play in the development of the enteric plexus **(145,146)**. Several studies have described Hox mutations (Hox9, Hox13) in human HSCR **(147,148)**, for instance, the colon of HSCR patients showed higher expression of Hox9 compared to normal controls. Hoxa9 and Hoxa13 play a role in the formation of the zebrafish ENS, as well **(149)**. The

expression of Hoxa9 was demonstrated in the posterior part of the small intestine and, interestingly, specifically in the ceca of chick embryos **(150)**. In the early stages of gut development, the expression of Hoxa13 in the endoderm of the hindgut and cloaca was demonstrated by using the chick model. Hox11L1 (also known as Tlx2) is a homeobox gene involved in the peripheral nervous system development and assumed to take part in NCC proliferation **(151)**. Two different Hox11L1 knockout mouse models have been generated **(151,152)**. Both developed megacolon and the histological and immunohistochemical examination showed an increase in the size and number of myenteric ganglia, which closely resemble the phenotype found in individuals with intestinal neuronal dysplasia (IND). It was observed that the perturbation of Hoxb5 resulted in Ret haploinsufficiency, which in turn constrained the migration of neural crest cells (NCCs), leading to hypoganglionosis and aganglionosis **(153)**. Megacolon is also exhibited in transgenic rodents that have overexpressed Hoxa4, along with hypoganglionosis in a short segment of the terminal colon and abnormally located ganglia **(154,155)**.

The Sonic hedgehog (Shh) and Indian hedgehog (Ihh) genes have been shown to affect the survival and development of neural crest cells (NCCs). In mice, the depletion of hedgehog leads to partial intestinal aganglionosis, as well as megacolon or ectopic ganglia **(156)**. Transcription factors Gli1, Gli2, and Gli3 play a crucial role in mediating hedgehog signaling in mammals **(156)**. The ectopic expression of Gli1 leads to hypoganglionosis, a phenotypic outcome comparable to the loss of Indian hedgehog (Ihh) signaling **(157,158)**. Transgenic mice that have an excessive amount of human Gli1 exhibit a phenotype similar to HSCR, and the severity of this phenotype is directly related to the level of expression of the Gli1 transgene **(156,158)**. Patients with HSCR have been identified to have missense mutations in the genes of Gli1, Gli2, and Gli3 **(156)**.

The ZFHX1B gene, commonly referred to as ZEB2 or SIP1 – a highly conserved gene that encodes zinc finger and homeodomain-like sequence-containing transcription factor – is expressed abundantly during embryological development **(159,160)**. The deletion of ZFHX1B in NCCs induces abnormalities in the peripheral nervous system of the digestive tract and leads to the loss of vagal NCCs **(161)**. Thus far, there have been no documented instances of ZFHX1B mutations in individuals with isolated HSCR. However, it is possible that the ZFHX1B gene could be a susceptibility gene for

syndromic HSCR **(162,163)** for instance in the case of congenital hypoventilation syndrome **(164)** and Mowat-Wilson syndrome **(165–167)**.

Loss of repression of the *Fam162b* gene in ENCDCs leads to a transgenic strain known as the *TashT* model. It is characterized by delayed migration of ENCDCs and partially penetrant aganglionic megacolon, exhibiting a pronounced male bias **(168,169)**. Altered expression of the *Col6a4* gene (excess collagen VI) also leads to a HSCR-like disease model named *Holstein*, presenting with delayed enteric NCC colonization of the embryonic intestine due to reduced cell migration. The myenteric ganglia in the ganglionated region are also encased by a substantial quantity of collagen VI microfibrils in the majority of patients in a cohort with HSCR, which implies a role in the HSCR phenotype **(170)**.

The role of β1 integrins in ENS development was investigated by the deletion in the NCCs of mice, resulting in aganglionosis of the descending colon, which is comparable to human HSCR **(171)**. Additionally, endothelial cells support the migration of enteric NCCs via the interaction of NCC surface-*β1 integrins* and extracellular matrix proteins expressed by the intestinal vasculature **(41)**. However, it has not been confirmed yet whether β1 integrins are involved in the impaired migration of ganglion cells observed in human HSCR **(172)**.

The Ercc1 gene plays a crucial role in nucleotide excision repair, recombination repair, and the repair of interstrand cross-links. Ercc1-deficient animals experienced the accumulation of unrepaired DNA damage in their colonic ganglia, resulting in a colonic blockage similar to the late-onset HSCR in humans **(173)**.

Numerous other non-genetic factors are also implicated in the control of ENS development. Previous studies have demonstrated the supportive effects of laminin **(41)**, fibronectin **(174)**, vitronectin **(175)**, and collagen type I **(176)** on enteric NCC migration. Conversely, collagen type VI **(170)** has been found to inhibit migration. Altered extracellular matrix (ECM) proteins, such as tenascin, fibronectin, and nidogen, have already been observed in individuals with HSCR **(177,178)**.

Next generation sequencing studies might provide new insights and potential genes which might contribute to the development of HSCR, for example TBX3 **(62,179)**.

1.4. The avian embryo as a model system for developmental studies

The selection of the appropriate animal model is an essential part of any embryonic research, as it is influenced by developmental differences. The challenge lies in the fact that the formation of the ENS varies across different animal species. In amphibians and reptiles, the submucosal plexus is located exclusively in the region encompassing the esophagus and stomach **(180,181)**. In mice, it develops only postnatally. The submucosal plexus is completely absent in zebrafish **(182)**. In birds and humans, both neural plexus appear uniformly, already in the embryonic age **(75)**. In most cases, the myenteric plexus is the first to form, except in birds where the submucosal plexus appears earlier. However, it is interesting to note that neuronal differentiation occurs earlier in the area of the myenteric plexus **(21,24,42,183)**.

Over the past few decades, the bird embryo has once again become the focus of attention. The most widely used species are the domestic chicken (Gallus gallus) and the Japanese quail (Coturnix japonica). Chicken embryos have long been used for this purpose due to their easy accessibility, sustainability, rapid development, manipulability and resilience. The successful sequencing of the chicken genome has further increased the strength of the model system, creating the possibility of genetic manipulations that could contribute to answering the fundamental questions of embryogenesis **(184–186)**.

In 1973, LeDouarin and Teillett, utilized the chimera technique to provide evidence for the neural crest origin of the neuronal and glial cells in the intestinal wall **(12)**. Ever since the neural crest origin of the ENS in chicken embryos was established, it has been extensively employed to investigate the migratory pathway and fate mapping of different stem cells. Embryo manipulation and cell tracing studies on bird embryos can also be used to determine the origin, migration and differentiation of a particular differentiated cell type. The hybridoma approach enables the production of monoclonal antibodies that can be used to monitor specific cell populations **(187–191)**.

The chick embryos have been extensively studied as a surgically created model for HSCR, due to their widespread availability and the extensive research conducted on the development of their ENS **(192)**. Meijers conducted a study on surgical ablation of the pre-migratory neural crest, which can be utilized to explore potential treatment approaches for the disease **(193)**. The recolonization of aganglionic bowel with NCCs was demonstrated through the transplantation of tissue obtained from the dorsal neural

tube **(33,194,195)**. In previous studies, it has been observed that neurons from different regions of the gut have the ability to recolonize the distal bowel and form enteric ganglia **(195,196)**. An insufficient number of ganglionic nerve cells and a decrease in parasympathetic nerves within the intestinal wall lead to megacolon, akin to what is observed proximally to the aganglionic section in HSCR. This condition is defined by a model resembling hypoganglionosis **(197)**.

1.5. The role of embryonic ceca in the formation of ENS in the hindgut

Although ENCDC-associated mutations are present in HSCR, the main portion of the intestine is colonized by ENCDCs, and aganglionosis is only shown in the colon in over 90% of cases. This implies that there might be something special related to the process of the hindgut ENCDC colonization. The current concept regarding the development of HSCR is that a lack of proliferation in enteric neural crest-derived cells (ENCDC) or early differentiation of neurons may result in an inadequate number of ENCDC progenitors successfully migrating from the foregut to the rectum. Nevertheless, the explanation of why cells are able to populate almost the entire gastrointestinal tract but only cease migrating in the colorectum remains unclear. This phenomenon could indicate that enteric neural crest-derived cells (ENCDCs) receive distinct molecular signals as they move from the midgut to the hindgut. It is possible that abnormalities in this particular region play an essential part in the development of HSCR.

The junction of the small and large intestine is marked by the cecum in mammals and by paired ceca in avians. It has been suggested that this structure plays a crucial role in the formation of the hindgut ENS. For instance, the expression of GDNF and EDN3, which are ligands involved in important pathways linked to HSCR pathogenesis, is limited to the cecal region in both mice **(94,114)** and chick **(176)** gut just prior to the arrival of ENCDCs. The role of EDN3-EDNRB signaling in mice is only necessary once ENCDCs reach the cecum, as it promotes ENCDC proliferation and hinders neuronal differentiation **(198–200)**. In addition, it has been demonstrated that the cecal environment can modify the migratory properties of the ENCDCs at the wavefront of migration, facilitating their colonization of the hindgut **(176,201)**. However, the unique role of the ceca during hindgut ENS development and how signaling pathways in the ceca impact migrating ENCDCs to promote their migration into the colon are not yet fully understood.

1.6. Pleiotropic effects of the bone morphogenetic proteins (BMPs) on the development of the ENS

BMPs are involved in neural crest induction and epithelial-to-mesenchymal transition and subsequent migration of NCCs. Following induction, NCCs utilize BMPs in varying ways, times, and anatomical regions throughout the development of the ENS **(202)**. In the fetal gut, BMP-2 and BMP-4, their receptors BMPR-IA, BMPR-IB, and BMPR-II, along with BMP inhibitors, such as noggin, gremlin, chordin and follistatin, are present at the stage when ENCDCs have completed their migration and first differentiated neurons become detectable. This expression pattern points to their possible paracrine or autocrine functions in ENS formation **(203–205)**. Studies using epithelium-mesenchyme recombination techniques have demonstrated that mesenchymal signals play an essential role in guiding the formation and spatial organization of enteric plexuses **(206–208)**. Furthermore, BMP-2 and BMP-4 promote the nuclear translocation of phosphorylated Smad-1 from the cytoplasm in enteric ganglia, confirming active signaling and the responsiveness of ENCDC to BMP stimulation.

BMP4 influences the migration of ENCDCs **(203,209)** as well as the differentiation of enteric neurons **(210)** and glial cells **(211)**. In addition, BMP signaling contributes to the development and spatial organization of enteric ganglia, ensuring correct neuronal distribution and connectivity, which is associated with changes in neural cell adhesion molecule (NCAM) expression **(209,212)**. Studies have shown that BMP signaling confines murine ENS precursors to the outer gut wall during their migratory phase. It also promotes colonization of the colon in mice, while reducing the formation of ganglionic aggregates and limiting neurite fasciculation. Such effects result in hypoganglionosis and a lower degree of neuronal clustering within ganglionic structures. The migration of ENCDCs throughout the intestine, as well as neurite fasciculation, may be influenced by BMP-mediated enhancement of polysialic-acid on Ncam1. Removal of polysialic acid from Ncam1 enzymatically eliminates BMP-induced effects on ENCDC migration and neurite fasciculation Consequently, BMP4 facilitates acid addition to neuronal Ncam, thereby supporting neuron aggregation into ganglionic clusters **(209,212)**.

Overexpression of Noggin, driven by a neuron-specific enolase promoter, increases neuronal numbers in both submucosal and myenteric plexuses of the postnatal gut in transgenic mice **(202)**. However, despite the overall rise in neuronal count, the population of TrkC-positive neurons decreases. By contrast, BMP2 and BMP4 appear to limit overall ENS size but promote differentiation of specific neuronal subtypes, including TrkC-expressing cells **(202)**.

Blocking BMP signaling in the intestinal mesenchyme disrupts smooth muscle development and causes abnormal ENS patterning **(204,205)**. Experimental data from avian and murine embryos, however, are not entirely consistent. In chicken embryos, Noggin overexpression leads to hindgut hypoganglionosis **(203)**, while excessive BMP4 in the mouse gut organ cultures hampers ENCDC migration **(209)**. Misexpression of BMP4 in the chicken gizzard mesenchyme produces hypertrophic and ectopic ganglia **(209)**. BMP2 enhances neuronal differentiation of mouse and rat ENCDCs **(213)** and upregulates GDNF receptor expression on NCCs, thereby increasing their responsiveness to GDNF **(214)**. Furthermore, combining GDNF treatment with elevated BMP2 or BMP4 in rat ENCDC cultures yields a higher neuronal output **(202)**.

The transcription factor Smad-interacting protein 1 (SIP1/ZEB2), a negative modulator of BMP4 signaling **(215)**, is involved in NCC specification, differentiation, and migration **(216)**. Mutations in SIP1 are associated with HSCR **(164,217,218)**. In summary, although the link between BMP4 and ENS development is well established, the precise mechanism by which BMP4 controls ENCDC colonization of the hindgut remains unclear.

2. Objectives

Although the exact etiology of Hirschsprung disease (HSCR) remains unclear, recent decades have yielded significant insights into the complexity of this congenital neurointestinal disorder and its variants. Advances in our understanding of ENS development and the molecular and genetic regulation of neurointestinal disorders have revealed that HSCR is a genetically complex and heterogeneous illness. It arises from abnormal development of neural crest cells and involves multiple mutations across various genes and signaling pathways, besides other molecular factors that are yet to be fully identified.

The primary objectives of this thesis are:

1. To characterize the role of the avian ceca in the development of the hindgut enteric nervous system using avian embryonic surgery techniques and molecular approaches.
2. To identify novel growth factors of cecal origin in hindgut ENS development and to experimentally validate their contribution to ENS formation.

<u>Specific aims include:</u>

- Characterizing the expression pattern of **BMP4** during avian hindgut ENS development and investigating the effects of BMP signaling on the migration and differentiation of enteric neural crest-derived cells.
- Characterizing the expression of non-canonical **WNT5A** and **WNT11** in the developing avian hindgut and elucidating previously unrecognized roles of WNT11 signaling in colorectum ENS development.

3. Methods

3.1. Animals / Embryos

Fertilized White Leghorn chicken (*Gallus gallus domesticus*) eggs were obtained from commercial breeders (Prophyl-BIOVO Ltd., Hungary and Charles River, USA) and maintained at 37.5 °C in a humidified incubator. Transgenic green fluorescent protein (GFP)-expressing chicken eggs were obtained from Prof. Helen Sang, The Roslin Institute, University of Edinburgh, UK **(219)**. Embryos were staged according to the number of embryonic (E) days or to Hamburger and Hamilton (HH) tables **(220,221)**. Gut stages were referenced to the chick embryo gut staging table **(222)** and the ENS formation timetable **(39)**.

3.2. Histological methods

3.2.1. Preparation of samples

For histological studies, whole embryos and embryonic intestinal sections were isolated under a stereomicroscope with micromanipulation tools (micro-scissors, tweezers, micro-dissecting needles, and embryo spoon). For immunohistochemistry and immunofluorescence studies, gelatin frozen blocks of organs were prepared **(190)**. The dissected organs were fixed in 4% buffered paraformaldehyde (PFA) for 1 hour, after which the fixative was washed out with phosphate buffered saline (PBS). The samples were incubated overnight at 4°C in 15% sucrose (Reanal puriss, 07140-0-08-38) solution prepared in 0.1 M PBS (pH=7.2). The next day, the solution was changed to 7.5% gelatin (Sigma, G2500; dissolved in 15% sucrose containing PBS) and incubated the samples for 1 hour at 37 °C. The impregnated organs were placed on a bed of gelatine and covered with a second layer. The blocks thus obtained were glued with Tissue-Tek matrix (Sakura Europe, 4583) to cardboard pieces. Isopentane (2-methylbutane; Sigma, M32632) was cooled to -50 °C in liquid nitrogen and the blocks were frozen in it. The cryo-sectioning was performed by using Shandon cryotome at a temperature of -24 °C. The 12 µm thick sections were taken on poly-L-lysine (Sigma, P8920) coated or SuperFrost adhesion slides. The sections were stored at -20 °C until processing.

3.2.2. Immunohistochemistry

Gelatin was dissolved from frozen sections in PBS heated to 37 °C (3-5 minutes) and then replaced to room temperature PBS for a further 5-7 minutes rehydration. The primary antibodies (50-80 µL/section) were applied to the slides (**Table 5**). Dilutions were performed in PBS containing 1% BSA and sodium azide (PBS-BSA). Sections were then incubated in a humidity chamber at room temperature for 1 hour and washed in PBS for 3 x 5 minutes. In the next step, the secondary antibody (**Table 6**) was measured and incubated for further 45 minutes at room temperature in the humidity chamber. After washing in PBS (3 x 5 minutes), the sections were placed in a 3% hydrogen peroxide solution (Sigma-Aldrich, H1009) to block the endogenous peroxidase activity of the tissue. After another washing series, the ABC complex (avidin-biotin-peroxidase complex, Vectastain Elite PK-6100; Vector Laboratories) was applied to the sections and incubated for half an hour. The ABC solution was diluted for 30 minutes prior to use according to the prescribed parameters (1:100 in PBS). After washing-off the solution in PBS, the bound peroxidase enzyme activity was determined with 4-chloro-1-naphtol (Sigma, C8890). The chloronaphthol stock solution was diluted in PBS: 100 µL stock in 100 mL PBS with 300 µL hydrogen peroxide mixed on a magnetic stirrer for 30 minutes, protected from light. After filtering this solution, we measured it to the sections and incubated them for 30 minutes. After developing the color reaction, we washed the slides for 3 x 5 minutes and mounted the samples with water-based media (Poly-Aqua Polyscience Inc., Washington PA, USA, 18606) and stored them at 4 °C until microscopy.

3.2.3. Immunofluorescence

Preparations of the sections and incubation with primary antibody (**Table 5**) were performed in the same way as described in the immunohistochemistry chapter (with the only exception in the case of pSMAD staining, where we used TBS during the whole procedure instead of PBS). Next, the fluorochrome-conjugated secondary antibody (**Table 7**) was pipetted dropwise on the section. Incubation was carried out at room temperature in a humidity chamber, protected from light for 45 minutes. Between incubation steps, the sections were washed with PBS (3 x 5 minutes). We counterstained nuclei with DAPI (4,6-diamino-2-phenylindole dihydrochloride) (Invitrogen, D1306) with a 1 µg/mL solution for 15 minutes. After the water-based mounting of the slides we stored them in the dark at 4 °C until microscopy.

Table 5. Primary antibodies used in immunostaining. The name of the primary antibodies indicated with their target, source, specificity, vendor, corresponding catalog numbers and Antibody registry IDs found on the Research Resource Identification (RRID) Portal (**https://rrid.site/**).

Target name (or clone)	**Source**	**Isotype**	**Dilution**	**Vendor, catalog number**	**Antibody registry ID**
CD57 (HNK-1)	mouse	IgM	1:50	Thermo Fisher, MA5-11605	AB_10980268
HuC/D (16A11)	mouse	IgG2b	1:100	Thermo Fisher, A-21271	AB_221448
nNOS	rabbit (polyclonal)	IgG (H+L)	1:200	Thermo Fisher, 61-7000	AB_2313734
N-cadherin (3B9)	mouse	IgG1	1:200	Thermo Fisher, 33-3900	AB_2313779
N-cadherin (GC-4)	mouse	IgG1	1:200	Sigma-Aldrich, C3865	AB_262097
p75	rabbit (polyclonal)	IgG (H+L)	1:1000	Promega, G3231	AB_430853
β3-tubulin, Tuj1 (AA10)	mouse	IgG2a	1:100	Santa Cruz Biotechnology, sc-80016	AB_2210523
SOX-10 (A-2)	mouse	IgG1	1:100	Santa Cruz Biotechnology, sc-365692	AB_10844002
Caspase-3 (5A1E)	rabbit (polyclonal)	IgG (H+L)	1:50	Cell Signaling, 9664	AB_2070042
pSMAD	rabbit (polyclonal)	IgG (H+L)	1:50	Cell Signaling, 9511	AB_331671
E-cadherin (8C2)	mouse	IgG1	1:2	DSHB	AB_528117

p19 gag protein (AMV-3C2)	mouse	IgG1	1:5	DSHB	AB_528098
SMA (1A4)	mouse	IgG2a	1:400	Dako, M0851	AB_2223500
Bfabp	rabbit (polyclonal)	IgG (H+L)	1:50	kind gift from Dr. Thomas Müller	

Table 6. Biotinylated secondary antibodies used in immunostaining. The name of the biotinylated secondary antibodies is indicated with their host species, specificity, target, vendor and corresponding catalog numbers and Antibody registry IDs found on the RRID Portal. We diluted the biotinylated secondary antibodies 1:200 in PBS-BSA prior to use.

Secondary antibody	Host species	Vendor	Catalog number	Antibody registry ID
biotinylated anti-mouse IgG (H+L)	horse	Vector Laboratories	BA-2000	AB_2313581
biotinylated anti-rabbit IgG (H+L)	goat	Vector Laboratories	BA-1000	AB_2313606
biotinylated anti-mouse IgM (μ chain)	goat	Vector Laboratories	BA-2020	AB_2336183

Table 7. Fluorochrome conjugated secondary antibodies used in immunostaining. The name of the fluorochrome conjugated secondary antibodies indicated with their host species, specificity, target, excitation wavelength of the certain fluorochrome used, vendor and Antibody registry IDs found on the RRID Portal. We diluted the fluorochrome conjugated secondary antibodies 1:200 in PBS prior to use.

Species reactivity and target	Host species and isotype	Excitation wavelength	Vendor	Catalog Number	Antibody registry ID
anti-mouse IgG (H+L)	goat	350 nm	Thermo Fisher	A21049	AB_141456
anti-mouse IgG (H+L)	donkey	488 nm	Thermo Fisher	A21202	AB_141607
anti-mouse IgG (H+L)	donkey	594 nm	Thermo Fisher	A21203	AB_2535789
anti-mouse IgG (H+L)	donkey	647 nm	Thermo Fisher	A31571	AB_162542
anti-mouse IgG1	goat	488 nm	Thermo Fisher	A21121	AB_2535764
anti-mouse IgG1	goat	594 nm	Thermo Fisher	A21125	AB_2535767
anti-mouse IgG2a	goat	488 nm	Thermo Fisher	A21131	AB_2535771
anti-mouse IgG2a	goat	594 nm	Thermo Fisher	A21135	AB_2535774
anti-mouse IgG2b	goat	594 nm	Thermo Fisher	A21145	AB_2535781
anti-rabbit IgG (H+L)	donkey	488 nm	Thermo Fisher	A21206	AB_2535792
anti-mouse IgM	goat	594 nm	Thermo Fisher	A21044	AB_2535713

3.2.4. Whole-mount immunostaining

For the whole mount immunostaining procedure distal gut segments were used. The samples were fixed in 4% PFA overnight at 4°C. The gut segments were immersed in 12-well plates and permeabilized with 0.1% Triton-X PBS overnight at 4°C. The primary antibody (β3-tubulin [Tuj1] clone: AA10; Santa Cruz, sc-80016) was diluted in 1:400 in PBS-BSA containing 1% goat serum. The gut segments were incubated with the primary antibody for 2 hours at room temperature, while shaking followed by an overnight washing step in PBS. The next day, the samples were incubated for 1 hour at room temperature, covered from light with the secondary antibody (goat anti-mouse IgG(H+L) AlexaFluor 488; Invitrogen A11001). After a brief washing the images were recorded with Nikon SMZ25 fluorescent stereomicroscope and analyzed with the NIS-Elements software.

3.3. In situ hybridization

3.3.1. Whole-mount in situ hybridization

Dissected gastrointestinal tracts were fixed in 4% paraformaldehyde (PFA), dehydrated in methanol, and stored at -20 °C until ready for processing **(223,224)**. Published chick probes were used: Wnt5a **(225)**, Wnt11 **(226)**, Fzd7 **(227)**, Bmp4 **(228,229)**. Digoxigenin riboprobe synthesis and whole-mount RNA in situ hybridization were performed as described by Acloque **(230)**.

3.3.2. In Situ Hybridization on FFPE sections and on primary cell cultures

For sections, embryonic gut segments were fixed in 4% PFA at room temperature for 1 hour, washed in PBS, gradually dehydrated in ethanol, and embedded in paraffin. Sections (10 µm) were cut using a microtome and collected on poly-L-lysine coated slides. In situ hybridization was performed following Faure and Nielsen **(231,232)**. All sections were hybridized for 18-24 hours. Detection was performed using BM purple, according to the manufacturer's instructions (Roche, 11442074001). Digoxigenin riboprobes were prepared as described by Riddle **(233)**. Published chick probes were used for FFPE sections and for primary cell cultures: Bmp4 **(228,229)**, BMPRII **(234)**, Fzd7 **(227)**.

3.4. Embryo manipulation techniques and *ex vivo* experiments

3.4.1. Collagen gel culture

In the first step, 700 µl of DMEM (Sigma), 6 µl of 1 N NaOH, and 294 µl of collagen (rat tail collagen I, 3.38 mg/ml; BD Biosciences, 354236) were added to an Eppendorf tube in the given order while keeping it on ice. 350 µl from this solution was measured into a Falcon Center-Well Organ Culture Dish (Corning, 353037) and incubated for 5 minutes at room temperature and another 5-10 minutes at 37 °C in a CO_2 incubator until polymerization. The preparations were placed on top of the collagen layer and embedded with a second layer. The gut segments were cultured for 24-72 hours.

3.4.2. Intestinal organ culture assay

Embryonic chicken intestinal segments were collected in PBS containing penicillin-streptomycin (PenStrep; Sigma, P0781) under sterile conditions to prepare suspended, so-called catenary organ cultures **(235,236)**. The sections were then attached to the bottom of sterile, non-toxic silicone-coated Petri dishes by using insect needles to suspend them in the surrounding liquid (culture media, DMEM; Gibco, 31966-021) and prevent adhesion to the silicone. The cultures were maintained for 2 to 3 days.

3.4.3. Chorioallantoic membrane (CAM) transplantation

Larger embryonic organs or *in vitro* recombinant tissues can be cultured for extended periods in an environment similar to *in vivo* conditions with the chorioallantoic membrane (CAM) transplantation technique (**Figure 4**). During the experiments the grafts were transferred to a 9-day-old chicken embryo's CAM and incubated further for 7-9 days. For embryonic ceca recombination chimeras, previously we cultured the organs embedded in collagen gel matrix to ensure the adhesion of tissues.

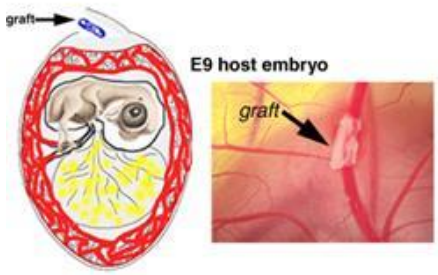

Figure 4. Schematic representation of CAM technique and an implanted hindgut segment sitting on an allantoic vessel

3.4.4. Viral overexpression

Retroviral vectors can be used to create targeted gain-of-function and loss-of-function mutations in avian embryos. The method involves amplifying a retroviral plasmid in E. coli strains, culturing it on embryonic fibroblast cell line DF1, concentrating the virus particles by ultracentrifugation, and injecting them into the mesenchyme of a specific intestinal segment of early chicken embryos. After being injected into the tissue, the virus infects dividing cells. The retrovirus is then incorporated into the genome of the newly formed cells. During our experiment, 2-5 µl of BMP4-RCAS retrovirus suspension with 0.1% Fast Green solution in PBS was injected into the E6 chicken hindgut mesenchyme by using the Narishige brand microinjector, 100 µl Hamilton syringe and thin glass capillary. The injected segments were further cultured on an E8 chick chorioallantoic membrane (CAM) for 9 days. Avian retroviruses have a specific tropism for mesenchymal cells and do not directly target ENCDCs **(208)**. The 3C2 antibody, which recognizes the RCAS P19 gag protein **(237)**, indicates successful and extensive viral replication in the intestinal wall.

3.4.5. Ceca ablation and recombination chimera

For ceca ablation experiments, ceca buds were separated from the midgut-hindgut segment of E6 (HH28) chicken embryonic guts by using Moria Pascheff-Wolff Spring scissors (Fine Science Tools, 15371-92). The remaining intestinal segments were cultured in catenary dishes. For the recombination experiment, ceca buds were removed from both GFP^+ and non-GFP chick embryonic guts in the same manner. The ceca buds of the non-GFP chick embryo were replaced with ceca isolated from a GFP-chick embryo. The proximal-distal and left-right orientations were maintained during recombination. To allow the tissues to adhere, ceca and intestine recombinants were embedded in a 3D collagen gel matrix. After three days, chimeric guts were removed, and immunofluorescence was performed.

3.4.6. Vital dye labeling

The vital lipophilic dye CellTracker CM-DiI (1,1'-dioctadecyl-3,3,3',3'-tetramethylindocarbocyanine perchlorate; Thermo Fisher Scientific, C7000) was dissolved in DMSO at a concentration of 1 mg/ml. The concentrated stock of DiI solution was diluted 1:100 in 15% sucrose containing PBS as described earlier **(238)**. To study the

colonization of ceca-derived or interceca-derived ENCDCs in the hindgut, intestinal tracts dissected from E5.5 (HH27) chick embryos were injected with approximately 0.5 µl DiI into the ceca buds (n=9) and interceca mesenchyme (n=7). CellTracker CM-DiI fluorescent dye can easily penetrate cell membranes and is converted into cell membrane-impermeant reaction products. This dye can be transferred to daughter cells through several generations, but not to adjacent cells in the population. Microinjection was processed by using Nikon SMZ25 epifluorescence stereomicroscope. DiI-injected guts were cultured for 72 hours, fixed in 4% PFA, cryo-embedded in gelatin, and sectioned at 12 µm. Sections were further processed for N-cadherin immunofluorescence staining.

3.5. Primary cell culture and *in vitro* experiments

3.5.1. Cell migration assay

For ENCDC migration assay, distal midgut without ceca and the cecal region was isolated from E6 (HH29) chick embryos and cultured on 20 µg/mL fibronectin coated plastic surface with GDNF (10 ng/mL; R&D Systems, Minneapolis, MN, USA, 212-GD-010; n=12) and GDNF in combination with different recombinant proteins (WNT11: 500 ng/mL, R&D Systems, 6179-WN; BMP4: 200 ng/mL, R&D Systems, 5020-BP or Noggin: 200 ng/mL, R&D Systems, 6997-NG-025) dissolved in DMEM culture medium.

3.5.2. Cell proliferation, EdU labeling

For cell proliferation, 5-ethynyl-2'-deoxyuridine (EdU) was added to the culture medium 2 or 3 hours before 4% PFA fixation. This can be used for direct measurement of *de novo* DNA synthesis or S-phase synthesis of the cell cycle by using click chemistry. Click chemistry is a method for covalently coupling of an azide with an alkyne. EdU incorporation was detected by using the Click-iT EdU Imaging Kit with Alexa Fluor 488 (Thermo Fisher Scientific, Click-iT EdU Proliferation Kit for Imaging, C10340) or 647 azides (C10337). The developed fluorescent signals were examined under fluorescent or confocal microscope.

3.6. Microscopic images

Images were recorded with a Nikon Eclipse E800 brightfield and fluorescence microscope and a Zeiss LSM 710 confocal microscope. Whole-mount images were recorded by using a Nikon SMZ25 with Prior L200 unit brightfield and fluorescence stereomicroscope. Image processing was carried out by using the proprietary software from Zeiss or Nikon, namely Zen Blue and NIS-Elements, respectively, and ImageJ.

3.7. RNA-Seq analysis

Segments from the mid-hindgut of embryonic chicks at day E5 (HH26) were collected. The cecal and intercecal regions were dissected (n=3 embryos per group), and total RNA was isolated using Trizol reagent according to manufacturer's guidelines. The RNA samples were sent to the Next Generation Sequencing Core Facility at Massachusetts General Hospital for mRNA library preparation and high-throughput sequencing, employing a 50 base-pair single-end read protocol on the Illumina HiSeq 2500 platform. Base calling was carried out using the HiSeq Control Software, and raw sequencing data were generated via the Illumina bcl2fastq pipeline. Sequence reads were aligned to the Gallus gallus reference genome (Galga4) using STAR, a splice-aware alignment program **(239)**. Gene-level read counts were obtained using HTSeq **(240)**. Transcriptome comparison between ceca and interceca were performed with the R package edgeR **(241)**. Differentially expressed genes (DEGs) were identified using a Benjamin-Hochberg adjusted $P < 0.001$ **(242)**. Genes with fewer than 0.3 counts per million on average in both groups and with minimal fold change (± 0.5 log) were excluded. Analysis of HSCR-related genes was conducted using the gene set from Gui et al. (2017) **(60)**. Functional enrichment analysis for biological processes was based on the Gene Ontology (GO) database **(243)** via PANTHER **(244)**. Enriched GO terms were summarized with the Revigo tool **(245)**, and heatmaps for selected terms were generated using ClustVis **(246)**. Protein-protein interaction (PPI) networks and related signaling modules were assembled with NetworkAnalyst 3.0 **(247)**, incorporating data from the STRING functional protein association database. Visualization of the interactome with overlaid gene ontologies was carried out within the same tool, considering only experimentally validated interactions.

Previously generated RNA-seq data were obtained from the GEO database (accession number: GSE182783) for re-analysis with a focus on the BMP signaling network. Differences in transcript expression between ceca and interceca were recalculated using edgeR (version 4.2.3) **(241)**, applying a false-discovery rate-adjusted $P < 0.01$ to define significant DEGs. Genes were considered expressed if they reached more than 1 read per kilobase per million mapped reads (RPKM) in at least three samples. To identify possible signaling hubs in the developing gut, PPI networks built from DEGs were visualized in NetworkAnalyst 3.0 **(247)** using STRING data with a high-confidence interaction score cutoff of 800. The top 20 nodes (extended to 23 in cases of tied values) ranked by degree (number of connections) on the network topology were considered key candidate hubs. BMP signaling pathway members were retrieved from Kyoto Encyclopedia of Genes and Genomes (KEGG) database TGF-β signaling pathway (hsa04350), substituting corresponding orthologous genes from the *Gallus gallus* genome.

3.8. Statistics

All statistical analyses were performed using GraphPad Prism version 10.0.2 for Windows, GraphPad Software, Boston, MA USA, www.graphpad.com or with R (R Core Team). The Shapiro-Wilk normality test was performed first. Based on the distribution and number of data points we carried out two-way ANOVA with Tukey's multiple comparisons test or Kruskal-Wallis test with post-hoc Dunn's test. A p-value <0.05 was considered significant. Error bars represent the standard error of mean (SEM) or the standard deviation (SD), as indicated in the corresponding figure legend.

4. Results

4.1. Avian ceca are required for normal enteric nervous system development

4.1.1. Characterization of ENCDC migration across the cecal and hindgut regions in chick embryo

The migration of enteric neural crest-derived cells (ENCDCs) across the distal intestine of chicks was assessed by using immunofluorescence at embryonic days 5 to 8 to determine the location of the migratory wavefront. SOX10^{+} ENCDCs are positioned just above the cecal buds at embryonic day 5 (E5) **(Figure 5A, inset)**. The migration continued in the next 24 hours as the wavefront passed through the ceca and intercecal midgut **(Figure 5B)**, and later reached the proximal hindgut **(Figure 5C)**. The NCADH^{+} wavefront was detected in the mid-hindgut at E7 and had progressed to the distal end by E8 **(Figure 5E)**. SOX10 and N-cadherin (NCADH) are both definitive markers for migrating neural crest cells; however, we could only employ SOX10 in the ceca due to

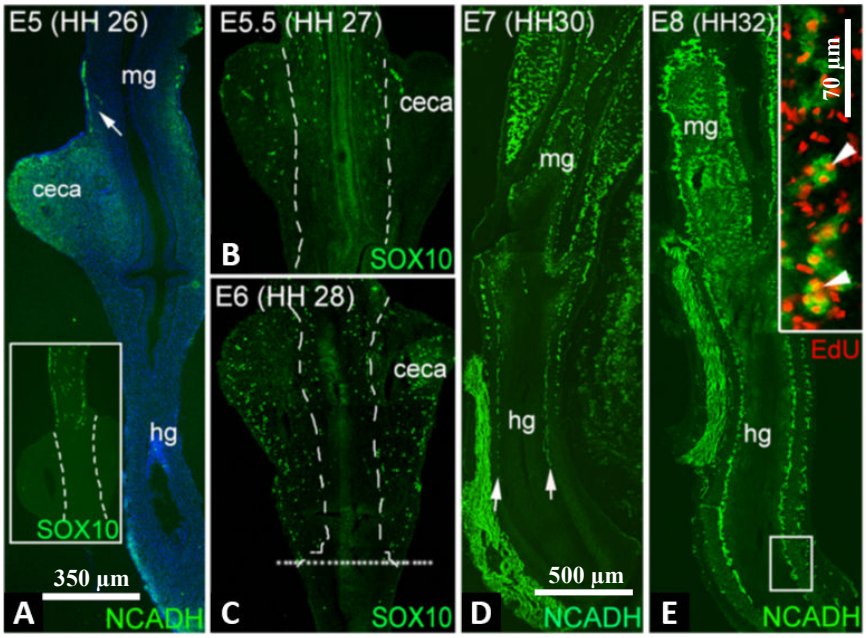

Figure 5. ENS development in the ceca and hindgut under *ex vivo* conditions. Chick intestines were immunostained with N-cadherin (A, D, E) and SOX10 (A inset, B, C) antibodies at E5-E8, demonstrating the progressive migration of ENCDCs towards the distal region of the hindgut. Arrows in A and D indicate the advancing front of migrating cells. Dashed lines indicate the boundary between ceca and interceca. SOX10^{+} ENCDCs colonize the cecal area between E5.5 (B) and E6 (C). The dotted horizontal line (in C) marks the distalmost cells in the migratory wavefront. Arrowheads in I indicate proliferating cells. hg, hindgut; mg, midgut. Scale bar in A represent 350 µm in A-C, 500 µm in D-E and 70 µm in the inset of E.

technological constraints. The utilization of various markers does not affect our findings concerning wavefront positions.

After explantation of isolated E5 gut segments to silicone-coated dishes **(Figure 6A)**, they were cultured under organotypic conditions for three days, which led to ENCDC colonization within a similar timeframe as previously observed *in vivo* **(Figure 6B,C)**. EdU labeling verified the existence of proliferating ENCDCs at the migration's leading edge **(Figure 6D)**.

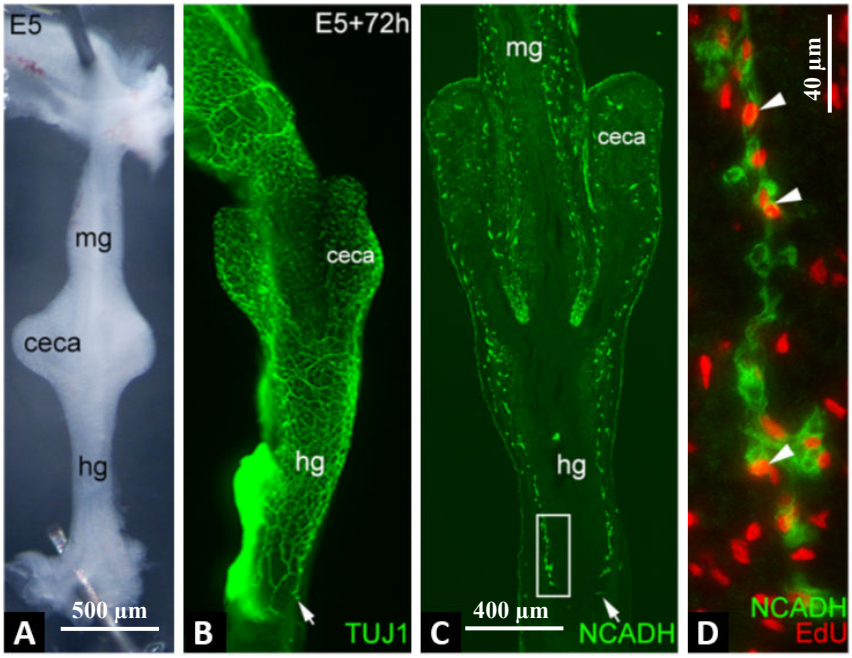

Figure 6. ENS development in the ceca and hindgut in the organotypic culture. Explanted E5 gut (A) has been entirely colonized by TUJ1^{+} ENCDCs after 72 h in culture (wholemount in B; longitudinal section in C; arrows mark position of migratory wavefront). N-cadherin^{+} ENCDCs proliferate at the wavefront (boxed area in C is enlarged in D). Arrowheads in D indicate proliferating cells. hg, hindgut; mg, midgut. Scale bar in A represents 500 µm in A-B, 400 µm in C and 40 µm in D.

To determine if the proliferation rate differs along the distal intestinal length, ENCDC proliferation was measured at multiple points in time by using cross-sections of the migratory wavefront and calculating the ratio of undifferentiated ENCDCs incorporating EdU **(Figure 7A)**. The undifferentiated wavefront cells can be defined by the expression of SOX10 without the presence of HU (ELAVL4) **(Figure 7B)** or BFABP (FABP7) **(Figure 7C)**. Measurements were performed when wavefront cells traveled in

the distalmost midgut (E5), in cecal region (E6) with separate quantification of ENCDC proliferation in the cecal buds and in the intercecal mesenchyme, and in the mid-hindgut (E7) and at the time colonization completed (E8). Our results revealed that wavefront ENCDCs exhibit maximal proliferation while migrating through the cecal buds at E6 **(Figure 7D)**. However, when the wavefront is positioned there, it is considerably elevated compared to the wavefront at the distal midgut (E5) or hindgut (E7). Although ENCDC proliferation was higher in the ceca compared to the intercecal region, the difference did not reach statistical significance. In summary, our findings suggest a critical role for thececal region in the development of the hindgut ENS.

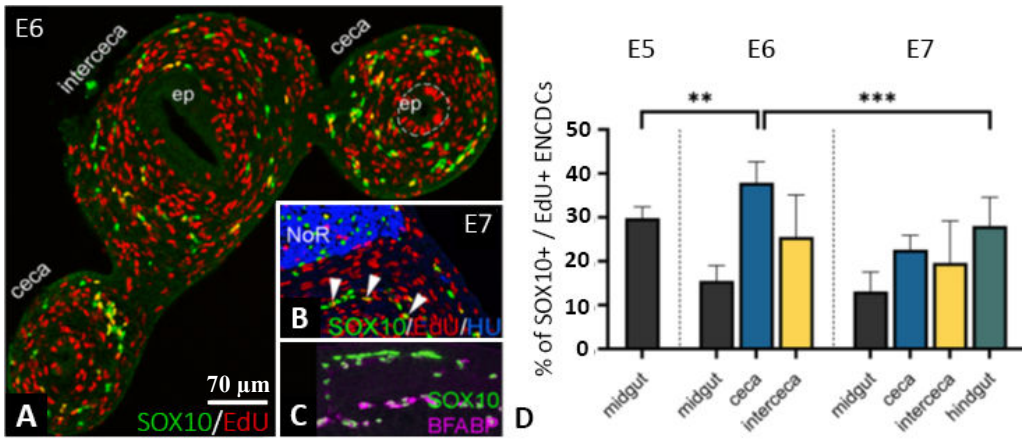

Figure 7. A cross-section of the ceca at embryonic day 6 (E6) (A) reveals SOX10^{+} ENCDCs distributed throughout the mesenchyme, lacking expression of both HU (B) and BFABP (C), and partially co-localizing with EdU—indicative of proliferating, undifferentiated cells, marked with arrowheads in B. Proliferation of the leading ENCDCs was assessed at various intestinal positions from E5 to E7 by calculating the proportion of SOX10^{+} cells incorporating EdU and those maintaining an undifferentiated SOX10^{+}/HU^{-}/BFABP^{-} phenotype. ep, epithelium; NoR, nerve of Remak. **p<0.01; ***p<0.001. Scale bar: 70 µm. n=9 guts per stage.

4.1.2. Embryonic cecal buds are required for normal ENS development

Cecal buds were microsurgically excised from E5 intestine shortly ahead of the arrival of migrating ENCDCs **(Figure 8A,B)** and the isolated guts were subsequently cultured for three days under organotypic conditions in catenary culture. Staining with TUJ1 (TUBB3) and N-cadherin (NCADH, CDH2) revealed that ENCDCs extended solely to the proximal hindgut, whereas the remainder of the hindgut remained aganglionic **(Figure 8C)**. The distalmost ENCDCs assembled into large aggregates of cells with substantially reduced cell proliferation **(Figure 8D)** compared to control **(Figure 8D)**, and this difference was statistically significant **(Figure 8G)**. The ENCDC

cells forming these aggregates were clearly differentiated and expressed nNOS (NOS1) **(Figure 8E)**, which indicates a subset of terminally differentiated enteric neurons. Caspase-3 staining revealed no apoptotic cells among ENCDCs **(Figure 8F)**. These results further demonstrate the importance of embryonic ceca in hindgut ENS formation.

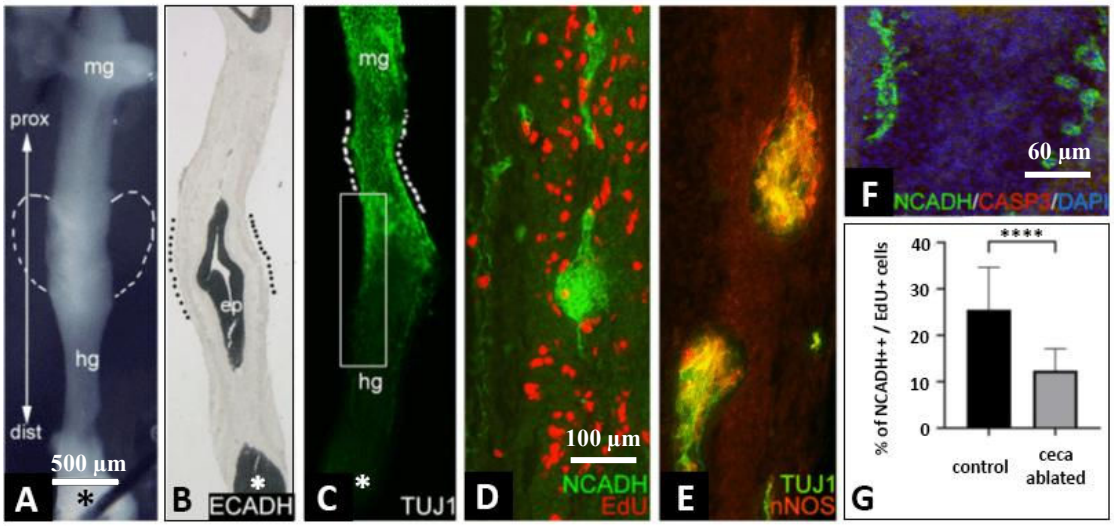

Figure 8. Ceca are essential for hindgut ENS colonization. When ceca were microsurgically excised from E5 intestines (A; dashed lines indicate the original cecal location), the remaining gut was stained with E-cadherin (ECADH) to verify structural integrity (B; dotted lines indicate the former cecal position). Asterisk marks the cloaca, the most caudal part of the gut tube (A-C) with endoderm-lined chamber visible (B). After 72 hours in organ culture, longitudinal sections were immunostained with TUJ1, revealing that ENCDC migration stopped at the proximal hindgut (C). This was accompanied by the formation of large N-cadherin–positive ($NCADH^+$) ENCDC aggregates, which showed minimal proliferation (D; magnified view of boxed region in C) and extensive nNOS expression, indicating premature differentiation (E). Consecutive sections of ceca-ablated intestines were stained for cleaved caspase-3 to detect apoptosis and NCADH to label ENCDCs (F). Following cecal ablation, ENCDC proliferation at the wavefront was markedly diminished in comparison to the control (G). n=8. ****$p<0.0001$. Scale bar in A represents 500 µm in A-C, 100 µm in D-E and 60 µm in F.

Next, we surgically removed the ceca at E6 and replaced them with freshly isolated ceca from age-matched green fluorescent protein (GFP)-expressing chick embryos **(Figure 9A)**. After 72 hours in culture, GFP-positive cells were observed migrating distally into the hindgut **(Figure 9B,C)**. Co-expression of N-cadherin (NCADH) in these cells **(Figure 9D,E)** confirmed that the migrating GFP^+ cells were ENCDCs. Moreover, all $NCADH^+$ cells in the hindgut co-expressed GFP **(Figure 9E)**, indicating that the hindgut ENS in these chimeric guts was formed exclusively by ceca-derived ENCDCs. Although ENCDCs were already present in the intercecal mesenchyme

at E6 **(Figure 1C)** and could have served as an alternative source, no contribution from the host gut to hindgut ENS formation was detected.

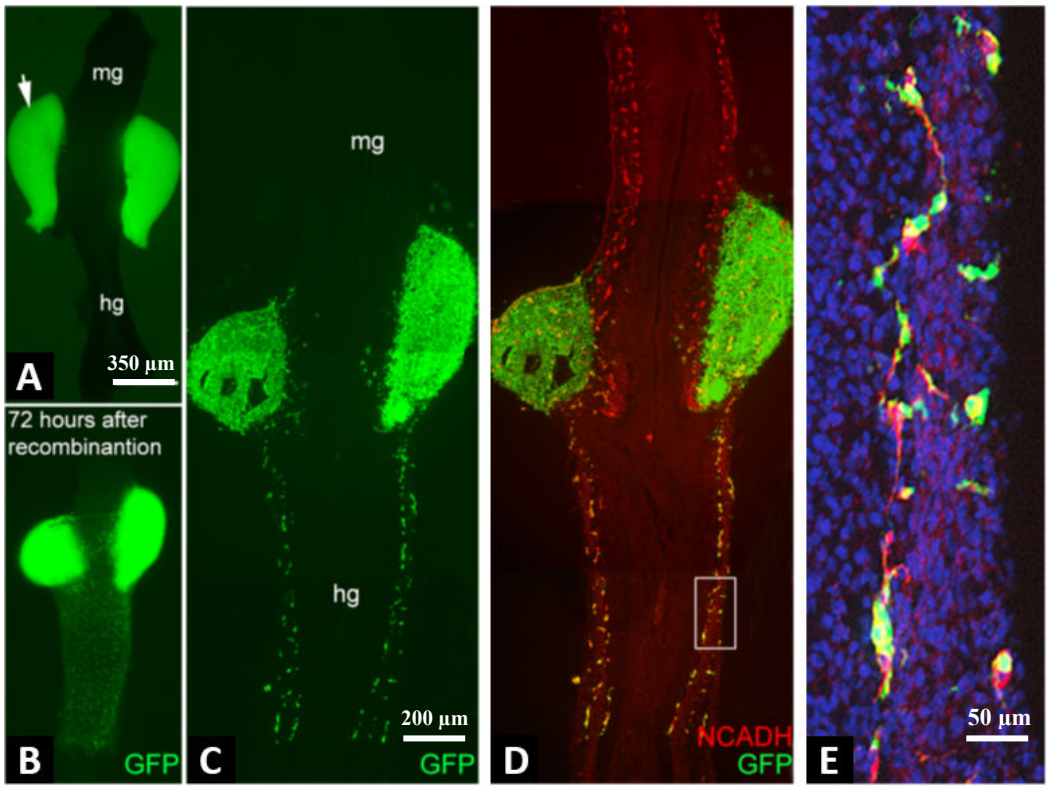

Figure 9. Cecal chimeras demonstrate that the hindgut ENS originates from the ceca-derived ENCDCs (A,B). Following the ablation of the ceca from E6 chicken intestine, it was replaced with new ceca from E6 GFP$^+$ chickens (A, marked with arrow) and the recombinants (B) were cultured for additional 72 hours; n=8. GFP$^+$ cells migrate out of the ceca distally to colonize the hindgut mesenchyme (C). Co-immunofluorescence with NCADH antibody shows that the hindgut ENS develops exclusively from GFP$^+$ ceca-derived cells (D, boxed area magnified in E). Scale bar in A represent 350 µm in A-B, 200 µm in C-D and 50 µm in E.

To further validate these findings, we injected a fluorescent lipophilic dye (DiI) into the cecal buds at E5.5 **(Figure 10A)**. After 72 hours, DiI-labeled cells were observed migrating into the hindgut **(Figure 10B,C)** and co-expressed NCADH **(Figure 10D)**. High-magnification quantification showed that 31% of NCADH$^+$ ENCDCs in the hindgut contained DiI crystals following cecal injection. In contrast, DiI injection into the intercecal region **(Figure 10E)** resulted in no detectable DiI-labeled cells in the hindgut

(Figure 10F–H), further supporting the exclusive contribution of cecal ENCDCs to hindgut colonization.

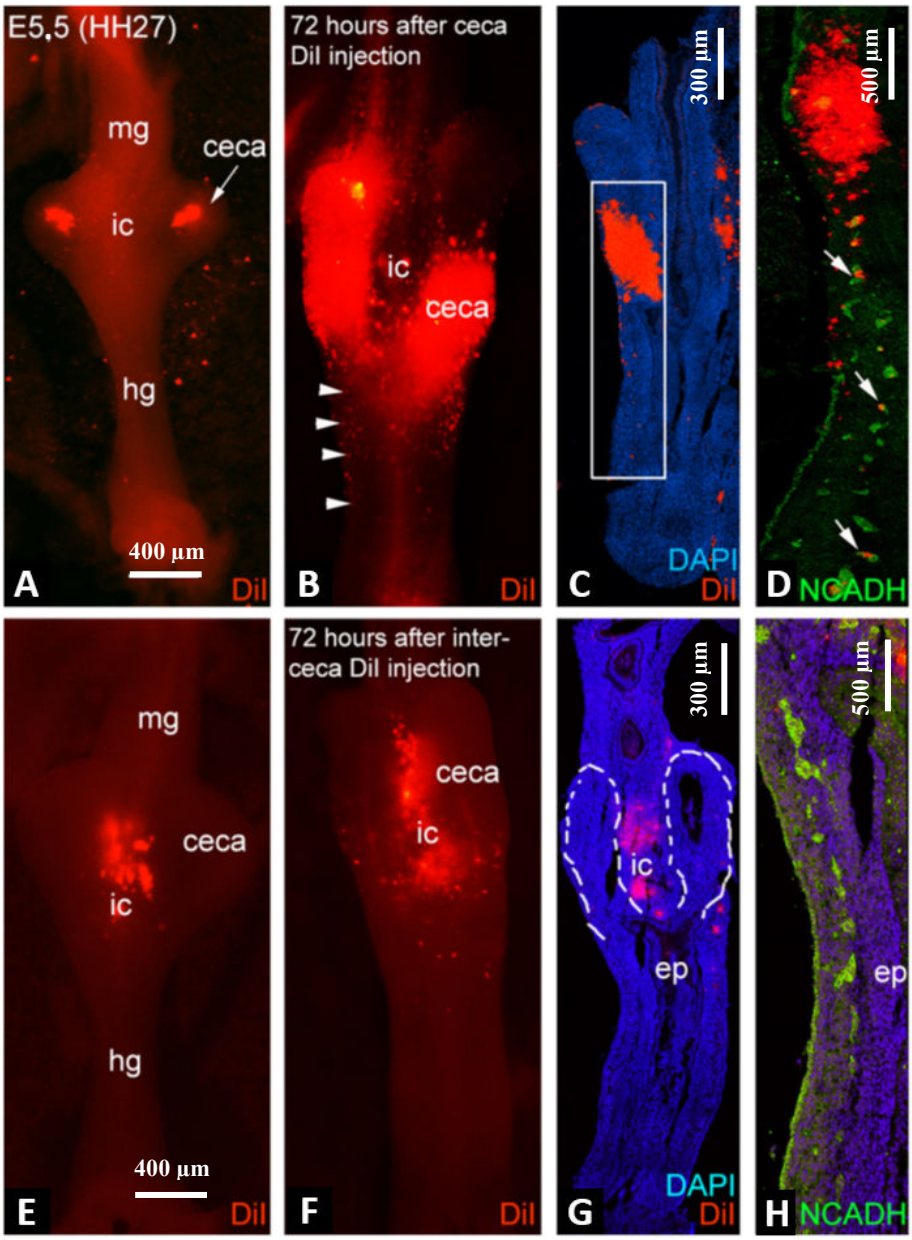

Figure 10. Hindgut ENCDCs originate from the ceca rather than the intercecal area (A,B). Vital lipophilic red fluorescent dye (DiI) was administered into the cecal buds at E5.5 (A). After 72 hours in culture (B), DiI^{+} cells were observed spreading throughout the proximal hindgut in wholemount (B, arrowheads). Longitudinal section shows DiI cells in the proximal hindgut (C), and a magnified view of the boxed region reveals co-expression of NCADH, indicative of ENCDCs (D, arrows). (E-H) Conversely, after DiI injection into the intercecal region (E), no DiI-labeled ENCDCs were observed in the hindgut (F-H; dashed lines in G indicate the ceca). Scale bar in A represents 400 µm in A-B and E-F, 300 µm in C and G, 500 µm in D and H.

4.2. Identifying ceca derived factors as new important signaling cues in ENS formation of avian hindgut

4.2.1. Role of WNT-related genes

The transcriptomes of the cecal and intercecal niches were characterized using RNA sequencing (RNA-seq). The ceca and intercecal regions were dissected at E5, just prior to ENCDC colonization, to identify region-specific transcriptional differences **(Figure 11A)**. E5 was chosen because it is the earliest stage at which the cecal buds can be morphologically distinguished and isolated. Importantly, this timing also allowed us to focus exclusively on the cecal microenvironment, free of ENCDC contamination, as ENCDCs have not yet migrated into the ceca at this stage.

We identified major differences in gene expression profiles, with 559 differentially expressed genes (DEGs) upregulated and 894 DEGs downregulated in the ceca compared to the interceca. HSCR-related genes **(60,248)** were substantially represented in the data set, with 51 out of 96 examined genes showing differential expression (FDR<0.05) between the ceca and intercecal regions **(Figure 11B)**. These comprised an increased expression of RET in the interceca and GDNF and EDN3 in the ceca, as previously described **(176)**. Upregulated DEGs in the ceca were linked to biological processes related to nervous system formation, cell migration, and digestive tract development, indicating that the ceca possess a molecular signature that facilitates ENCDC colonization.

We performed a topological analysis of protein–protein interaction (PPI) networks derived from RNA-seq data to identify key cecal factors influencing ENCDC migration. This approach enables the identification of central regulatory proteins – so-called hub proteins – based on their degree of connectivity within the network. By ranking proteins according to the number of predicted interactions, we generated a list of candidate hub proteins with the highest connectivity. Wnt signaling emerged as a prominent regulatory module. Components of this pathway – both ligands and receptors – overlapped extensively with biological processes such as neurogenesis and cell migration, both of which were highly represented in the PPI network. These findings suggest that Wnt signaling may play a critical role in regulating ENCDC behavior within the ceca. Specifically, we identified upregulation of several key Wnt ligands, including WNT11, WNT2B, and WNT5A, along with receptors FZD4 and FZD10, in the ceca. In contrast,

the related receptor FZD7, as well as non-canonical Wnt/planar cell polarity (PCP) pathway co-receptors RYK and PRICKLE1, were more prominently expressed in the intercecal region **(Figure 11C,E)**.

To further evaluate signaling pathways, we quantified the expression of receptors, intracellular mediators, and other pathway components in both regions using reads per kilobase per million (RPKM) values. Interestingly, BMP4 was upregulated 1.8-fold in the ceca and ranked as the top-expressed secreted protein, highlighting its potential as a major paracrine signaling factor for ENCDCs. Receptors for BMP4, including ACVR1, ACVR2A, and BMPRII, were expressed in both the cecal and intercecal regions **(Figure 11D,F)**. In summary, these transcriptomic data suggest that the embryonic ceca—and specifically, WNT and BMP signaling within them—may function as critical signaling centers in the developing gut, enabling proper ENS formation in the hindgut.

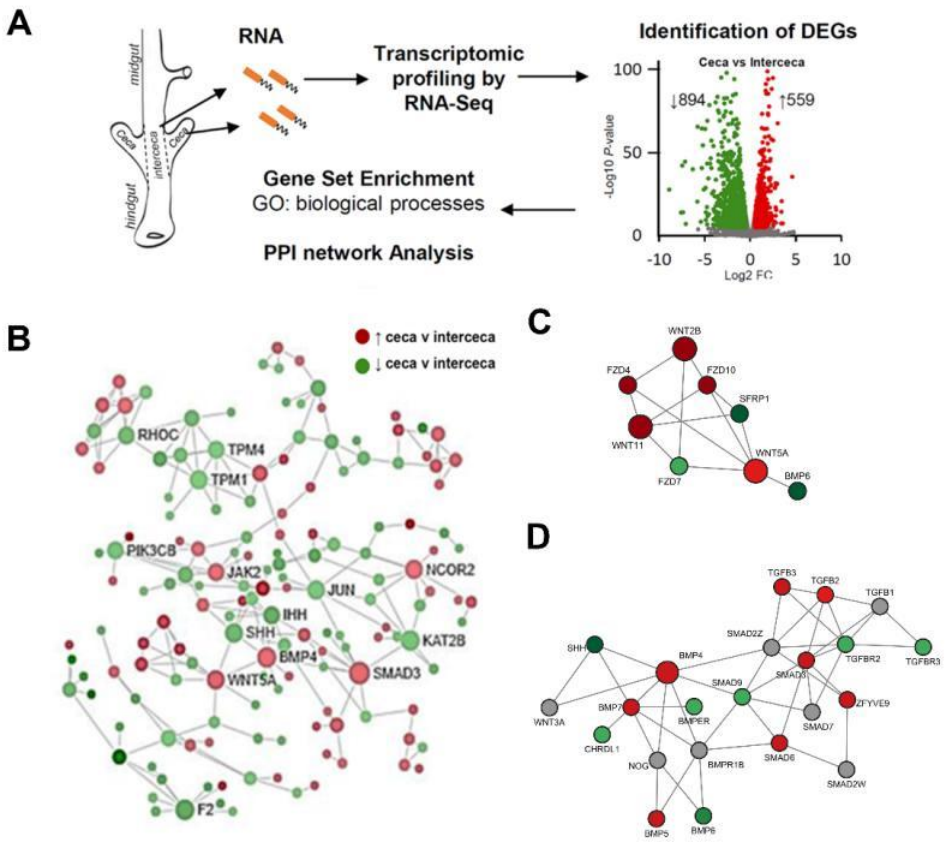

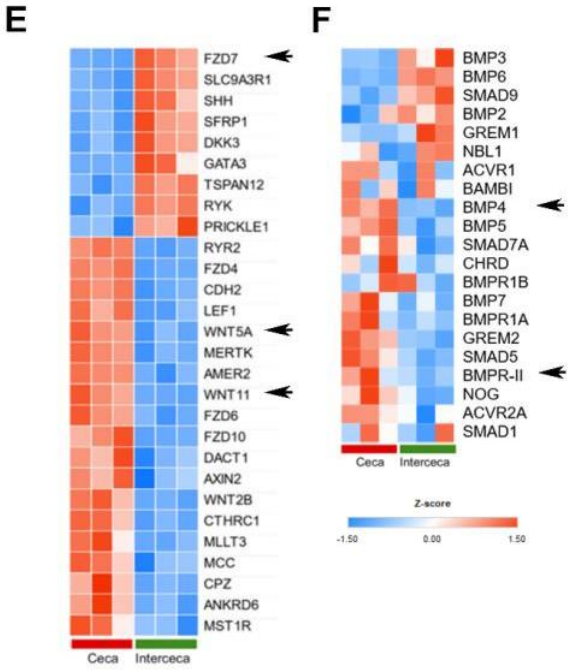

Figure 11. Transcriptional profile of E5 chicken embryonic ceca and interceca (A) Total RNA was extracted and RNA-seq performed to profile respective transcriptomes. Differentially expressed genes (DEGs) were compared between the two regions and analyzed for over-representation analysis of biological processes by using the Gene Ontology (GO) database, as well as for protein-protein interaction (PPI) networks. **(B)** A PPI network comprising DEGs that are upregulated (red) and downregulated (green) in the ceca compared to the interceca was constructed. **(C-D)** Analysis of PPIs revealed a significant module linked to Wnt (C) and BMP (D) ligands and receptors, which were either upregulated (red) or downregulated (green) in the ceca relative to the interceca. **(E-F)** Hierarchical clustered heatmaps illustrate the identified DEGs linked to Wnt (E) and BMP (F) signaling, displaying Z-scores of RPKM values from cecal and intercecal areas. The expression and function of the major signaling molecules denoted by arrows were subsequently validated. experimentally. The samples of ceca and interceca sent for bulk RNA-seq are biological replicates (n=3 for each).

4.2.1.1. Validation of Wnt pathway genes expression in the ceca

Cecal region of 5-day-old (E5) chick embryo showed robust expression of Wnt5a and Wnt11 **(Figure 12A-C)**. Conversely, despite its presence in the gut epithelium at this stage, Fzd7 was not expressed in E5 ceca **(Figure 12D,E)**. Later, at E6 Fzd7 mesenchymal expression appeared throughout both the cecal and intercecal region **(Figure 12F)**. The expression of Fzd7 in ENCDCs was validated *ex vivo* by culturing E6 ceca with GDNF to stimulate the migration of ENCDCs from the explants and co-immunostaining them with HNK-1 antibody. It seems that only a fraction of HNK1^{+} ENCDCs express Fzd7, indicating that the ENCDCs compose a heterogeneous group with varying Fzd7 expression **(Figure 12G,H)**.

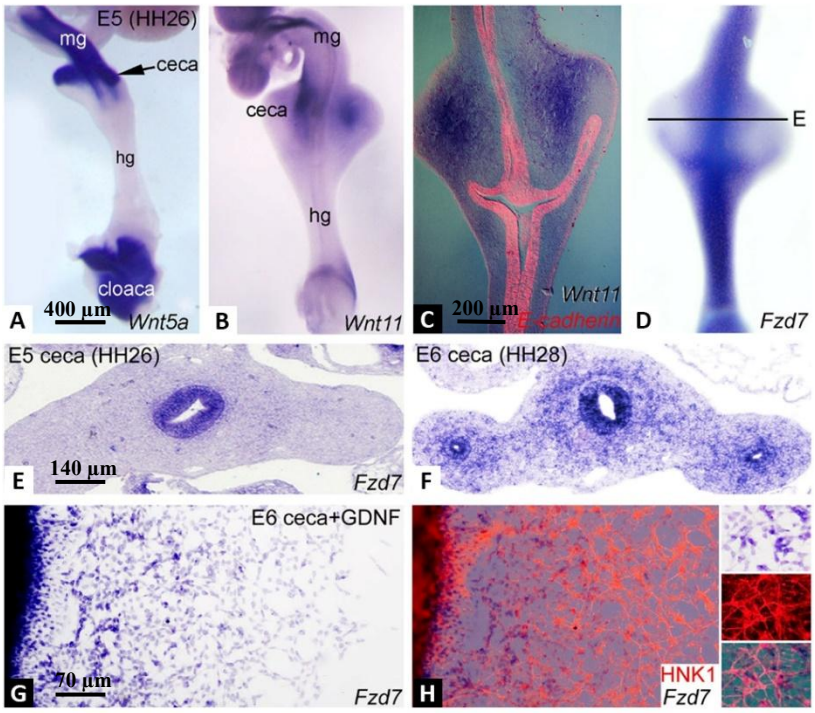

Figure 12. Wnt pathway genes are expressed in the ceca and migrating ENCDCs. (A) Whole-mount in situ hybridization (ISH) of E5 distal intestine shows Wnt5a expressed in the midgut, ceca and cloaca. (B,C) Wnt11 is specifically expressed in the E5 ceca as demonstrated by whole-mount ISH (B) and in a longitudinal section double-stained with E-cadherin to mark the epithelium (C). (D-F) At E5, Fzd7 is expressed throughout the gut epithelium, apart from the cecal buds (D,E) and at E6, Fzd7 is also expressed in the ceca and hindgut mesenchyme (F). (G,H) Explanted E6 chick ceca was cultured in presence of GDNF, which promotes ENCDC migration from the gut. Insets show an enlarged view of Fzd7-expressing ENCDCs. Scale bar in A represents 400 µm in A, B and D; 200 µm in C; 140 µm in E, F; 70 µm in G, H and insets.

4.2.1.2. WNT11 inhibits neuronal differentiation

To further investigate the influence of non-canonical Wnt signaling on ENCDCs during their migration through the cecal domain, E6 ceca were excised and grown on a fibronectin-coated surface in the presence of recombinant GDNF and/or Wnt11 protein. GDNF promoted ENCDC migration to the fibronectin-coated surface within 24 hours which expanded further by 48 hours **(Figure 13A)**. The majority of these ENCDCs expressed the neuronal differentiation marker TUJ1 **(Figure 13B)**. This assay offers a framework for assessing the direct impact of signaling elements on the ENCDCs independently of their mesenchymal environment. Upon the removal of GDNF from the culture medium after 24 hours, further migration over the following 24 hours was

restricted, resulting in cell aggregation into substantial ganglion-like clusters exhibiting aberrant network topology **(Figure 13C-E)**. In contrast, with the addition of WNT11 to the medium following GDNF, withdrawal at 24 hours reinstated migration and prevented aberrant cell aggregation **(Figure 13F)**. Notably, in contrast to GDNF treatment alone, WNT11-treated cultures presented far more undifferentiated ENCDCs **(Figure 13G)**. Moreover, WNT11 alone did not promote the migration of ENCDCs from the ceca (data not shown). To assess the role of WNT11 in neuronal differentiation, we quantified the proportion of HNK1^{+} ENCDCs co-expressing TUJ1 in GDNF-treated cultures, with or without the addition of WNT11 protein. The presence of WNT11 significantly reduced the percentage of ENCDCs undergoing enteric neuronal differentiation **(Figure 13H)**.

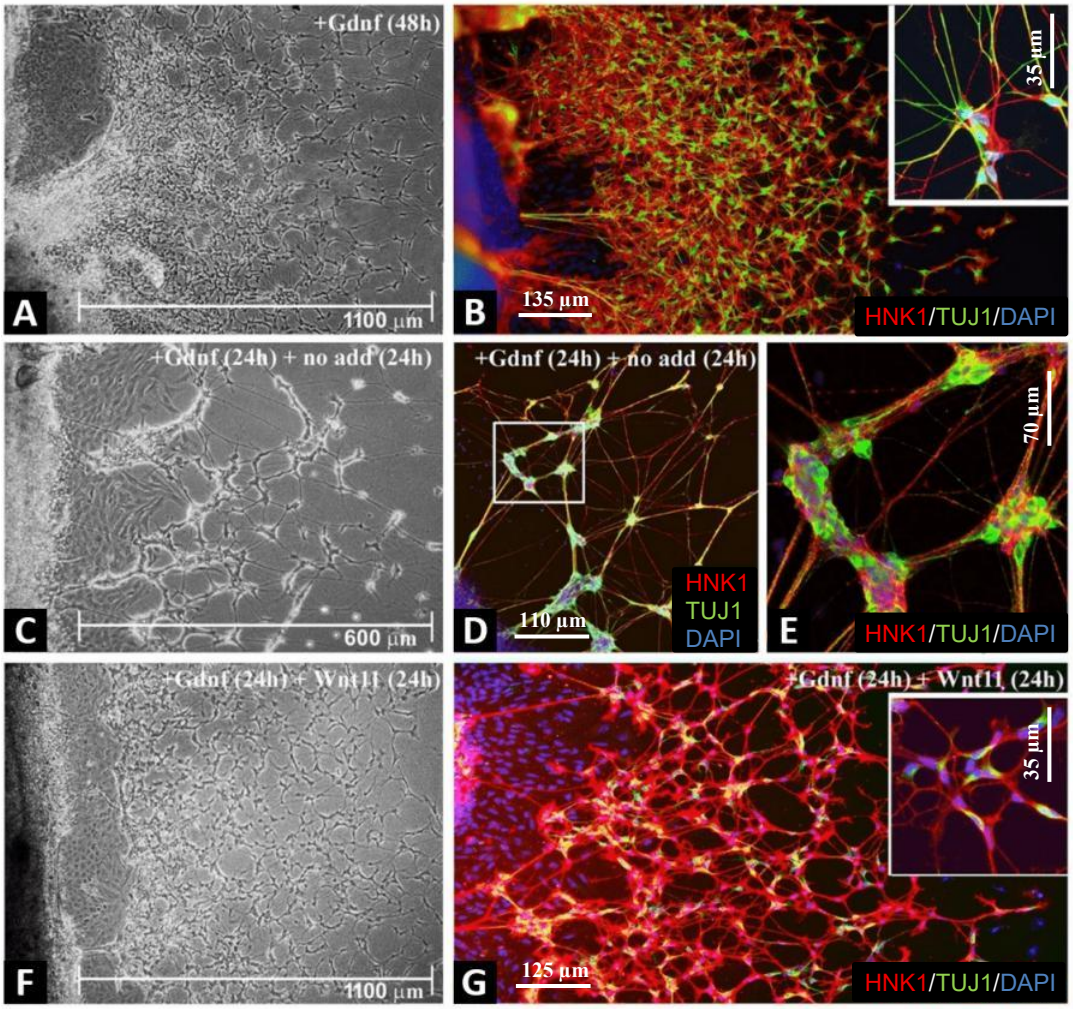

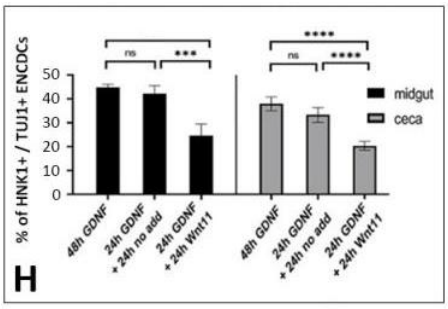

Figure 13. WNT11 suppresses enteric neuronal differentiation. (A–D) E6 ceca were cultured on fibronectin-coated plates with GDNF for 24 hours (A) or 48 hours (C), followed by immunostaining with HNK1 and TUJ1 antibodies (B, D) to assess ENCDC migration distance and neuronal differentiation. The inset in (D) shows a magnified view of differentiated neurons. (E–I) In subsequent experiments, GDNF was withdrawn after the first 24 hours, and cultures were maintained for an additional 24 hours either without further treatment (E, G) or with the addition of WNT11 protein (H, I). The inset in (I) highlights undifferentiated ENCDCs. (J–L) E6 ceca cultured with WNT11 protein alone for 24 hours (J) or 48 hours (K, L) showed no ENCDC migration. (M) The presence of WNT11 significantly inhibited neuronal differentiation of ENCDCs. n=7-10 cell cultures/experiment. ***p<0.001, ****p<0.0001. ns, not significant.

We examined the effect of WNT11 on ENCDC proliferation with the same *in vitro* assay. Incorporation of EdU **(Figure 14B)** was used to quantify cell proliferation. The presence of GDNF enhanced ENCDC proliferation, but adding WNT11 markedly reduced **(Figure 14D)**. The proliferation rate was also quantified in ex vivo cultured E6 intestines. Supplementation of culture media with WNT11 recombinant protein significantly (p<0.001) reduced the number of $NCADH^{+}/EdU^{+}$ cells (from 25.5±9.1% to 16.8±6.1%).

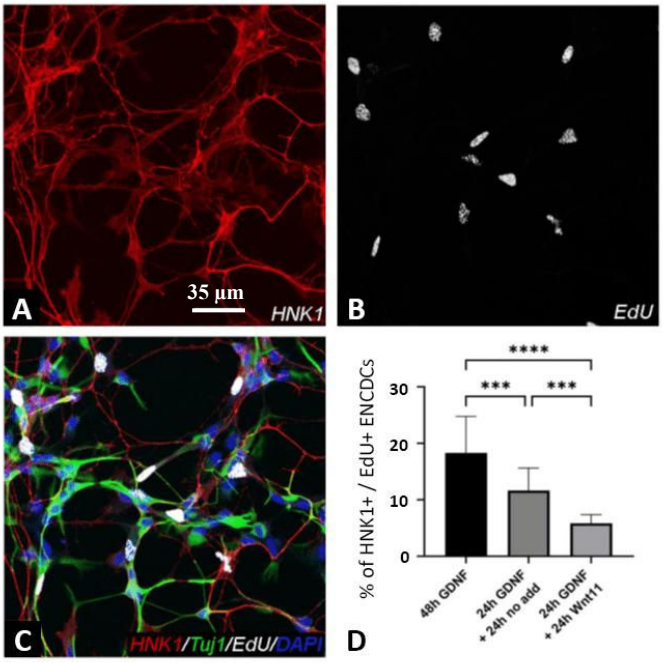

Figure 14. Wnt11 inhibits ENCDC proliferation. E6 ceca and midgut were cultured on fibronectin-coated plates in the presence of GDNF to promote ENCDC migration away from the guts. Addition of EdU to the cultures allowed quantitative comparison of the rate of ENCDC proliferation in the three different culture conditions tested. ***p<0.001; ****p<0.0001. Scale bar represents 35 µm. 5 different fields were quantified for each gut segments and n=4-5 segments were used for each condition.

We investigated whether nNOS-expressing neurons were present in hindgut explants to assess the effect of WNT11 on enteric neuronal differentiation in the intact gut. In the ENS, nNOS marks a specific subset of terminally differentiated neurons, whereas TUJ1 and HU are general markers of early neuronal identity. E6 chick intestines, including the ceca and hindgut, were cultured for three days with or without WNT11 protein. Under control conditions, ENCDCs successfully colonized the hindgut, and nNOS$^+$ neurons were detected at the distal end **(Figure 15A–B')**. While WNT11 did not interfere with ENCDC migration **(Figure 15C)**, it inhibited neuronal differentiation, as indicated by the absence of nNOS-expressing neurons in the distal hindgut **(Figure 15D-D')**. This was further confirmed by measuring the distance between the most distal NCADH$^+$ cell and the nearest nNOS$^+$ neuron. These findings indicate that WNT11 delays the neuronal differentiation of ENCDCs without affecting their migration.

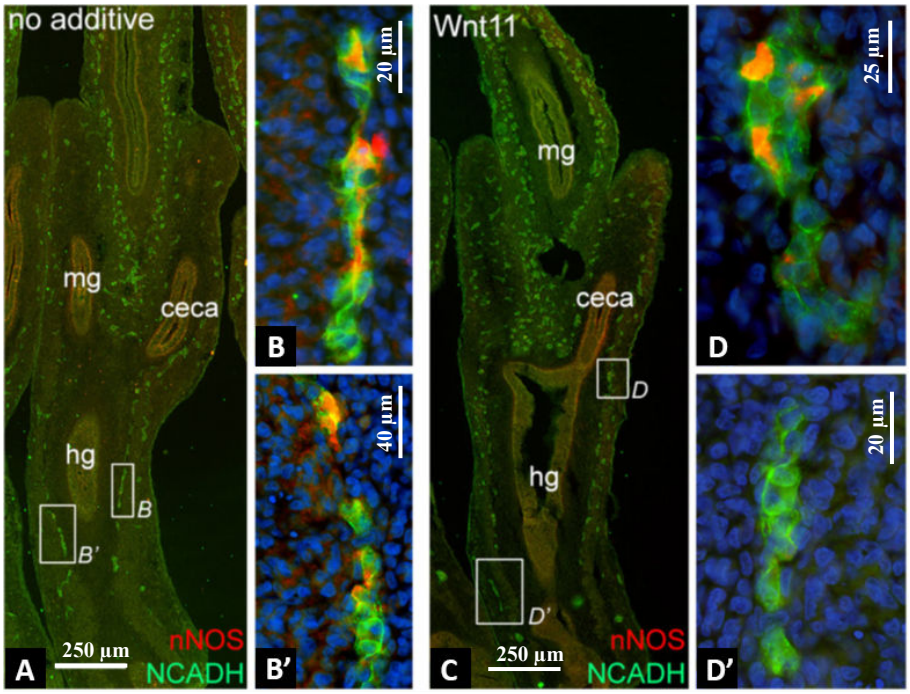

Figure 15. WNT11 suppresses neuronal differentiation in the hindgut ENS. (A) Following a 3-day culture of E6 chick gut, the hindgut ENS is completely populated by N-cadherin$^+$ ENCDCs. The boxed regions in (A) are enlarged in (B, B'), where cells exhibiting dual immunoreactivity for N-cadherin and nNOS are distributed throughout the hindgut. Upon the addition of WNT11 protein to the culture, N-cadherin$^+$ cells continue to populate the whole hindgut (C), whereas on the enlarged areas nNOS immunoreactivity is observed solely at the proximal end (D, D'). The distance from the furthest NCADH$^+$ cell at the wavefront to the furthest nNOS$^+$ cell was measured, demonstrating that WNT11 postpones neuronal differentiation. n=9. ***P<0.001.

4.2.2. The role of BMP4 in hindgut ENS development

4.2.2.1. Expression of BMP4 signaling components implies a contribution to hindgut ENS development.

The expression of BMP4 has been previously reported in the gastrointestinal tract of various vertebrates **(203,205,209,228,249)**; however, its role during avian hindgut development and ENS formation has remained unclear. To investigate the spatial distribution of BMP4 in the developing colorectum, whole-mount in situ hybridization was performed shortly after ENCDCs colonized the post-umbilical midgut at embryonic day 5 (E5) **(Figure 16A,B)** and the ceca at E6 **(Figure 16C)**. Undifferentiated ENCDCs were identified by the expression of markers such as p75 (nerve growth factor receptor), SOX10 (indicative of ENCDCs and enteric glia), N-cadherin (CDH2), and HNK1. At E5, BMP4 expression was restricted to the cecal mesenchyme **(Figure 16B)**, while expression

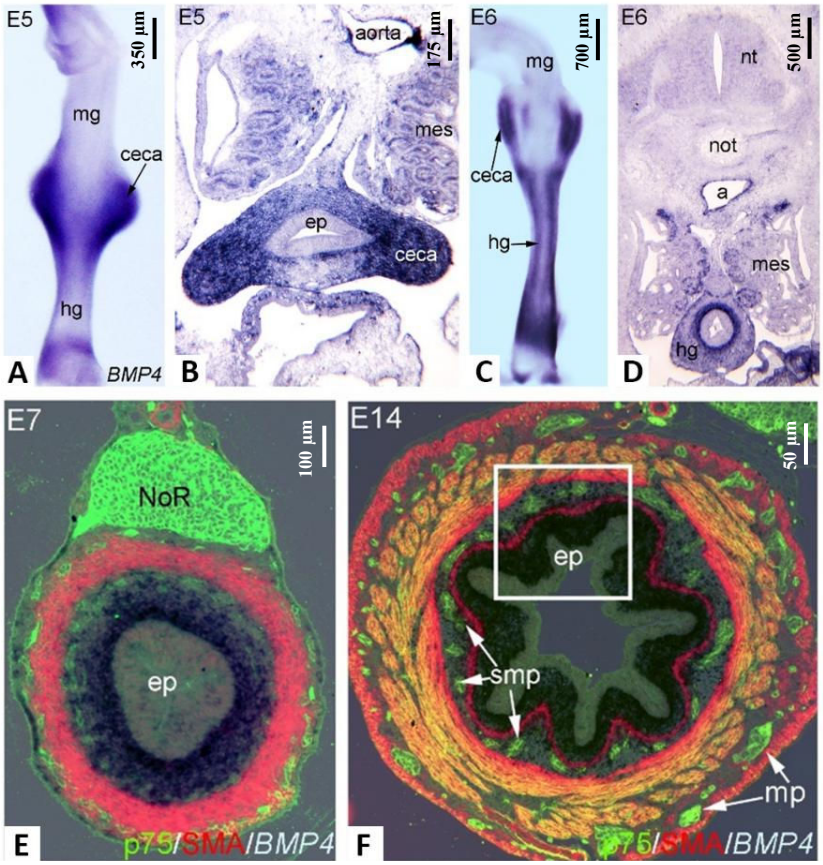

Figure 16. Expression of BMP4 during hindgut development. *In situ* hybridization of the wholemount tissues and sections of an E5 gut shows BMP4 expression primarily in the ceca (A,B). From E6 through E14, BMP4 is expressed in the inner mesenchyme, but not by $p75^{+}$ ENCDCs. *a, aorta; ep, epithelium; hg, hindgut; lp, lamina propria; mes, mesonephros; mg, midgut; mp, myenteric plexus; NoR, nerve of Remak; nt, neural tube; not, notochord; smp, submucosal plexus.*

in the hindgut mesenchyme emerged only at E6 **(Figure 16D)**. Transverse sections showed BMP4 transcripts localized specifically within the mesenchyme, adjacent to the hindgut epithelium **(Figure 16D,E)**. In contrast, BMP4 was absent from the midgut mesenchyme at both E5 and E6 **(Figure 16A,C)**. By E14, BMP4 expression became confined to the prospective lamina propria, without co-localization with p75$^+$ ENCDCs **(183)** or SMA$^+$ smooth muscle cells in the intestine **(Figure 16F)**.

The expression of BMPR2 was examined using in situ hybridization at multiple developmental stages **(Figure 17A,B)**. Since BMPR2 alone does not bind BMP2, BMP4, or BMP7 with high affinity unless co-expressed with a type I BMP receptor, we verified functional BMP signaling at the same stages using an antibody that recognizes the phosphorylated (active) form of SMAD1, 5, and 8 **(Figure 17C,D)**. At E6, the nerve of Remak also showed positive BMPR2 expression **(Figure 17A,B)**. Co-expression of BMPR2 mRNA and the p75 protein in ENCDCs of the E8 hindgut was demonstrated by

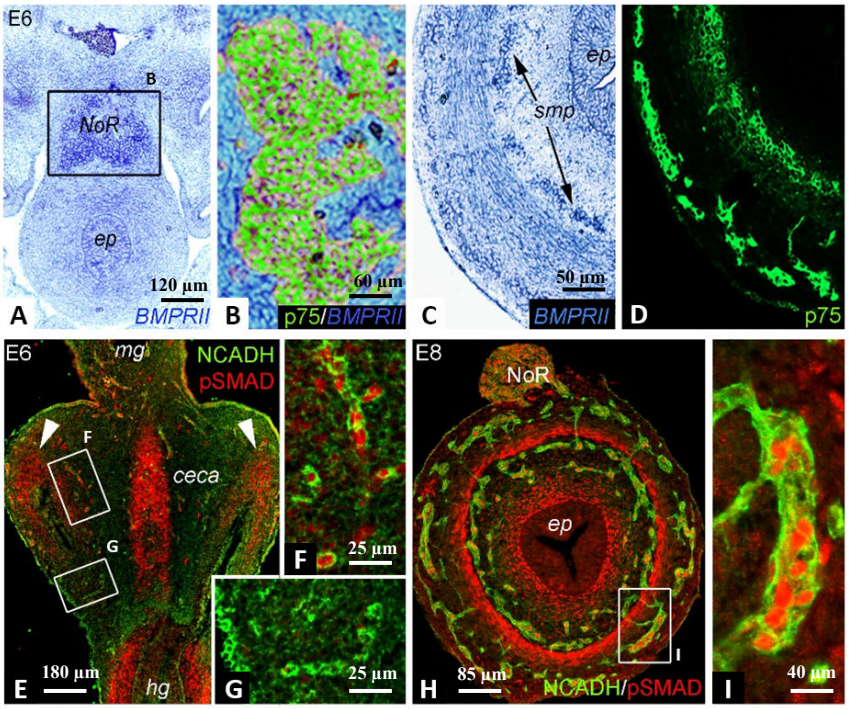

Figure 17. Expression of BMPRII and phospho-SMADs during hindgut development. *In situ* hybridization of an E6 gut shows BMPRII expression concentrated in p75$^+$ ENCDCs (A-D). In addition, functional BMP activity was confirmed at the same stages with an anti-pSMAD antibody (E-I), recognizing the active, phosphorylated form of Smad 1,5 and 8 in the ceca mesenchyme (arrowheads in E) with subsequent expression in NCADH$^+$ nerve of Remak (H), enteric ganglia (H,I), inner layer of the muscularis propria, and subepithelial mesenchyme (H). Interestingly, pSMAD expression is not present in the NCADH$^+$ wavefront of ENCDCs (G). *ep, epithelium; hg, hindgut; mg, midgut; NoR, nerve of Remak; smp, submucosal plexus.*

double labeling **(Figure 17C,D)**. To further confirm active BMP signaling in ENCDCs, immunostaining for phosphorylated SMAD (pSMAD) and N-cadherin was performed on longitudinal sections of the E6 hindgut. pSMAD protein was detected in the cecal mesenchyme at E6 **(Figure 17E)**. Interestingly, pSMAD expression was absent in N-cadherin^{+} ENCDCs at the migratory wavefront **(Figure 17E,G)**. However, by E8, when the wavefront had reached the distal hindgut, enteric ganglia began to express pSMADs, indicating activation of BMP signaling at later stages of ENS development **(Figure 17I)**.

The expression of BMPR2 and pSMAD was also confirmed in ex vivo cultures of E6 chick midguts, were GDNF (10 ng/mL) was added for 24h, leading to migration of ENCDCs onto the fibronectin-coated surface. BMPRII was broadly expressed by the ENCDCs **(Figure 18A-C)**, whereas pSMAD immunoreactivity was heterogeneous **(Figure 18D-F)**, confirming that ENCDCs possess the ability to respond to BMP signaling.

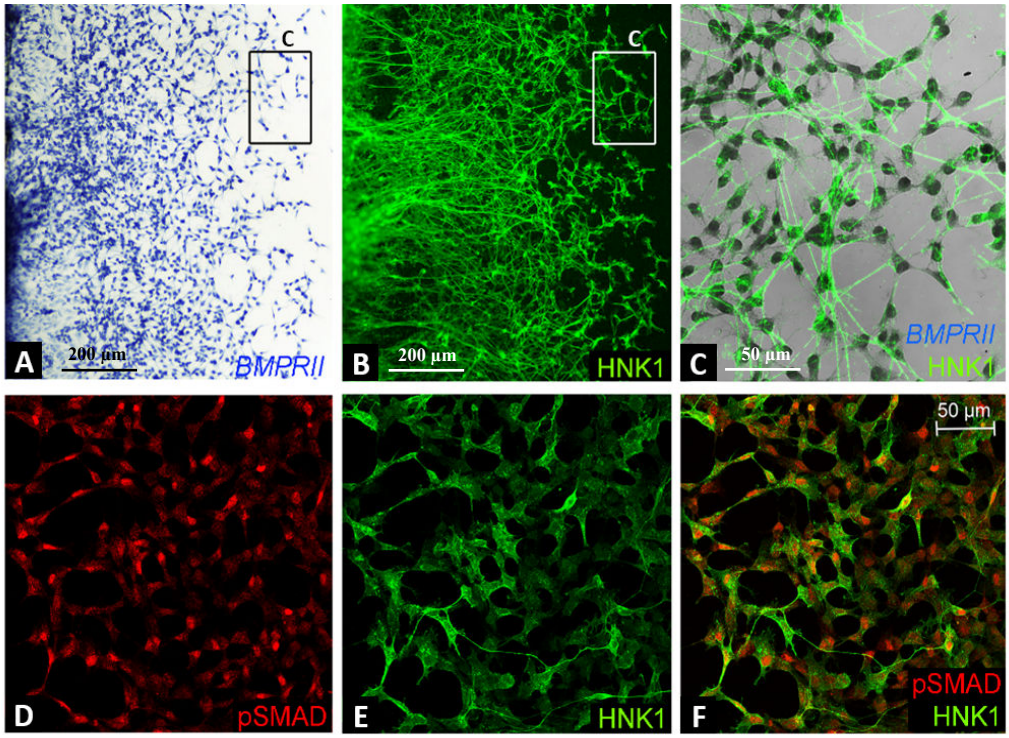

Figure 18. Explanted E6 chick midgut was cultured with GDNF, which promotes significant ENCDC migration from the intestinal tissue. Both BMPRII (A,C) and pSMAD (D,F) are highly expressed by the migratory HNK1^{+} ENCDCs.

4.2.2.2. Blocking of BMP4 signaling results in hindgut hypoganglionosis

Based on our findings that the E6 cecal mesenchyme expresses BMP4, while the hindgut at this stage lacks both ENCDCs and BMP4 expression, we hypothesized that cecal BMP4 is essential for proper hindgut colonization. To test this, E6 intestines were cultured in a catenary setup for 2 days in the presence or absence of recombinant BMP4 or Noggin proteins **(Figure 19A–C)**. Tuj1 antibody was used to label neurons, and SOX10 to identify all enteric neural crest-derived cells (ENCDCs) and early enteric glial cells **(183)**. Culturing E6 intestines in control DMEM medium (no supplement) resulted in complete colonization of the hindgut. Tuj1^{+} neurons were detected in both enteric plexuses throughout the entire length of the hindgut **(Figure 19A)**. In contrast, BMP4-treated gut segments showed Tuj1^{+} neurons clustered in large aggregates, suggesting that BMP4 promotes hyperganglionosis and accelerates early ganglion formation **(Figure 19B)**. Noggin treatment led to the formation of smaller ganglia **(Figure 19C)**.

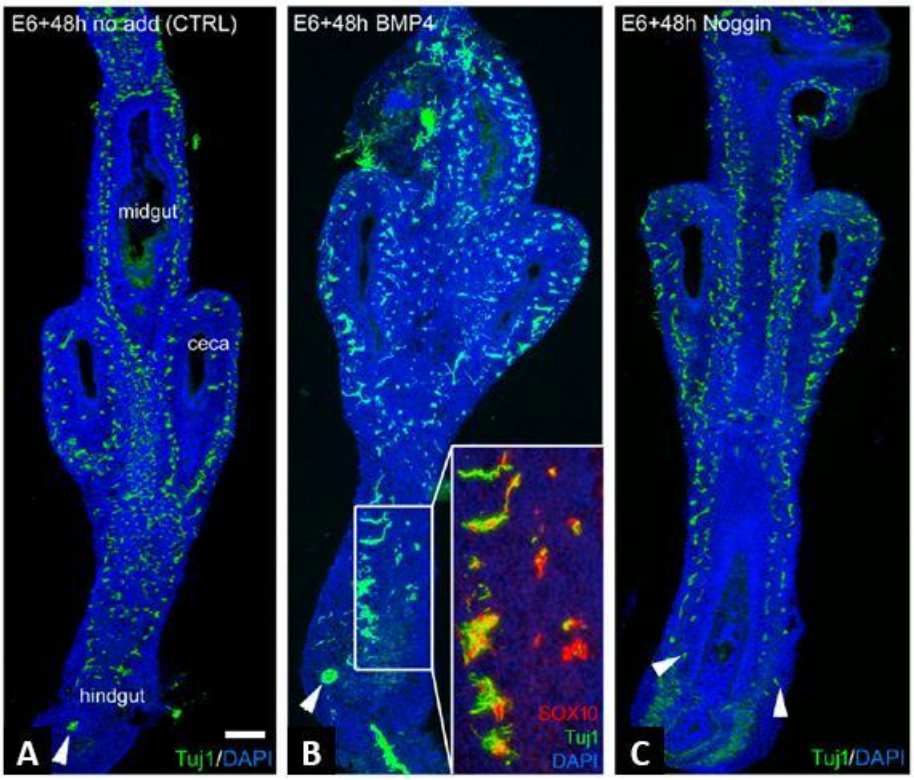

Figure 19. BMP4 signaling is required for hindgut colonization. E6 chick gut was cultured in the catenary culture for 2 days in the absence of additives (A) with BMP4 protein (B), or with Noggin protein (C), and their longitudinal sections are shown. Arrowheads indicate wavefront cells. Addition of BMP4 induced large ganglion formation in the hindgut (see (B) and inset in (B)), whereas inhibition of BMP4 signaling with Noggin led to small ganglia formation (C). Cells in the ganglion expressed neuronal markers Tuj1 and SOX10, which label ENCDCs and enteric glial cells (B). Scale bar represents 350 μm.

To determine whether BMP4 promotes glial differentiation in addition to premature ganglion formation, double immunofluorescence staining was performed using the enteric neuron-specific anti-HU antibody (ELAV-like protein 4) and the enteric glia-specific anti-BFABP antibody (brain fatty acid binding protein; FABP7). After a two-day culture of E6 intestines without additives, BFABP$^+$ cells were detected dispersed throughout the nerve of Remak and enteric plexuses. Consistent with the presence of hyperganglionosis, BFABP$^+$ glial cells were distributed throughout the intestine in large ganglia **(Figure 14B)**. This finding supports the conclusion that BMP4 promotes enteric glial differentiation, as most cells in the nerve of Remak expressed BFABP, aligning with previous reports on the role of BMPs in glial fate determination **(211)**. In contrast, Noggin-treated explants exhibited hindgut hypoganglionosis, characterized by a reduced number of Tuj1$^+$ neurons **(Figure 19C)**. Additionally, Remak cells in these cultures did not express BFABP, suggesting that BMP inhibition suppresses glial differentiation.

Quantification of enteric ganglion size and hindgut colonization length under different treatment conditions revealed statistically significant differences **(Figure 20A-C)**. Notably, Noggin treatment accelerated ENCDC colonization of the hindgut **(Figure 20A)**. Ganglion size differed significantly between control and BMP4-treated intestines ($p < 0.01$), and even more so between BMP4- and Noggin-treated samples ($p < 0.001$). However, no significant difference in ganglion diameter was found between control and Noggin-treated intestines **(Figure 20B)**. The opposing effects of BMP4 and Noggin on ganglion formation may reflect differences in ENCDC proliferation. To investigate this, we assessed proliferation by quantifying EdU

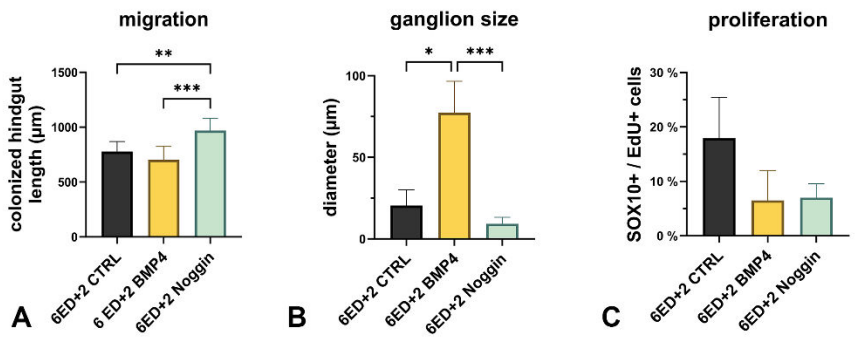

Figure 20. Transverse sections of the catenary cultured guts through the mid-hindgut were used for quantification. The length of colonized hindgut segment (A) from the ceca by SOX10$^+$ ENCDCs and enteric glial cells and the average diameter of the SOX10$^+$/Tuj1$^+$ enteric ganglia (B) and ENCDC proliferation (C) were compared among treatment groups. Kruskal-Wallis with Dunn's multiple comparison test was used for statistical analysis. For migration n=7 guts were measured, for ganglion size measurement and proliferation 3 different areas were quantified / treatment group. *** $p < 0.001$, ** $p < 0.01$, * $p < 0.05$.

incorporation in SOX10$^+$ cells exposed to BMP4 or Noggin. In control cultures, EdU$^+$ cells constituted 20.9% of SOX10$^+$ cells, primarily in the mesenchyme **(Figure 20C)**. Both treatments showed a trend toward reduced ENCDC proliferation, suggesting that a delicate balance and spatial regulation of BMP signaling is essential for normal ENCDC proliferation and ENS development. To assess macroscopic gut features, we measured hindgut length (from the ileocecal junction to the distal end) and hindgut diameter (in the mid-region) in each group (n = 12). The average length of BMP4-treated hindguts (877.3 µm ± 80.23 µm) was significantly shorter ($p < 0.001$) compared to both the control (1240 µm ± 100.8 µm) and Noggin-treated (1344 µm ± 81.29 µm) groups. However, no significant differences were observed in hindgut diameter among the groups (data not shown).

4.2.2.3. The overexpression of BMP4 via retrovirus leads to extensive gangliogenesis

Using a replication-competent retrovirus (RCAS), which expressed the chicken BMP4, we further dissected the effect of BMP signaling on the hindgut ENS development (**Figure 21**). The RCAS virus was administered into the E6 chicken hindgut mesenchyme. Subsequently, the gut segments were cultured on an E8 chick chorioallantoic membrane (CAM) for a duration of 9 days (**Figure 21A**). Avian retroviruses replicate particularly in the mesenchymal cells, and they do not affect ENCDCs **(205,208)**. The 3C2 antibody targeting the RCAS P19 gag protein demonstrated effective and widespread viral replication within the intestinal wall (**Figure 21F,G**). BMP4 overexpression resulted in considerable enteric hypoganglionosis, characterized by extensive and disordered ganglia within the gut wall, coupled with the absence of the characteristic organization into myenteric and submucosal plexuses (**Figure 21H,I**). The architecture of the smooth muscle was similarly disrupted (**Figure 21J**), exhibiting no distinct differentiation into the three muscle layers (muscularis mucosae, circular muscle, longitudinal muscle) typically observed (**Figure 21E**).

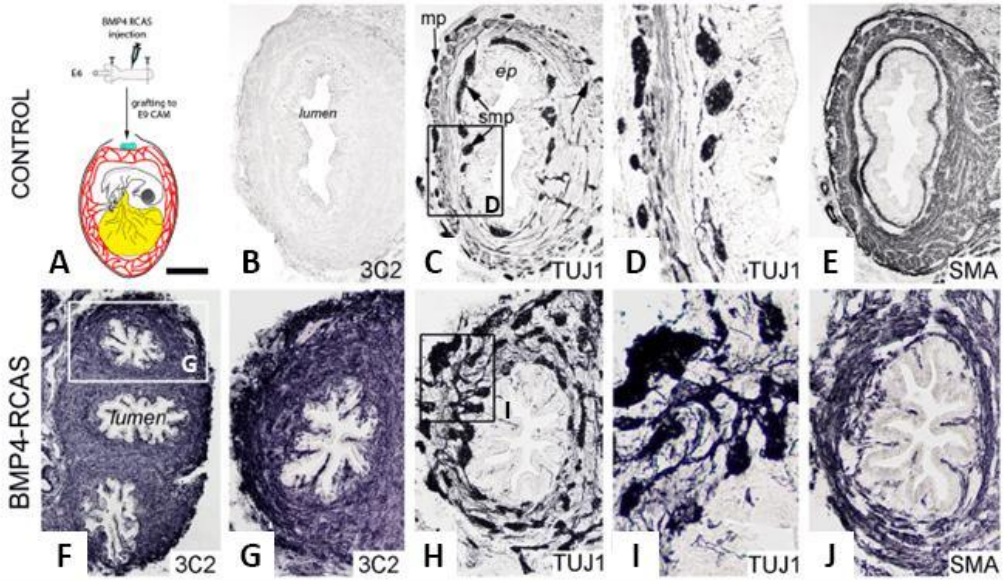

Figure 21. Overexpression of BMP4 via retroviral transduction promotes enteric gangliogenesis *in vivo*. To examine the effects of BMP4 on hindgut enteric nervous system (ENS) development in vivo, a replication-competent retrovirus (RCAS) encoding the chicken BMP4 gene was injected into the hindgut mesenchyme of E6 chick embryos, followed by culture on the chorioallantoic membrane (CAM) for 9 days (A). Viral infection and replication were confirmed by immunostaining with the 3C2 antibody, which detects the RCAS p19 gag protein, revealing widespread viral expression throughout the intestinal wall in RCAS-BMP4-treated samples (F, G) compared to controls (B). RCAS-BMP4 treatment induced marked enteric hyperganglionosis, as evidenced by large, disorganized ganglia spread throughout the gut wall (I vs. D), and a loss of the distinct organization of myenteric and submucosal plexuses typically observed in control intestines (H vs. C). Additionally, the morphology of the smooth muscle layers was disrupted in RCAS-BMP4-infected guts (J vs. E), further supporting a broad impact of BMP4 overexpression on gut structure and ENS organization. The scale bar is on the figure: 250 µm (B,C,E,J), 80 µm (D), 560 µm (F), 280 µm (G,H), 140 µm (I). *ep, epithelium; mp, myenteric plexus; smp, submucosal plexus.*

4.2.2.4. GDNF suppresses the aggregation of ENCDC induced by BMP4.

In congenital neurointestinal pathogenesis the role of GDNF signaling is well known. Just prior to the arrival of the ENCDCs to the midgut-hindgut boundary, just like BMP4, its expression is spatially and temporally limited to the cecal region. To test whether these factors have a combined effect on ENCDCs during their journey through the ceca, we explanted E6 ceca and cultured with BMP4 in the absence (**Figure 22**) or presence of GDNF (**Figure 23**). ENCDCs demonstrated substantial migration from cecal explants after 48 hours of culture in response to GDNF. A significant proportion of ENCDCs presented the neuronal marker Tuj1 (**Figure 22E**). Upon the removal of GDNF from the culture media during the initial 24 hours and its substitution with a culture media

devoid of additives, cell migration during the subsequent 24 hours was markedly diminished (**Figure 22B,I**). Furthermore, ENCDCs joined into an organized network of interlinked ganglia (**Figure 22F**). Upon substituting GDNF containing media after 24 hours with either an additional BMP4 **(Figure 22C,G)** or Noggin **(Figures 23D,H)** containing ones for an additional 24-hour duration, significant alterations were noted. The BMP4 treatment produced substantial ENCDC aggregates exhibiting significant Tuj1 expression (**Figure 22G,K**) and drastically lowered ENCDC proliferation (**Figure 22J**). Noggin inhibited normal ganglion formation and interfered with the establishment of interganglionic connections (**Figure 22D,H**). On the migration and proliferation of ENCDCs (**Figure 22I**) (**Figure 22J)** Noggin had no substantial effect but significantly reduced the rate of neuronal differentiation (**Figure 22H,K**).

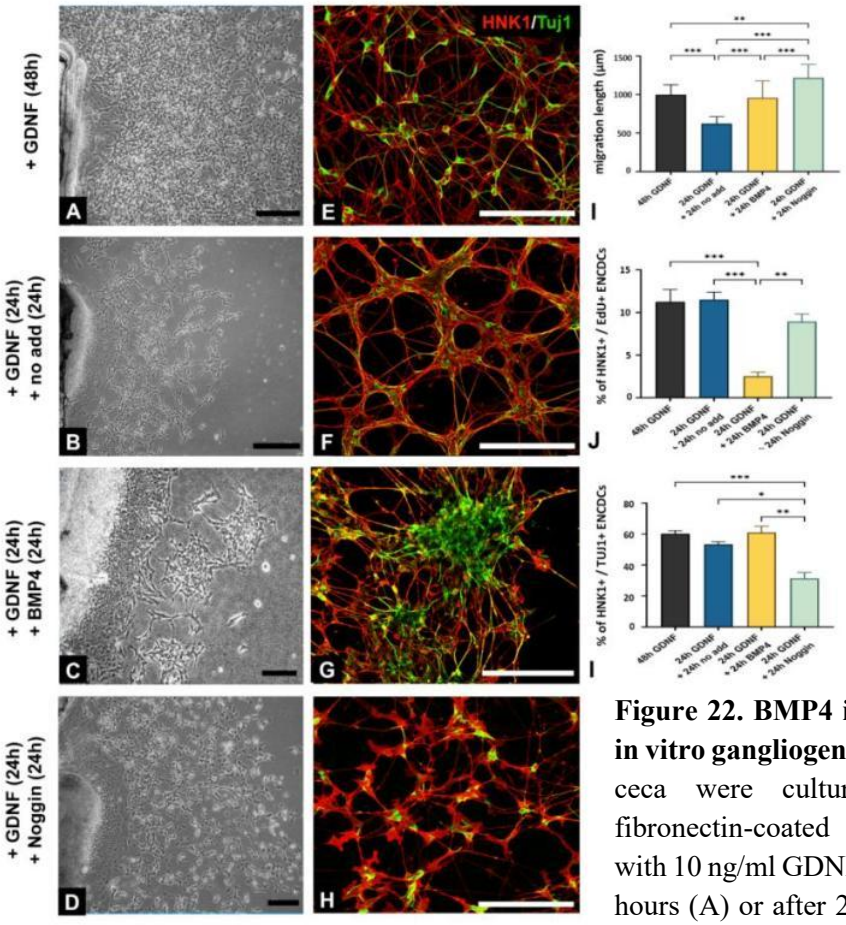

Figure 22. BMP4 induces in vitro gangliogenesis. E6 ceca were cultured on fibronectin-coated surface with 10 ng/ml GDNF for 48 hours (A) or after 24 hours the GDNF was removed and followed by 24 hours with either no added factors (B) or additional 200 ng/ml BMP4 (C) and 200 ng/ml Noggin (D) recombinant protein. There is no difference in percentage of $Tuj1^{+}/HNK1^{+}$ cells between 48h-GDNF or 24h-GDNF + 24h-no-additive groups. Excess of BMP4 not induced significant neuronal differentiation of ENCDCs, but initiated their aggregation. In contrast, the presence of Noggin markedly reduced the neuronal differentiation and inhibited the aggregation. All scale bars represent 200 µm. n = 7-10 cell cultures/experiment. Kruskal-Wallis with Dunn's multiple comparison test was used for statistical analysis. *** $p < 0.001$, ** $p < 0.01$,* $p < 0.05$.

Ultimately, we assessed the effect of BMP4 treatment in combination with GDNF on cecal explants **(Figure 23)**. When both BMP4 and GDNF were present in the culture medium, no cell aggregates form **(Figure 23B, D)**. These findings suggest that BMP4 directly reduces ENCDC proliferation and promotes their aggregation into ganglia. However, this effect is counteracted by GDNF in the cecal mesenchyme, which prevents premature ganglion formation and allows the ENCDC wavefront to migrate into the hindgut.

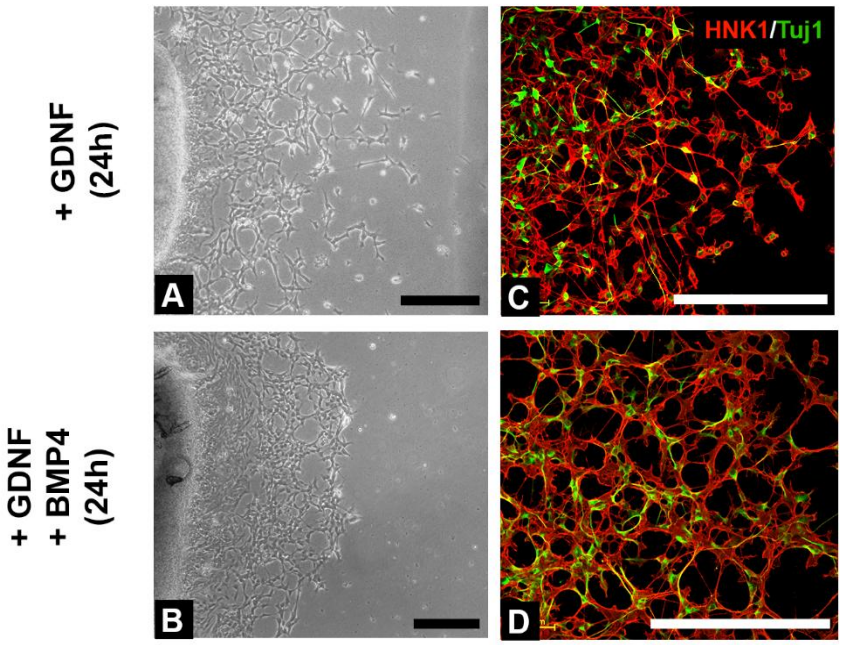

Figure 23. The co-administration of GDNF and BMP4 blocks the ganglion-inducing effect of BMP4. E6 ceca were cultured on fibronectin-coated surface with GDNF for 24 hours (A) or GDNF+BMP4 (B) for 24 hours. Cell cultures were immunostained with HNK1 and Tuj1 antibodies (A',B') to evaluate ganglion formation. The migration of ENCDCs from E6 ceca mediated by GDNF was substantial at 24 hours, as evidenced by the distance of cell migration depicted (A). No marking difference was observed between the GDNF and GDNF+BMP4 treated groups; however, the concurrent administration of GDNF and BMP4 impeded the aggregation of $Tuj1^{+}/HNK1^{+}$ cells. All-scale bars represent 200 µm.

5. Discussion

Over the past few decades, extensive data have been generated on the morphology and function of the ENS, but relatively little is known about the embryonic development and etiology of congenital neurointestinal diseases. Among the developmental disorders affecting the ENS, intestinal neuronal dysplasia associated with hypoganglionosis or hyperganglionosis and HSCR with aganglionosis are the most common congenital disorders. The only current treatment option for HSCR is the surgical resection of the gut segment. There is an emerging need from clinicians to develop a novel stem cell transplantation-based treatment as an alternative therapy in the future. Our results on enteric neural crest-derived cells (ENCDCs) could contribute to the better understanding of the normal and pathological ENS development, ultimately supporting the ENCDC propagation and preparation for transplantation to reinnervate the aganglionic segment.

The avian ceca are a pair of blind-ended sacs that emerge at the junction of the ileum and colon. They exhibit a wide range of morphological types across bird species – from nearly absent structures to small lymphoid or large glandular forms **(250)**. In adult birds, the ceca serve various physiological functions, including fermentation, water and electrolyte absorption, digestion and immune defense. These roles highly depend on the species and on cecal morphology. In herbivorous birds that consume fiber-rich plant material, the ceca contain a microbiome that helps in fiber breakdown through anaerobic fermentation, producing ammonia and volatile fatty acids **(251,252)**. Water balance is another critical function, as sodium and water are extensively reabsorbed in the ceca **(253,254)**. Additionally, many species possess a cecal tonsil composed of organized lymphoid tissue, indicating an important role in mucosal immunity. This region contains myeloid cells, T-, and B lymphocytes, plasma cells producing immunoglobulins (IgA, IgY and IgM) and germinal centers **(255,256)**. The ceca also function as a microbial "safe compartment", maintaining beneficial bacteria that can re-colonize the gut following illnesses such as diarrhea **(257,258)**. Interestingly, there is a strong correlation between the relative length of the cecum and colon across bird species **(259)**; however, no definitive evolutionary or developmental explanation has yet been established for this relationship.

Besides all the earlier known functions of ceca described in the adult animals, we have described another important function of the ceca in the development of the hindgut ENS, along with the finding that hindgut ENCDCs originate exclusively from the cecal buds, rather than the intercecal region. Our findings indicate that the typical caudal migration of vagal crest-derived ENCDCs does not only advance as a wave through the midgut-hindgut junction. Cells migrating into the mesenchyme between the paired ceca are blocked, whereas those entering the cecal buds undergo proliferation and continue their caudal migration. Moreover, ENCDC proliferation at the migratory wavefront peaks when the wavefront is located in the cecal buds. Although previous studies have shown increased ENCDC proliferation at the migration wavefront **(260,261)**, our findings demonstrate that this proliferation specifically increased in the cecal buds, suggesting that migrating cells receive localized mitogenic signals in this region to optimize their numbers for effective hindgut colonization.

5.1. Ceca-specific non-canonical WNT11 signaling balances ENCDC migration and differentiation in the developing hindgut

HSCR arises from inadequate colonization of the distal intestine by migrating ENCDCs. In over 90% of cases, aganglionosis is restricted to the distal colorectum, suggesting that this terminal segment of the gut presents unique developmental challenges for the ENS. Emerging evidence indicates that abnormalities at the cecal region may by responsible for the pathogenesis of HSCR. Our avian embryo-manipulation results show that surgical removal of the cecal buds prior to ENCDC arrival disrupts cell migration into the proximal hindgut, leaving the distal segment aganglionic. Rather than simply stopping, ENCDCs aggregate into large clusters of $TUJ1^{+}$/$nNOS^{+}$ differentiated neurons. This observation suggests that signals normally present in the ceca inhibit premature neuronal differentiation, thereby preserving ENCDCs in a progenitor state to support continues migration into the distal colorectum.

Motivated by these findings, we performed comparative transcriptomic analysis of the cecal buds, and the intercecal mesenchymal region at the critical time of wavefront arrival. This revealed significant differences in gene expression, including the activation of genes related to ENCDC migration and neurogenesis in the cecal buds. Notably, *Gdnf* was highly expressed in the ceca, while gene encoding its cognate receptor *Ret* was

upregulated in the intercecal region. We also observed increased expression of genes encoding non-canonical Wnt signaling molecules, particularly *Wnt11* and *Wnt5a*, in the ceca mesenchyme. These findings support the hypothesis that non-canonical WNT11 growth factor, besides known morphogens such as GDNF and EDN3 **(88,176)**, functions to delay neuronal differentiation and maintain a pool of migratory progenitors for hindgut colonization.

Members of the Wnt protein family are known to play diverse roles in neural crest biology, including migration, proliferation, differentiation, and survival **(262)**, and are essential regulators of gut development **(263,264)**. Canonical Wnt/β-catenin signaling is critical for neural crest induction, while non-canonical Wnt signaling, which is β-catenin dependent, controls neural crest migration by promoting lamellipodia and filopodia formation necessary for delamination and directed cell movement (265–268). WNT11, acting through its transmembrane FZD7 receptor, is essential for early neural crest migration – its inhibition disrupts this process, while intracellular activation of non-canonical Wnt signaling can rescue the phenotype **(269)**. Downstream effectors such as ROCK1/2 kinases **(270)**, particularly ROCK2 **(271)**, play a key role in mediating WNT11-induced migratory behavior by regulating cell shape and motility through the RhoA-ROCK pathway **(272)**.

Although WNT11 is not directly chemoattractive to ENCDCs, it supports their responsiveness to the pro-migratory effects of GDNF. WNT11 is also required for maintaining *Gdnf* expression in the kidney **(273,274)**, essential for uretric branching. Moreover, *Wnt11* transcription itself stimulated by GDNF-RET signaling **(275)**, suggesting a potential positive feedback loop between WNT11 and GDNF that could also be present in the ceca. Wnt signaling is similarly implicated in EDNRB-mediated regulation of melanocyte stem cell proliferation and differentiation **(276)**, indicating a complex interaction between Wnt, GDNF/RET, and EDN3/EDNRB pathways during ENS development.

Surprisingly, we found that WNT11 exerts an anti-mitogenic effect on ENCDCs, despite the high proliferation rates observed in the ceca where WNT11 is expressed. This seeming contradiction suggests a fine balance between WNT11-mediated suppression of premature ENCDC differentiation and the proliferative effects of GDNF and EDN3, which together synergistically maintain an optimal progenitor pool for successful

colonization of the distal gut. Further molecular and *in vitro* studies are needed to clarify how these signaling pathways act in complex and are coordinated during ENS development.

5.2. BMP4 promotes enteric gangliogenesis following GDNF dependent ENCDC migration in the ceca

We also observed a notable increase in the BMP signaling pathway components in the cecal transcriptome, particularly the BMP4. A multitude of data substantiates the concept that BMP4 – akin to GDNF and EDN3, produced by cecal mesenchymal cells – plays a critical role in the development of the hindgut ENS. Nevertheless, investigations utilizing diverse *in vivo* and *in vitro* experiments across multiple model organisms have yielded inconsistent findings regarding BMP4's exact function **(201–203,209,249,277)**. BMP4 and its receptors (BMPRI, BMPRII) have been documented during both mammalian **(202,209)** and avian **(203,205)** ENS development. Previous results suggest that BMP signaling components are expressed throughout the mesenchyme of the developing chicken gut, with the exception of the stomach and hindgut **(228,234)**. More recent data show that BMP2, BMP4, and BMP7 are symmetrically expressed in the E12 chicken midgut and mesentery **(204)**.

Moreover, BMP signaling has also been implicated in regulating intestinal villus morphogenesis, smooth muscle differentiation, and gut looping **(204,278,279)**. During ENS formation, BMP components guide ENCDC migration **(203,205,209)** and their differentiation into neurons and glial cells **(202,213)**, partly by regulating gene expression patterns essential for enteric ganglia formation and organization. For instance, Smad-interacting protein 1 (SIP1 or ZEB2) – a negative regulator of BMP4 signaling **(215)** – is involved in neural crest specification, migration, and differentiation **(216)** and mutations in ZEB2 are associated with HSCR **(164,217,218)**.

Although involvement of the BMP4 in ENS development is well-established, its specific role in hindgut colonization has remained unclear. To investigate this question, we used RCAS retrovirus-mediated overexpression of BMP4 in the pre-colonized hindgut mesenchyme, subsequently cultured on CAM surface. This resulted in ectopic and robust enteric ganglia formation. These findings agree with previous BMP inhibition experiments, in which Noggin overexpression in early chicken embryos led to

hypoganglionosis and impaired ENS formation **(203)**. Our organotypic and *in vitro* cultures further confirmed that disrupting BMP4 signaling yields various ENS phenotypes, including hypoganglionosis and impaired neuronal/glial differentiation. However, when the BMP4 inhibitor recombinant Noggin protein was applied to intestinal exolants, ENCDC migration was enhanced, but ganglion formation was impaired, leading to ectopic distribution of enteric neurons – recapitulating the results obtained from mouse embryo models **(209)**. Misexpression of Noggin in early chick embryos caused delayed ENCDC migration and smaller ganglia **(203)**, consistent with earlier studies showing that BMP4 inhibition at the neural tube blocks neural crest emigration **(9)** and thus depletes ENCDC pool.

The varying effects observed between early RCAS-Noggin injection and later recombinant Noggin protein treatment likely reflect differences in delivery methods and timing. To directly assess role of BMP4 in ENCDC development, we added GDNF to the pre-colonized E6 cecal explants, facilitating ENCDC migration onto a fibronectin-caoted surface. As reported in embryonic mouse gut, BMP4 alone did not promote ENCDC migration **(280)**, but recombinant Noggin inhibited ENCDC aggregation *in vitro,* as previously described **(202)**. Conversely, BMP4 promoted aggregation in our explant system, mimicking the phenotype of RCAS-BMP4-infected hindguts. Interestingly, simultaneous application of BMP4 and GDNF growth factors before migration started, prevented ENCDC aggregation. This suggests that expression of GDNF in the ceca may temporarily override the aggregation-inducing effects of the BMP4, thereby maintaining a migratory ENCDC population for hindgut colonization.

Although the ceca will eventually develop enteric ganglia, our findings suggest that ENCDCs deplete local GDNF levels as they migrate. During this developmental window, pSMADs are not detected in wavefront ENCDCs, indicating that BMP signaling is inactive and ganglion formation is suppressed to maintain migratory capacity. Once GNDF levels decline, BMP4 can act on the trailing ENCDC population, promoting aggregation and initiating neuronal differentiation (**Figure 24**).

5.3. Cecal regulation of ENCDCs: a model of progenitor expansion and migration via balanced BMP4, GDNF, and WNT11 signaling

Our data implies that the cecal buds in the avian embryonic intestine function as a staging area where ENCDC proliferation is supported, while differentiation is prevented in order to increase the number of undifferentiated progenitors available to migrate to the hindgut. (**Figure 24**). Interestingly, a study in mice did not find an increased rate of cecal ENCDC proliferation **(281)**. Considering that the hindgut represents the most distant location for vagal crest-derived ENCDCs to colonize during migration, each species may have individually evolved to the challenges this imposes on ENS growth. In avians, our findings indicate that the cecal buds are utilized as an optimal location to instruct the incoming ENCDCs to proliferate, maintain a non-differentiated state, and proceed with their craniocaudal migration into the colorectum.

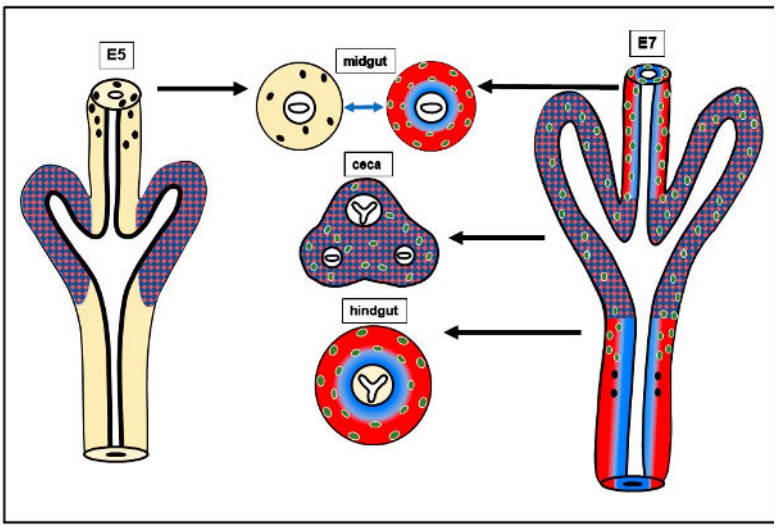

Figure 24. Model of hindgut ENCDC colonization and the roles of BMP4, GDNF, and WNT11 growth factors. Model of hindgut colonization by ENCDCs highlights the specific roles of BMP4, GDNF, and WNT11 signaling in the ceca mesenchyme. BMP4 (blue colour) reduces ENCDC proliferation, promotes differentiation, and induces premature gangliogenesis, while GDNF (red) stimulates ENCDC proliferation, migration, and differentiation. Both signals are expressed in the ceca mesenchyme just before ENCDCs arrive, suggesting that their overlapping local activity regulates the migratory wavefront. We propose that the co-expression of BMP4 and GDNF is essential for hindgut ENS formation: GDNF counteracts the gangliogenic effect of BMP4 in the cecum, allowing wavefront cells to remain undifferentiated and continue migrating into the hindgut. Once past the ceca, ENCDCs enter a BMP4-free, GDNF-rich outer mesenchyme, where they differentiate and form enteric ganglia in the colorectum. WNT11, similarly restricted to the ceca, also inhibits premature neuronal differentiation, further ensuring that ENCDCs remain migratory and prevent early aggregation into ganglia-like clusters. This coordinated signaling mechanism ensures that a sufficient pool of undifferentiated progenitors reaches the distal gut to complete the ENS. Undifferentiated ENCDCs and wavefront cells are shown as black dots, differentiated ENS cells in green, mesenchymal compartment coloured in yellow, while GDNF expression in red, and BMP4 expression in blue.

5.4. Future perspectives

Current research is intensively focused on both stem cell therapy to replace absent neurons and glia in the aganglionic segment, and possible treatments to stimulate the transdifferentiation of endogenous enteric glial cells into enteric neurons. Enteric neural stem cells (ENSCs) can be extracted from the gut wall of both children **(282–284)** and adults **(285)**, specifically from the small intestine and colon **(286)**, via mucosal and full-thickness biopsies **(287)**. These ENSCs possess self-renewal capabilities, demonstrate elevated neurogenesis rates in vitro, and proliferate in culture to create clusters of concentrated neural stem cells known as neurospheres **(284,285,288)**.

In animal models, enteric neurospheres can be transplanted into the colon using laparotomy, a peri-anal route, or endoscopic injection in mice **(289)** and swine **(65)**. After transplantation, ENSCs engraft and differentiate into functional neurons and glial cells **(290)**. Embryonic ENSCs have also demonstrated successful engraftment in aganglionic embryonic gut explants and contributed to the regulation of tissue contractility **(283)**. Despite these promising outcomes, most postnatal transplantation studies have been limited by inadequate engraftment, migration, and proliferation of donor cells **(16,291,292)**.

Ongoing research is focused on optimizing the efficacy of ENSC-based therapies. Strategies include co-transplanting cells with bioactive molecules encapsulated in liposomal nanoparticles **(293)**, genetically modifying donor cells using viral vectors **(294)**, and enriching culture conditions with specific growth factors **(286)**. For example, co-delivery of ENSCs with nanoparticles containing 5-hydroxytryptamine type 4 (5-HT4) receptor agonists significantly enhanced neuronal density and proliferation *in vivo* **(293)**. Similarly, transduction of donor cells with a lentivirus that reduced the expression of agrin – a heparan sulfate proteoglycan – improved cell migration in both gut explants and *in vivo* **(295)**. Additionally, GDNF treatment enhances the neurogenic potential of neurospheres *in vitro* **(286,296)**.

Based on our findings, testing the effects of BMP4 and WNT11 supplementation during neurosphere preparation could further enhance regenerative potential prior to transplantation. Supporting this, when human embryonic stem cell-derived neural crest progenitors were directly transplanted into the ceca of *Ednrb*-/- mice, the cells colonized the entire colon and improved survival rates, though without a corresponding

improvement in gut motility. The mechanism behind this enhanced survival remain unclear **(297)**, but these results further emphasize the functional significance of the ceca and support the relevance of our findings for translational applications.

Future studies could benefit from a more detailed characterization of cecal mesenchyme-derived signals using advanced techniques such as spatial transcriptomics, multiplexed RNAscope labeling, or CRISPR-based conditional gene silencing. However, these approaches are either unavailable or not yet optimized for avian model systems. Single-cell RNA sequencing (scRNA-seq) has only recently been applied to ENS **(298)**. In the mouse embryo, FZD3 (a Wnt receptor) and Sfrp1 (a secreted Wnt inhibitor) are robustly expressed at the ENCDC wavefront; this expression is disrupted in *Ednrb* mutant mice and HSCR patient samples **(299)**. It has been proposed that defective WNT/FZD3 signaling in HSCR leads to premature ENCDC differentiation, thereby compromising their ability to colonize the distal gut and resulting in aganglionosis – a mechanism that aligns with our observations.

Moreover, recent transcriptomic comparisons between control and HSCR patient samples revealed significant downregulation of BMP-modulating genes in endothelial cells within the aganglionic segment. In addition, germline mutations in *BMPR1* and missense variants in *BMP4* have been identified in multiple HSCR patients, highlighting the crucial role of BMP signaling in ENS development **(300)**.

6. Conclusions

Using avian embryo-surgery and molecular analyses, we demonstrate that the cecal buds in the avian gut act as a critical staging area for enteric neural crest-derived cells (ENCDCs). In this intestinal mesenchyme environment, ENCDC proliferation is promoted, while differentiation is inhibited, thereby maximizing the pool of undifferentiated progenitors available for hindgut colonization.

We have identified several cecal-derived growth factors that create a unique niche for the expansion of the undifferentiated ENCDCs and supporting their craniocaudal migration into the colorectum. Specifically, we characterized the expression and developmental biology roles of BMP4, WNT5A, and WNT11 in the developing avian hindgut, demonstrating their regulatory roles in ENCDC proliferation, migration, and differentiation, during development of the colorectum ENS.

Our findings significantly contribute to understanding the key signaling pathways controlling ENCDC migration and differentiation, which are disrupted in enteric neurocristopathies, such as Hirschsprung disease. By integrating classical embryology and developmental biology methods as well as molecular biology studies, this research may contribute to new regenerative medicine approaches, leading to the development of more targeted, effective stem cell-based therapies.

7. Summary

The enteric nervous system (ENS), originating from enteric neural crest-derived cells (ENCDCs), forms the complex neuronal innervation of the gastrointestinal tract. Disruption of ENCDC migration can result in Hirschsprung disease, characterized by the absence of enteric ganglia in the distal colorectum. We observed that ENCDC proliferation is specifically high during their migration throughout the ceca, a paired structure of the avian intestine at the midgut-hindgut junction level. Microsurgical ablation of the ceca leads to hindgut aganglionosis, highlighting their essential role in colorectal ENS development. Comparative transcriptomic analysis revealed that non-canonical Wnt signaling, especially WNT11, is highly expressed in the ceca mesenchyme. RNA *in situ* hybridization confirmed the ceca mesenchyme-specific expression of the WNT11 gene. Addition of recombinant WNT11 protein in organ culture experiments showed to inhibit enteric neuronal differentiation, suggesting a role in maintaining ENCDCs in the undifferentiated progenitor state. Furthermore, transcriptomic profiling also identified bone morphogenetic proteins (BMPs) as critical regulators. In situ hybridization revealed strong BMP4 expression in the cecal mesenchyme, suggesting a critical role for cecal-derived BMP4 in hindgut ENS formation. To investigate this, we modulated BMP4 activity using embryonic intestinal organ culture and retroviral-mediated gene manipulation. Both overexpression and inhibition of BMP4 in the ceca disrupted hindgut ENS development, indicating that precise regulation of BMP4 is necessary. Our findings demonstrate that BMP, non-canonical WNT and GDNF signaling pathways are essential for normal ENCDC migration and enteric ganglia formation in the hindgut. This study identifies novel molecular players in avian hindgut ENS development and provides new insights into the regulation of ENCDC proliferation, migration, and differentiation.

8. References

1. Schneider S, Wright CM, Heuckeroth RO. Unexpected Roles for the Second Brain: Enteric Nervous System as Master Regulator of Bowel Function. Annu Rev Physiol. 2019;81:235–259. doi: 10.1146/annurev-physiol-021317-121515. Cited: in: : PMID: 30379617.

2. Furness JB. Types of neurons in the enteric nervous system. J Auton Nerv Syst. 2000;81:87–96. doi: 10.1016/s0165-1838(00)00127-2. Cited: in: : PMID: 10869706.

3. Gershon MD, Erde SM. The nervous system of the gut. Gastroenterology. 1981;80:1571–1594. Cited: in: : PMID: 6112192.

4. Timmermans JP, Hens J, Adriaensen D. Outer submucous plexus: an intrinsic nerve network involved in both secretory and motility processes in the intestine of large mammals and humans. Anat Rec. 2001;262:71–78. doi: 10.1002/1097-0185(20010101)262:1<71::AID-AR1012>3.0.CO;2-A. Cited: in: : PMID: 11146430.

5. Dora D, Arciero E, Hotta R, Barad C, Bhave S, Kovacs T, Balic A, Goldstein AM, Nagy N. Intraganglionic macrophages: a new population of cells in the enteric ganglia. J Anat. 2018;233:401–410. doi: 10.1111/joa.12863. Cited: in: : PMID: 30022489.

6. Dora D, Ferenczi S, Stavely R, Toth VE, Varga ZV, Kovacs T, Bodi I, Hotta R, Kovacs KJ, Goldstein AM, et al. Evidence of a Myenteric Plexus Barrier and Its Macrophage-Dependent Degradation During Murine Colitis: Implications in Enteric Neuroinflammation. Cell Mol Gastroenterol Hepatol. 2021;12:1617–1641. doi: 10.1016/j.jcmgh.2021.07.003. Cited: in: : PMID: 34246810.

7. Gershon MD. The enteric nervous system: a second brain. Hosp Pract 1995. 1999;34:31–32, 35–38, 41-42 passim. doi: 10.3810/hp.1999.07.153. Cited: in: : PMID: 10418549.

8. Liem KF, Tremml G, Roelink H, Jessell TM. Dorsal differentiation of neural plate cells induced by BMP-mediated signals from epidermal ectoderm. Cell. 1995;82:969–979. doi: 10.1016/0092-8674(95)90276-7. Cited: in: : PMID: 7553857.

9. Sela-Donenfeld D, Kalcheim C. Regulation of the onset of neural crest migration by coordinated activity of BMP4 and Noggin in the dorsal neural tube. Dev Camb Engl. 1999;126:4749–4762. doi: 10.1242/dev.126.21.4749. Cited: in: : PMID: 10518492.

10. Burstyn-Cohen T, Stanleigh J, Sela-Donenfeld D, Kalcheim C. Canonical Wnt activity regulates trunk neural crest delamination linking BMP/noggin signaling with G1/S transition. Dev Camb Engl. 2004;131:5327–5339. doi: 10.1242/dev.01424. Cited: in: : PMID: 15456730.

11. Yntema CL, Hammond WS. The origin of intrinsic ganglia of trunk viscera from vagal neural crest in the chick embryo. J Comp Neurol. 1954;101:515–541. doi: 10.1002/cne.901010212. Cited: in: : PMID: 13221667.

12. Le Douarin NM, Teillet MA. The migration of neural crest cells to the wall of the digestive tract in avian embryo. J Embryol Exp Morphol. 1973;30:31–48. Cited: in: : PMID: 4729950.

13. Stoller JZ, Epstein JA. Cardiac neural crest. Semin Cell Dev Biol. 2005;16:704–715. doi: 10.1016/j.semcdb.2005.06.004. Cited: in: : PMID: 16054405.

14. Porras D, Brown CB. Temporal-spatial ablation of neural crest in the mouse results in cardiovascular defects. Dev Dyn Off Publ Am Assoc Anat. 2008;237:153–162. doi: 10.1002/dvdy.21382. Cited: in: : PMID: 18058916.

15. Kuo BR, Erickson CA. Regional differences in neural crest morphogenesis. Cell Adhes Migr. 2010;4:567–585. doi: 10.4161/cam.4.4.12890. Cited: in: : PMID: 20962585.

16. Nagy N, Goldstein AM. Enteric nervous system development: A crest cell's journey from neural tube to colon. Semin Cell Dev Biol. 2017;66:94–106. doi: 10.1016/j.semcdb.2017.01.006. Cited: in: : PMID: 28087321.

17. Espinosa-Medina I, Jevans B, Boismoreau F, Chettouh Z, Enomoto H, Müller T, Birchmeier C, Burns AJ, Brunet J-F. Dual origin of enteric neurons in vagal Schwann cell precursors and the sympathetic neural crest. Proc Natl Acad Sci U S A. 2017;114:11980–11985. doi: 10.1073/pnas.1710308114. Cited: in: : PMID: 29078343.

18. Burns AJ, Champeval D, Le Douarin NM. Sacral neural crest cells colonise aganglionic hindgut in vivo but fail to compensate for lack of enteric ganglia. Dev Biol. 2000;219:30–43. doi: 10.1006/dbio.1999.9592. Cited: in: : PMID: 10677253.

19. Catala M, Teillet MA, Le Douarin NM. Organization and development of the tail bud analyzed with the quail-chick chimaera system. Mech Dev. 1995;51:51–65. doi: 10.1016/0925-4773(95)00350-a. Cited: in: : PMID: 7669693.

20. Pomeranz HD, Gershon MD. Colonization of the avian hindgut by cells derived from the sacral neural crest. Dev Biol. 1990;137:378–394. doi: 10.1016/0012-1606(90)90262-h. Cited: in: : PMID: 2406176.

21. Burns AJ, Douarin NML. The sacral neural crest contributes neurons and glia to the post-umbilical gut: spatiotemporal analysis of the development of the enteric nervous system. Development. 1998;125:4335–4347. doi: 10.1242/dev.125.21.4335.

22. Pomeranz HD, Rothman TP, Gershon MD. Colonization of the post-umbilical bowel by cells derived from the sacral neural crest: direct tracing of cell migration using an intercalating probe and a replication-deficient retrovirus. Dev Camb Engl. 1991;111:647–655. doi: 10.1242/dev.111.3.647. Cited: in: : PMID: 1879333.

23. Erickson CA, Goins TL. Sacral neural crest cell migration to the gut is dependent upon the migratory environment and not cell-autonomous migratory properties. Dev Biol. 2000;219:79–97. doi: 10.1006/dbio.1999.9597. Cited: in: : PMID: 10677257.

24. Nagy N, Brewer KC, Mwizerwa O, Goldstein AM. Pelvic plexus contributes ganglion cells to the hindgut enteric nervous system. Dev Dyn Off Publ Am Assoc Anat. 2007;236:73–83. doi: 10.1002/dvdy.20933. Cited: in: : PMID: 16937371.

25. Halasy V, Szőcs E, Soós Á, Kovács T, Pecsenye-Fejszák N, Hotta R, Goldstein AM, Nagy N. CXCR4 and CXCL12 signaling regulates the development of extrinsic innervation to the colorectum. Dev Camb Engl. 2023;150:dev201289. doi: 10.1242/dev.201289. Cited: in: : PMID: 37039233.

26. Yu Q, Liu L, Du M, Müller D, Gu Y, Gao Z, Xin X, Gu Y, He M, Marquardt T, et al. Sacral Neural Crest-Independent Origin of the Enteric Nervous System in Mouse. Gastroenterology. 2024;166:1085–1099. doi: 10.1053/j.gastro.2024.02.034. Cited: in: : PMID: 38452824.

27. Serbedzija GN, Burgan S, Fraser SE, Bronner-Fraser M. Vital dye labelling demonstrates a sacral neural crest contribution to the enteric nervous system of chick and mouse embryos. Dev Camb Engl. 1991;111:857–866. doi: 10.1242/dev.111.4.857. Cited: in: : PMID: 1879357.

28. Young HM, Hearn CJ, Ciampoli D, Southwell BR, Brunet JF, Newgreen DF. A single rostrocaudal colonization of the rodent intestine by enteric neuron precursors is revealed by the expression of Phox2b, Ret, and p75 and by explants grown under the kidney capsule or in organ culture. Dev Biol. 1998;202:67–84. doi: 10.1006/dbio.1998.8987. Cited: in: : PMID: 9758704.

29. Kapur RP. Colonization of the murine hindgut by sacral crest-derived neural precursors: experimental support for an evolutionarily conserved model. Dev Biol. 2000;227:146–155. doi: 10.1006/dbio.2000.9886. Cited: in: : PMID: 11076683.

30. Uesaka T, Nagashimada M, Enomoto H. Neuronal Differentiation in Schwann Cell Lineage Underlies Postnatal Neurogenesis in the Enteric Nervous System. J Neurosci Off J Soc Neurosci. 2015;35:9879–9888. doi: 10.1523/JNEUROSCI.1239-15.2015. Cited: in: : PMID: 26156989.

31. Nishiyama C, Uesaka T, Manabe T, Yonekura Y, Nagasawa T, Newgreen DF, Young HM, Enomoto H. Trans-mesenteric neural crest cells are the principal source of the colonic enteric nervous system. Nat Neurosci. 2012;15:1211–1218. doi: 10.1038/nn.3184. Cited: in: : PMID: 22902718.

32. Rothstein M, Bhattacharya D, Simoes-Costa M. The molecular basis of neural crest axial identity. Dev Biol. 2018;444 Suppl 1:S170–S180. doi: 10.1016/j.ydbio.2018.07.026. Cited: in: : PMID: 30071217.

33. Gershon MD, Chalazonitis A, Rothman TP. From neural crest to bowel: development of the enteric nervous system. J Neurobiol. 1993;24:199–214. doi: 10.1002/neu.480240207. Cited: in: : PMID: 8445388.

34. Erickson CS, Lee SJ, Barlow-Anacker AJ, Druckenbrod NR, Epstein ML, Gosain A. Appearance of cholinergic myenteric neurons during enteric nervous system development: comparison of different ChAT fluorescent mouse reporter lines.

Neurogastroenterol Motil. 2014;26:874–884. doi: 10.1111/nmo.12343. Cited: in: : PMID: 24712519.

35. Kang Y-N, Fung C, Vanden Berghe P. Gut innervation and enteric nervous system development: a spatial, temporal and molecular tour de force. Dev Camb Engl. 2021;148:dev182543. doi: 10.1242/dev.182543. Cited: in: : PMID: 33558316.

36. Goldstein AM, Hofstra RMW, Burns AJ. Building a brain in the gut: development of the enteric nervous system. Clin Genet. 2013;83:307–316. doi: 10.1111/cge.12054. Cited: in: : PMID: 23167617.

37. Laddach A, Chng SH, Lasrado R, Progatzky F, Shapiro M, Erickson A, Sampedro Castaneda M, Artemov AV, Bon-Frauches AC, Amaniti E-M, et al. A branching model of lineage differentiation underpinning the neurogenic potential of enteric glia. Nat Commun. 2023;14:5904. doi: 10.1038/s41467-023-41492-3. Cited: in: : PMID: 37737269.

38. Stavely R, Rahman AA, Mueller JL, Leavitt AR, Han CY, Pan W, Kaiser KN, Ott LC, Ohkura T, Guyer RA, et al. Mature enteric neurons have the capacity to reinnervate the intestine with glial cells as their guide. Neuron. 2024;112:3143-3160.e6. doi: 10.1016/j.neuron.2024.06.018. Cited: in: : PMID: 39019043.

39. Allan IJ, Newgreen DF. The origin and differentiation of enteric neurons of the intestine of the fowl embryo. Am J Anat. 1980;157:137–154. doi: 10.1002/aja.1001570203.

40. Conner PJ, Focke PJ, Noden DM, Epstein ML. Appearance of neurons and glia with respect to the wavefront during colonization of the avian gut by neural crest cells. Dev Dyn Off Publ Am Assoc Anat. 2003;226:91–98. doi: 10.1002/dvdy.10219. Cited: in: : PMID: 12508228.

41. Nagy N, Mwizerwa O, Yaniv K, Carmel L, Pieretti-Vanmarcke R, Weinstein BM, Goldstein AM. Endothelial cells promote migration and proliferation of enteric neural crest cells via beta1 integrin signaling. Dev Biol. 2009;330:263–272. doi: 10.1016/j.ydbio.2009.03.025. Cited: in: : PMID: 19345201.

42. McKeown SJ, Chow CW, Young HM. Development of the submucous plexus in the large intestine of the mouse. Cell Tissue Res. 2001;303:301–305. doi: 10.1007/s004410000303. Cited: in: : PMID: 11291776.

43. Uesaka T, Nagashimada M, Enomoto H. GDNF signaling levels control migration and neuronal differentiation of enteric ganglion precursors. J Neurosci Off J Soc Neurosci. 2013;33:16372–16382. doi: 10.1523/JNEUROSCI.2079-13.2013. Cited: in: : PMID: 24107967.

44. Rolle U, Nemeth L, Puri P. Nitrergic innervation of the normal gut and in motility disorders of childhood. J Pediatr Surg. 2002;37:551–567. doi: 10.1053/jpsu.2002.31610. Cited: in: : PMID: 11912511.

45. Bolande RP. The neurocristopathies: A unifying concept of disease arising in neural crest maldevelopment. Hum Pathol. 1974;5:409–429. doi: 10.1016/S0046-8177(74)80021-3.

46. Bolande RP. Neurocristopathy: its growth and development in 20 years. Pediatr Pathol Lab Med J Soc Pediatr Pathol Affil Int Paediatr Pathol Assoc. 1997;17:1–25. Cited: in: : PMID: 9050057.

47. Etchevers HC, Amiel J, Lyonnet S. Molecular bases of human neurocristopathies. Adv Exp Med Biol. 2006;589:213–234. doi: 10.1007/978-0-387-46954-6_14. Cited: in: : PMID: 17076285.

48. Burns AJ, Goldstein AM, Newgreen DF, Stamp L, Schäfer K-H, Metzger M, Hotta R, Young HM, Andrews PW, Thapar N, et al. White paper on guidelines concerning enteric nervous system stem cell therapy for enteric neuropathies. Dev Biol. 2016;417:229–251. doi: 10.1016/j.ydbio.2016.04.001. Cited: in: : PMID: 27059883.

49. Kapur RP. Developmental disorders of the enteric nervous system. Gut. 2000;47 Suppl 4:iv81-83; discussion iv87. doi: 10.1136/gut.47.suppl_4.iv81. Cited: in: : PMID: 11076927.

50. Ehrenpreis T. Hirschsprung's disease. Am J Dig Dis. 1971;16:1032–1052. doi: 10.1007/BF02235017. Cited: in: : PMID: 4942817.

51. Sergi C. Hirschsprung's disease: Historical notes and pathological diagnosis on the occasion of the 100(th) anniversary of Dr. Harald Hirschsprung's death. World J Clin Pediatr. 2015;4:120–125. doi: 10.5409/wjcp.v4.i4.120. Cited: in: : PMID: 26566484.

52. Leenders E, Sieber WK. Congenital megacolon observation by Frederick Ruysch--1691. J Pediatr Surg. 1970;5:1–3. doi: 10.1016/0022-3468(70)90512-9. Cited: in: : PMID: 4907731.

53. Ehrenpreis T. Megacolon in the newborn; a clinical and röntgenological study with special regard to the pathogenesis; a preliminary report. Acta Paediatr. 1945;32:358–370. Cited: in: : PMID: 21007848.

54. Whitehouse FR, Kernohan JW. Myenteric plexus in congenital megacolon; study of 11 cases. Arch Intern Med Chic Ill 1908. 1948;82:75–111. doi: 10.1001/archinte.1948.00220250085005. Cited: in: : PMID: 18110761.

55. Passarge E. The genetics of Hirschsprung's disease. Evidence for heterogeneous etiology and a study of sixty-three families. N Engl J Med. 1967;276:138–143. doi: 10.1056/NEJM196701192760303. Cited: in: : PMID: 4224912.

56. Romeo G, Ronchetto P, Luo Y, Barone V, Seri M, Ceccherini I, Pasini B, Bocciardi R, Lerone M, Kääriäinen H. Point mutations affecting the tyrosine kinase domain of the RET proto-oncogene in Hirschsprung's disease. Nature. 1994;367:377–378. doi: 10.1038/367377a0. Cited: in: : PMID: 8114938.

57. Iwashita T, Kruger GM, Pardal R, Kiel MJ, Morrison SJ. Hirschsprung disease is linked to defects in neural crest stem cell function. Science. 2003;301:972–976. doi: 10.1126/science.1085649. Cited: in: : PMID: 12920301.

58. Gershon MD. Neural crest development. Do developing enteric neurons need endothelins? Curr Biol CB. 1995;5:601–604. doi: 10.1016/s0960-9822(95)00120-5. Cited: in: : PMID: 7552166.

59. Kusafuka T, Wang Y, Puri P. Mutation analysis of the RET, the endothelin-B receptor, and the endothelin-3 genes in sporadic cases of Hirschsprung's disease. J Pediatr Surg. 1997;32:501–504. doi: 10.1016/s0022-3468(97)90616-3. Cited: in: : PMID: 9094028.

60. Gui H, Schriemer D, Cheng WW, Chauhan RK, Antiňolo G, Berrios C, Bleda M, Brooks AS, Brouwer RWW, Burns AJ, et al. Whole exome sequencing coupled with unbiased functional analysis reveals new Hirschsprung disease genes. Genome Biol. 2017;18:48. doi: 10.1186/s13059-017-1174-6. Cited: in: : PMID: 28274275.

61. Stavely R, Hotta R, Guyer RA, Picard N, Rahman AA, Omer M, Soos A, Szocs E, Mueller J, Goldstein AM, et al. A distinct transcriptome characterizes neural crest-derived cells at the migratory wavefront during enteric nervous system development. Dev Camb Engl. 2023;150:dev201090. doi: 10.1242/dev.201090. Cited: in: : PMID: 36779913.

62. Yang Q, Wang F, Wang Z, Guo J, Chang T, Dalielihan B, Yang G, Lei C, Dang R. mRNA sequencing provides new insights into the pathogenesis of Hirschsprung's disease in mice. Pediatr Surg Int. 2023;39:268. doi: 10.1007/s00383-023-05544-5. Cited: in: : PMID: 37676292.

63. Ziogas IA, Kuruvilla KP, Fu M, Gosain A. Hirschsprung-associated enterocolitis: a comprehensive review. World J Pediatr Surg. 2024;7:e000878. doi: 10.1136/wjps-2024-000878. Cited: in: : PMID: 39410939.

64. Rahman AA, Ohkura T, Bhave S, Pan W, Ohishi K, Ott L, Han C, Leavitt A, Stavely R, Burns AJ, et al. Enteric neural stem cell transplant restores gut motility in mice with Hirschsprung disease. JCI Insight. 2024;9:e179755. doi: 10.1172/jci.insight.179755. Cited: in: : PMID: 39042470.

65. Hotta R, Pan W, Bhave S, Nagy N, Stavely R, Ohkura T, Krishnan K, de Couto G, Myers R, Rodriguez-Borlado L, et al. Isolation, Expansion, and Endoscopic Delivery of Autologous Enteric Neuronal Stem Cells in Swine. Cell Transplant. 2023;32:9636897231215233. doi: 10.1177/09636897231215233. Cited: in: : PMID: 38049927.

66. Kapur RP. Histology of the Transition Zone in Hirschsprung Disease. Am J Surg Pathol. 2016;40:1637–1646. doi: 10.1097/PAS.0000000000000711. Cited: in: : PMID: 27526297.

67. Best KE, Addor M-C, Arriola L, Balku E, Barisic I, Bianchi F, Calzolari E, Curran R, Doray B, Draper E, et al. Hirschsprung's disease prevalence in Europe: a register based study. Birt Defects Res A Clin Mol Teratol. 2014;100:695–702. doi: 10.1002/bdra.23269. Cited: in: : PMID: 25066220.

68. Russell MB, Russell CA, Niebuhr E. An epidemiological study of Hirschsprung's disease and additional anomalies. Acta Paediatr Oslo Nor 1992. 1994;83:68–71. doi: 10.1111/j.1651-2227.1994.tb12955.x. Cited: in: : PMID: 8193476.

69. Suita S, Taguchi T, Ieiri S, Nakatsuji T. Hirschsprung's disease in Japan: analysis of 3852 patients based on a nationwide survey in 30 years. J Pediatr Surg. 2005;40:197–201; discussion 201-202. doi: 10.1016/j.jpedsurg.2004.09.052. Cited: in: : PMID: 15868585.

70. Suita S, Taguchi T, Kamimura T, Yanai K. Total colonic aganglionosis with or without small bowel involvement: a changing profile. J Pediatr Surg. 1997;32:1537–1541. doi: 10.1016/s0022-3468(97)90446-2. Cited: in: : PMID: 9396519.

71. Nakamura H, Henderson D, Puri P. A meta-analysis of clinical outcome of intestinal transplantation in patients with total intestinal aganglionosis. Pediatr Surg Int. 2017;33:837–841. doi: 10.1007/s00383-017-4107-2. Cited: in: : PMID: 28600659.

72. Sharif K, Beath SV, Kelly DA, McKiernan P, van Mourik I, Mirza D, Mayer AD, Buckels J a. C, de Ville de Goyet J. New perspective for the management of near-total or total intestinal aganglionosis in infants. J Pediatr Surg. 2003;38:25–28; discussion 25-28. doi: 10.1053/jpsu.2003.50004. Cited: in: : PMID: 12592613.

73. Ryan ET, Ecker JL, Christakis NA, Folkman J. Hirschsprung's disease: associated abnormalities and demography. J Pediatr Surg. 1992;27:76–81. doi: 10.1016/0022-3468(92)90111-j. Cited: in: : PMID: 1552451.

74. Ikeda K, Goto S. Diagnosis and treatment of Hirschsprung's disease in Japan. An analysis of 1628 patients. Ann Surg. 1984;199:400–405. doi: 10.1097/00000658-198404000-00005. Cited: in: : PMID: 6712314.

75. Wallace AS, Burns AJ. Development of the enteric nervous system, smooth muscle and interstitial cells of Cajal in the human gastrointestinal tract. Cell Tissue Res. 2005;319:367–382. doi: 10.1007/s00441-004-1023-2. Cited: in: : PMID: 15672264.

76. Parisi MA, Kapur RP. Genetics of Hirschsprung disease. Curr Opin Pediatr. 2000;12:610–617. doi: 10.1097/00008480-200012000-00017. Cited: in: : PMID: 11106284.

77. Passarge E. Dissecting Hirschsprung disease. Nat Genet. 2002;31:11–12. doi: 10.1038/ng878. Cited: in: : PMID: 11953748.

78. Gariepy CE. Developmental disorders of the enteric nervous system: genetic and molecular bases. J Pediatr Gastroenterol Nutr. 2004;39:5–11. doi: 10.1097/00005176-200407000-00003. Cited: in: : PMID: 15187773.

79. Amiel J, Sproat-Emison E, Garcia-Barcelo M, Lantieri F, Burzynski G, Borrego S, Pelet A, Arnold S, Miao X, Griseri P, et al. Hirschsprung disease, associated syndromes and genetics: a review. J Med Genet. 2008;45:1–14. doi: 10.1136/jmg.2007.053959. Cited: in: : PMID: 17965226.

80. Heuckeroth RO, Schäfer K-H. Gene-environment interactions and the enteric nervous system: Neural plasticity and Hirschsprung disease prevention. Dev Biol. 2016;417:188–197. doi: 10.1016/j.ydbio.2016.03.017. Cited: in: : PMID: 26997034.

81. Amiel J, Lyonnet S. Hirschsprung disease, associated syndromes, and genetics: a review. J Med Genet. 2001;38:729–739. doi: 10.1136/jmg.38.11.729. Cited: in: : PMID: 11694544.

82. Wartiovaara K, Salo M, Sariola H. Hirschsprung's disease genes and the development of the enteric nervous system. Ann Med. 1998;30:66–74. doi: 10.3109/07853899808999386. Cited: in: : PMID: 9556091.

83. Chalazonitis A, Rothman TP, Chen J, Gershon MD. Age-dependent differences in the effects of GDNF and NT-3 on the development of neurons and glia from neural crest-derived precursors immunoselected from the fetal rat gut: expression of GFRalpha-1 in vitro and in vivo. Dev Biol. 1998;204:385–406. doi: 10.1006/dbio.1998.9090. Cited: in: : PMID: 9882478.

84. Hearn CJ, Murphy M, Newgreen D. GDNF and ET-3 differentially modulate the numbers of avian enteric neural crest cells and enteric neurons in vitro. Dev Biol. 1998;197:93–105. doi: 10.1006/dbio.1998.8876. Cited: in: : PMID: 9578621.

85. Heuckeroth RO, Lampe PA, Johnson EM, Milbrandt J. Neurturin and GDNF promote proliferation and survival of enteric neuron and glial progenitors in vitro. Dev Biol. 1998;200:116–129. doi: 10.1006/dbio.1998.8955. Cited: in: : PMID: 9698461.

86. Taraviras S, Marcos-Gutierrez CV, Durbec P, Jani H, Grigoriou M, Sukumaran M, Wang L-C, Hynes M, Raisman G, Pachnis V. Signalling by the RET receptor tyrosine kinase and its role in the development of the mammalian enteric nervous system. Development. 1999;126:2785–2797. doi: 10.1242/dev.126.12.2785.

87. Barlow A, de Graaff E, Pachnis V. Enteric nervous system progenitors are coordinately controlled by the G protein-coupled receptor EDNRB and the receptor tyrosine kinase RET. Neuron. 2003;40:905–916. doi: 10.1016/s0896-6273(03)00730-x. Cited: in: : PMID: 14659090.

88. Mwizerwa O, Das P, Nagy N, Akbareian SE, Mably JD, Goldstein AM. Gdnf is mitogenic, neurotrophic, and chemoattractive to enteric neural crest cells in the embryonic colon. Dev Dyn Off Publ Am Assoc Anat. 2011;240:1402–1411. doi: 10.1002/dvdy.22630. Cited: in: : PMID: 21465624.

89. Mason I. The RET receptor tyrosine kinase: activation, signalling and significance in neural development and disease. Pharm Acta Helv. 2000;74:261–264. doi: 10.1016/s0031-6865(99)00048-5. Cited: in: : PMID: 10812967.

90. Pattyn A, Morin X, Cremer H, Goridis C, Brunet JF. The homeobox gene Phox2b is essential for the development of autonomic neural crest derivatives. Nature. 1999;399:366–370. doi: 10.1038/20700. Cited: in: : PMID: 10360575.

91. Hellmich HL, Kos L, Cho ES, Mahon KA, Zimmer A. Embryonic expression of glial cell-line derived neurotrophic factor (GDNF) suggests multiple developmental roles in neural differentiation and epithelial-mesenchymal interactions. Mech Dev. 1996;54:95–105. doi: 10.1016/0925-4773(95)00464-5. Cited: in: : PMID: 8808409.

92. Worley DS, Pisano JM, Choi ED, Walus L, Hession CA, Cate RL, Sanicola M, Birren SJ. Developmental regulation of GDNF response and receptor expression in the enteric nervous system. Dev Camb Engl. 2000;127:4383–4393. doi: 10.1242/dev.127.20.4383. Cited: in: : PMID: 11003838.

93. Focke PJ, Schiltz CA, Jones SE, Watters JJ, Epstein ML. Enteric neuroblasts require the phosphatidylinositol 3-kinase pathway for GDNF-stimulated proliferation. J Neurobiol. 2001;47:306–317. doi: 10.1002/neu.1037. Cited: in: : PMID: 11351341.

94. Young HM, Hearn CJ, Farlie PG, Canty AJ, Thomas PQ, Newgreen DF. GDNF Is a Chemoattractant for Enteric Neural Cells. Dev Biol. 2001;229:503–516. doi: 10.1006/dbio.2000.0100.

95. Takahashi M, Buma Y, Iwamoto T, Inaguma Y, Ikeda H, Hiai H. Cloning and expression of the ret proto-oncogene encoding a tyrosine kinase with two potential transmembrane domains. Oncogene. 1988;3:571–578. Cited: in: : PMID: 3078962.

96. Uesaka T, Jain S, Yonemura S, Uchiyama Y, Milbrandt J, Enomoto H. Conditional ablation of GFRalpha1 in postmigratory enteric neurons triggers unconventional neuronal death in the colon and causes a Hirschsprung's disease phenotype. Dev Camb Engl. 2007;134:2171–2181. doi: 10.1242/dev.001388. Cited: in: : PMID: 17507417.

97. Pichel JG, Shen L, Sheng HZ, Granholm AC, Drago J, Grinberg A, Lee EJ, Huang SP, Saarma M, Hoffer BJ, et al. Defects in enteric innervation and kidney development in mice lacking GDNF. Nature. 1996;382:73–76. doi: 10.1038/382073a0. Cited: in: : PMID: 8657307.

98. Sánchez MP, Silos-Santiago I, Frisén J, He B, Lira SA, Barbacid M. Renal agenesis and the absence of enteric neurons in mice lacking GDNF. Nature. 1996;382:70–73. doi: 10.1038/382070a0. Cited: in: : PMID: 8657306.

99. Kusafuka T, Puri P. Altered RET gene mRNA expression in Hirschsprung's disease. J Pediatr Surg. 1997;32:600–604. doi: 10.1016/s0022-3468(97)90716-8. Cited: in: : PMID: 9126763.

100. Edery P, Lyonnet S, Mulligan LM, Pelet A, Dow E, Abel L, Holder S, Nihoul-Fékété C, Ponder BA, Munnich A. Mutations of the RET proto-oncogene in Hirschsprung's disease. Nature. 1994;367:378–380. doi: 10.1038/367378a0. Cited: in: : PMID: 8114939.

101. Butler Tjaden NE, Trainor PA. The developmental etiology and pathogenesis of Hirschsprung disease. Transl Res J Lab Clin Med. 2013;162:1–15. doi: 10.1016/j.trsl.2013.03.001. Cited: in: : PMID: 23528997.

102. Martucciello G, Ceccherini I, Lerone M, Jasonni V. Pathogenesis of Hirschsprung's disease. J Pediatr Surg. 2000;35:1017–1025. doi: 10.1053/jpsu.2000.7763. Cited: in: : PMID: 10917288.

103. Uesaka T, Nagashimada M, Yonemura S, Enomoto H. Diminished Ret expression compromises neuronal survival in the colon and causes intestinal aganglionosis in mice. J Clin Invest. 2008;118:1890–1898. doi: 10.1172/JCI34425. Cited: in: : PMID: 18414682.

104. Cacalano G, Fariñas I, Wang LC, Hagler K, Forgie A, Moore M, Armanini M, Phillips H, Ryan AM, Reichardt LF, et al. GFRalpha1 is an essential receptor component for GDNF in the developing nervous system and kidney. Neuron. 1998;21:53–62. doi: 10.1016/s0896-6273(00)80514-0. Cited: in: : PMID: 9697851.

105. Enomoto H, Araki T, Jackman A, Heuckeroth RO, Snider WD, Johnson EM, Milbrandt J. GFR alpha1-deficient mice have deficits in the enteric nervous system and kidneys. Neuron. 1998;21:317–324. doi: 10.1016/s0896-6273(00)80541-3. Cited: in: : PMID: 9728913.

106. Moore MW, Klein RD, Fariñas I, Sauer H, Armanini M, Phillips H, Reichardt LF, Ryan AM, Carver-Moore K, Rosenthal A. Renal and neuronal abnormalities in mice lacking GDNF. Nature. 1996;382:76–79. doi: 10.1038/382076a0. Cited: in: : PMID: 8657308.

107. Schuchardt A, D'Agati V, Larsson-Blomberg L, Costantini F, Pachnis V. Defects in the kidney and enteric nervous system of mice lacking the tyrosine kinase receptor Ret. Nature. 1994;367:380–383. doi: 10.1038/367380a0. Cited: in: : PMID: 8114940.

108. Gianino S, Grider JR, Cresswell J, Enomoto H, Heuckeroth RO. GDNF availability determines enteric neuron number by controlling precursor proliferation. Dev Camb Engl. 2003;130:2187–2198. doi: 10.1242/dev.00433. Cited: in: : PMID: 12668632.

109. Shen L, Pichel JG, Mayeli T, Sariola H, Lu B, Westphal H. Gdnf haploinsufficiency causes Hirschsprung-like intestinal obstruction and early-onset lethality in mice. Am J Hum Genet. 2002;70:435–447. doi: 10.1086/338712. Cited: in: : PMID: 11774071.

110. Heuckeroth RO, Enomoto H, Grider JR, Golden JP, Hanke JA, Jackman A, Molliver DC, Bardgett ME, Snider WD, Johnson EM, et al. Gene targeting reveals a critical role for neurturin in the development and maintenance of enteric, sensory, and parasympathetic neurons. Neuron. 1999;22:253–263. doi: 10.1016/s0896-6273(00)81087-9. Cited: in: : PMID: 10069332.

111. Doray B, Salomon R, Amiel J, Pelet A, Touraine R, Billaud M, Attié T, Bachy B, Munnich A, Lyonnet S. Mutation of the RET ligand, neurturin, supports multigenic inheritance in Hirschsprung disease. Hum Mol Genet. 1998;7:1449–1452. doi: 10.1093/hmg/7.9.1449. Cited: in: : PMID: 9700200.

112. Baynash AG, Hosoda K, Giaid A, Richardson JA, Emoto N, Hammer RE, Yanagisawa M. Interaction of endothelin-3 with endothelin-B receptor is essential for development of epidermal melanocytes and enteric neurons. Cell. 1994;79:1277–1285. doi: 10.1016/0092-8674(94)90018-3. Cited: in: : PMID: 8001160.

113. Hosoda K, Hammer RE, Richardson JA, Baynash AG, Cheung JC, Giaid A, Yanagisawa M. Targeted and natural (piebald-lethal) mutations of endothelin-B receptor gene produce megacolon associated with spotted coat color in mice. Cell. 1994;79:1267–1276. doi: 10.1016/0092-8674(94)90017-5. Cited: in: : PMID: 8001159.

114. Leibl MA, Ota T, Woodward MN, Kenny SE, Lloyd DA, Vaillant CR, Edgar DH. Expression of endothelin 3 by mesenchymal cells of embryonic mouse caecum. Gut. 1999;44:246–252. doi: 10.1136/gut.44.2.246. Cited: in: : PMID: 9895385.

115. Lane PW. Association of megacolon with two recessive spotting genes in the mouse. J Hered. 1966;57:29–31. doi: 10.1093/oxfordjournals.jhered.a107457. Cited: in: : PMID: 5917257.

116. Amiel J, Attié T, Jan D, Pelet A, Edery P, Bidaud C, Lacombe D, Tam P, Simeoni J, Flori E, et al. Heterozygous endothelin receptor B (EDNRB) mutations in isolated Hirschsprung disease. Hum Mol Genet. 1996;5:355–357. doi: 10.1093/hmg/5.3.355. Cited: in: : PMID: 8852660.

117. Kusafuka T, Wang Y, Puri P. Novel mutations of the endothelin-B receptor gene in isolated patients with Hirschsprung's disease. Hum Mol Genet. 1996;5:347–349. doi: 10.1093/hmg/5.3.347. Cited: in: : PMID: 8852658.

118. Bidaud C, Salomon R, Van Camp G, Pelet A, Attié T, Eng C, Bonduelle M, Amiel J, Nihoul-Fékété C, Willems PJ, et al. Endothelin-3 gene mutations in isolated and syndromic Hirschsprung disease. Eur J Hum Genet EJHG. 1997;5:247–251. Cited: in: : PMID: 9359047.

119. Kusafuka T, Puri P. Mutations of the endothelin-B receptor and endothelin-3 genes in Hirschsprung's disease. Pediatr Surg Int. 1997;12:19–23. doi: 10.1007/BF01194795. Cited: in: : PMID: 9035203.

120. Oue T, Puri P. Altered endothelin-3 and endothelin-B receptor mRNA expression in Hirschsprung's disease. J Pediatr Surg. 1999;34:1257–1260. doi: 10.1016/s0022-3468(99)90163-x. Cited: in: : PMID: 10466607.

121. Abe Y, Sakurai T, Yamada T, Nakamura T, Yanagisawa M, Goto K. Functional analysis of five endothelin-B receptor mutations found in human Hirschsprung disease patients. Biochem Biophys Res Commun. 2000;275:524–531. doi: 10.1006/bbrc.2000.3291. Cited: in: : PMID: 10964697.

122. Gershon MD. Endothelin and the development of the enteric nervous system. Clin Exp Pharmacol Physiol. 1999;26:985–988. doi: 10.1046/j.1440-1681.1999.03176.x. Cited: in: : PMID: 10626067.

123. McCallion AS, Chakravarti A. EDNRB/EDN3 and Hirschsprung disease type II. Pigment Cell Res. 2001;14:161–169. doi: 10.1034/j.1600-0749.2001.140305.x. Cited: in: : PMID: 11434563.

124. Puffenberger EG, Hosoda K, Washington SS, Nakao K, deWit D, Yanagisawa M, Chakravart A. A missense mutation of the endothelin-B receptor gene in multigenic Hirschsprung's disease. Cell. 1994;79:1257–1266. doi: 10.1016/0092-8674(94)90016-7. Cited: in: : PMID: 8001158.

125. Edery P, Attié T, Amiel J, Pelet A, Eng C, Hofstra RM, Martelli H, Bidaud C, Munnich A, Lyonnet S. Mutation of the endothelin-3 gene in the Waardenburg-Hirschsprung disease (Shah-Waardenburg syndrome). Nat Genet. 1996;12:442–444. doi: 10.1038/ng0496-442. Cited: in: : PMID: 8630502.

126. Hofstra RM, Osinga J, Tan-Sindhunata G, Wu Y, Kamsteeg EJ, Stulp RP, van Ravenswaaij-Arts C, Majoor-Krakauer D, Angrist M, Chakravarti A, et al. A homozygous mutation in the endothelin-3 gene associated with a combined Waardenburg type 2 and Hirschsprung phenotype (Shah-Waardenburg syndrome). Nat Genet. 1996;12:445–447. doi: 10.1038/ng0496-445. Cited: in: : PMID: 8630503.

127. Attié T, Till M, Pelet A, Amiel J, Edery P, Boutrand L, Munnich A, Lyonnet S. Mutation of the endothelin-receptor B gene in Waardenburg-Hirschsprung disease. Hum Mol Genet. 1995;4:2407–2409. doi: 10.1093/hmg/4.12.2407. Cited: in: : PMID: 8634719.

128. Auricchio A, Casari G, Staiano A, Ballabio A. Endothelin-B receptor mutations in patients with isolated Hirschsprung disease from a non-inbred population. Hum Mol Genet. 1996;5:351–354. doi: 10.1093/hmg/5.3.351. Cited: in: : PMID: 8852659.

129. Angrist M, Bolk S, Thiel B, Puffenberger EG, Hofstra RM, Buys CH, Cass DT, Chakravarti A. Mutation analysis of the RET receptor tyrosine kinase in Hirschsprung disease. Hum Mol Genet. 1995;4:821–830. doi: 10.1093/hmg/4.5.821. Cited: in: : PMID: 7633441.

130. Yanagisawa H, Yanagisawa M, Kapur RP, Richardson JA, Williams SC, Clouthier DE, de Wit D, Emoto N, Hammer RE. Dual genetic pathways of endothelin-mediated intercellular signaling revealed by targeted disruption of endothelin converting enzyme-1 gene. Dev Camb Engl. 1998;125:825–836. doi: 10.1242/dev.125.5.825. Cited: in: : PMID: 9449665.

131. Kuhlbrodt K, Herbarth B, Sock E, Hermans-Borgmeyer I, Wegner M. Sox10, a novel transcriptional modulator in glial cells. J Neurosci Off J Soc Neurosci. 1998;18:237–250. doi: 10.1523/JNEUROSCI.18-01-00237.1998. Cited: in: : PMID: 9412504.

132. Southard-Smith EM, Kos L, Pavan WJ. Sox10 mutation disrupts neural crest development in Dom Hirschsprung mouse model. Nat Genet. 1998;18:60–64. doi: 10.1038/ng0198-60. Cited: in: : PMID: 9425902.

133. Kapur RP. Early death of neural crest cells is responsible for total enteric aganglionosis in Sox10(Dom)/Sox10(Dom) mouse embryos. Pediatr Dev Pathol Off J Soc Pediatr Pathol Paediatr Pathol Soc. 1999;2:559–569. doi: 10.1007/s100249900162. Cited: in: : PMID: 10508880.

134. Paratore C, Eichenberger C, Suter U, Sommer L. Sox10 haploinsufficiency affects maintenance of progenitor cells in a mouse model of Hirschsprung disease. Hum Mol Genet. 2002;11:3075–3085. doi: 10.1093/hmg/11.24.3075. Cited: in: : PMID: 12417529.

135. Bondurand N, Natarajan D, Barlow A, Thapar N, Pachnis V. Maintenance of mammalian enteric nervous system progenitors by SOX10 and endothelin 3 signalling. Dev Camb Engl. 2006;133:2075–2086. doi: 10.1242/dev.02375. Cited: in: : PMID: 16624853.

136. Nagashimada M, Ohta H, Li C, Nakao K, Uesaka T, Brunet J-F, Amiel J, Trochet D, Wakayama T, Enomoto H. Autonomic neurocristopathy-associated mutations in PHOX2B dysregulate Sox10 expression. J Clin Invest. 2012;122:3145–3158. doi: 10.1172/JCI63401. Cited: in: : PMID: 22922260.

137. Lane PW, Liu HM. Association of megacolon with a new dominant spotting gene (Dom) in the mouse. J Hered. 1984;75:435–439. doi: 10.1093/oxfordjournals.jhered.a109980. Cited: in: : PMID: 6512238.

138. Herbarth B, Pingault V, Bondurand N, Kuhlbrodt K, Hermans-Borgmeyer I, Puliti A, Lemort N, Goossens M, Wegner M. Mutation of the Sry-related Sox10 gene in Dominant megacolon, a mouse model for human Hirschsprung disease. Proc Natl Acad Sci U S A. 1998;95:5161–5165. doi: 10.1073/pnas.95.9.5161. Cited: in: : PMID: 9560246.

139. Kuhlbrodt K, Schmidt C, Sock E, Pingault V, Bondurand N, Goossens M, Wegner M. Functional analysis of Sox10 mutations found in human Waardenburg-Hirschsprung patients. J Biol Chem. 1998;273:23033–23038. doi: 10.1074/jbc.273.36.23033. Cited: in: : PMID: 9722528.

140. Pingault V, Bondurand N, Kuhlbrodt K, Goerich DE, Préhu MO, Puliti A, Herbarth B, Hermans-Borgmeyer I, Legius E, Matthijs G, et al. SOX10 mutations in patients with Waardenburg-Hirschsprung disease. Nat Genet. 1998;18:171–173. doi: 10.1038/ng0298-171. Cited: in: : PMID: 9462749.

141. Pattyn A, Morin X, Cremer H, Goridis C, Brunet JF. Expression and interactions of the two closely related homeobox genes Phox2a and Phox2b during neurogenesis. Dev Camb Engl. 1997;124:4065–4075. doi: 10.1242/dev.124.20.4065. Cited: in: : PMID: 9374403.

142. Amiel J, Laudier B, Attié-Bitach T, Trang H, de Pontual L, Gener B, Trochet D, Etchevers H, Ray P, Simonneau M, et al. Polyalanine expansion and frameshift mutations of the paired-like homeobox gene PHOX2B in congenital central hypoventilation syndrome. Nat Genet. 2003;33:459–461. doi: 10.1038/ng1130. Cited: in: : PMID: 12640453.

143. Vega-Lopez GA, Cerrizuela S, Tribulo C, Aybar MJ. Neurocristopathies: New insights 150 years after the neural crest discovery. Dev Biol. 2018;444 Suppl 1:S110–S143. doi: 10.1016/j.ydbio.2018.05.013. Cited: in: : PMID: 29802835.

144. Rings E, van den Berg M, Stokkers P. Expression of homeobox genes in the gastrointestinal tract. J Pediatr Gastroenterol Nutr. 1998;27:122–123. doi: 10.1097/00005176-199807000-00026. Cited: in: : PMID: 9669743.

145. Pitera JE, Smith VV, Thorogood P, Milla PJ. Coordinated expression of 3' hox genes during murine embryonal gut development: an enteric Hox code. Gastroenterology. 1999;117:1339–1351. doi: 10.1016/s0016-5085(99)70284-2. Cited: in: : PMID: 10579975.

146. Fu M, Lui VCH, Sham MH, Pachnis V, Tam PKH. Sonic hedgehog regulates the proliferation, differentiation, and migration of enteric neural crest cells in gut. J Cell Biol. 2004;166:673–684. doi: 10.1083/jcb.200401077. Cited: in: : PMID: 15337776.

147. Méchine-Neuville A, Lefebvre O, Bellocq J-P, Kedinger M, Simon-Assmann P. [Increased expression of HOXA9 gene in Hirschsprung disease]. Gastroenterol Clin Biol. 2002;26:1110–1117. Cited: in: : PMID: 12520199.

148. Warot X, Fromental-Ramain C, Fraulob V, Chambon P, Dollé P. Gene dosage-dependent effects of the Hoxa-13 and Hoxd-13 mutations on morphogenesis of the terminal parts of the digestive and urogenital tracts. Dev Camb Engl. 1997;124:4781–4791. doi: 10.1242/dev.124.23.4781. Cited: in: : PMID: 9428414.

149. Doodnath R, Wride M, Puri P. The spatio-temporal patterning of Hoxa9 and Hoxa13 in the developing zebrafish enteric nervous system. Pediatr Surg Int. 2012;28:115–121. doi: 10.1007/s00383-011-2992-3. Cited: in: : PMID: 21971947.

150. Yokouchi Y, Sakiyama J, Kuroiwa A. Coordinated expression of Abd-B subfamily genes of the HoxA cluster in the developing digestive tract of chick embryo. Dev Biol. 1995;169:76–89. doi: 10.1006/dbio.1995.1128. Cited: in: : PMID: 7750659.

151. Shirasawa S, Yunker AM, Roth KA, Brown GA, Horning S, Korsmeyer SJ. Enx (Hox11L1)-deficient mice develop myenteric neuronal hyperplasia and megacolon. Nat Med. 1997;3:646–650. doi: 10.1038/nm0697-646. Cited: in: : PMID: 9176491.

152. Hatano M, Aoki T, Dezawa M, Yusa S, Iitsuka Y, Koseki H, Taniguchi M, Tokuhisa T. A novel pathogenesis of megacolon in Ncx/Hox11L.1 deficient mice. J Clin Invest. 1997;100:795–801. doi: 10.1172/JCI119593. Cited: in: : PMID: 9259577.

153. Lui VCH, Cheng WWC, Leon TYY, Lau DKC, Garcia-Barcelo M-M, Miao XP, Kam MKM, So MT, Chen Y, Wall NA, et al. Perturbation of hoxb5 signaling in vagal neural crests down-regulates ret leading to intestinal hypoganglionosis in mice. Gastroenterology. 2008;134:1104–1115. doi: 10.1053/j.gastro.2008.01.028. Cited: in: : PMID: 18395091.

154. Tennyson VM, Gershon MD, Sherman DL, Behringer RR, Raz R, Crotty DA, Wolgemuth DJ. Structural abnormalities associated with congenital megacolon in transgenic mice that overexpress the Hoxa-4 gene. Dev Dyn Off Publ Am Assoc Anat. 1993;198:28–53. doi: 10.1002/aja.1001980105. Cited: in: : PMID: 7904838.

155. Tennyson VM, Gershon MD, Wade PR, Crotty DA, Wolgemuth DJ. Fetal development of the enteric nervous system of transgenic mice that overexpress the Hoxa-4 gene. Dev Dyn Off Publ Am Assoc Anat. 1998;211:269–291. doi: 10.1002/(SICI)1097-0177(199803)211:3<269::AID-AJA8>3.0.CO;2-F. Cited: in: : PMID: 9520114.

156. Liu JA-J, Lai FP-L, Gui H-S, Sham M-H, Tam PK-H, Garcia-Barcelo M-M, Hui C-C, Ngan ES-W. Identification of GLI Mutations in Patients With Hirschsprung Disease That Disrupt Enteric Nervous System Development in Mice. Gastroenterology. 2015;149:1837-1848.e5. doi: 10.1053/j.gastro.2015.07.060. Cited: in: : PMID: 26261006.

157. Bondurand N, Southard-Smith EM. Mouse models of Hirschsprung disease and other developmental disorders of the enteric nervous system: Old and new players. Dev Biol. 2016;417:139–157. doi: 10.1016/j.ydbio.2016.06.042. Cited: in: : PMID: 27370713.

158. Yang JT, Liu CZ, Villavicencio EH, Yoon JW, Walterhouse D, Iannaccone PM. Expression of human GLI in mice results in failure to thrive, early death, and patchy Hirschsprung-like gastrointestinal dilatation. Mol Med Camb Mass. 1997;3:826–835. Cited: in: : PMID: 9440116.

159. Dastot-Le Moal F, Wilson M, Mowat D, Collot N, Niel F, Goossens M. ZFHX1B mutations in patients with Mowat-Wilson syndrome. Hum Mutat. 2007;28:313–321. doi: 10.1002/humu.20452. Cited: in: : PMID: 17203459.

160. Takagi T, Nishizaki Y, Matsui F, Wakamatsu N, Higashi Y. De novo inbred heterozygous Zeb2/Sip1 mutant mice uniquely generated by germ-line conditional knockout exhibit craniofacial, callosal and behavioral defects associated with Mowat-Wilson syndrome. Hum Mol Genet. 2015;24:6390–6402. doi: 10.1093/hmg/ddv350. Cited: in: : PMID: 26319231.

161. Van de Putte T, Francis A, Nelles L, van Grunsven LA, Huylebroeck D. Neural crest-specific removal of Zfhx1b in mouse leads to a wide range of neurocristopathies reminiscent of Mowat-Wilson syndrome. Hum Mol Genet. 2007;16:1423–1436. doi: 10.1093/hmg/ddm093. Cited: in: : PMID: 17478475.

162. Amiel J, Espinosa-Parrilla Y, Steffann J, Gosset P, Pelet A, Prieur M, Boute O, Choiset A, Lacombe D, Philip N, et al. Large-scale deletions and SMADIP1 truncating mutations in syndromic Hirschsprung disease with involvement of midline structures. Am J Hum Genet. 2001;69:1370–1377. doi: 10.1086/324342. Cited: in: : PMID: 11595972.

163. Pan Z-W, Li J-C. Advances in molecular genetics of Hirschsprung's disease. Anat Rec Hoboken NJ 2007. 2012;295:1628–1638. doi: 10.1002/ar.22538. Cited: in: : PMID: 22815266.

164. Cacheux V, Dastot-Le Moal F, Kääriäinen H, Bondurand N, Rintala R, Boissier B, Wilson M, Mowat D, Goossens M. Loss-of-function mutations in SIP1 Smad interacting protein 1 result in a syndromic Hirschsprung disease. Hum Mol Genet. 2001;10:1503–1510. doi: 10.1093/hmg/10.14.1503. Cited: in: : PMID: 11448942.

165. Coyle D, Puri P. Hirschsprung's disease in children with Mowat-Wilson syndrome. Pediatr Surg Int. 2015;31:711–717. doi: 10.1007/s00383-015-3732-x. Cited: in: : PMID: 26156877.

166. Mowat DR, Wilson MJ, Goossens M. Mowat-Wilson syndrome. J Med Genet. 2003;40:305–310. doi: 10.1136/jmg.40.5.305. Cited: in: : PMID: 12746390.

167. Wilson M, Mowat D, Dastot-Le Moal F, Cacheux V, Kääriäinen H, Cass D, Donnai D, Clayton-Smith J, Townshend S, Curry C, et al. Further delineation of the phenotype associated with heterozygous mutations in ZFHX1B. Am J Med Genet A. 2003;119A:257–265. doi: 10.1002/ajmg.a.20053. Cited: in: : PMID: 12784289.

168. Bergeron K-F, Cardinal T, Touré AM, Béland M, Raiwet DL, Silversides DW, Pilon N. Male-biased aganglionic megacolon in the TashT mouse line due to perturbation of silencer elements in a large gene desert of chromosome 10. PLoS Genet. 2015;11:e1005093. doi: 10.1371/journal.pgen.1005093. Cited: in: : PMID: 25786024.

169. Cardinal T, Bergeron K-F, Soret R, Souchkova O, Faure C, Guillon A, Pilon N. Male-biased aganglionic megacolon in the TashT mouse model of Hirschsprung disease involves upregulation of p53 protein activity and Ddx3y gene expression. PLoS Genet. 2020;16:e1009008. doi: 10.1371/journal.pgen.1009008. Cited: in: : PMID: 32898154.

170. Soret R, Mennetrey M, Bergeron KF, Dariel A, Neunlist M, Grunder F, Faure C, Silversides DW, Pilon N, Ente-Hirsch Study Group. A collagen VI-dependent pathogenic mechanism for Hirschsprung's disease. J Clin Invest. 2015;125:4483–4496. doi: 10.1172/JCI83178. Cited: in: : PMID: 26571399.

171. Breau MA, Pietri T, Eder O, Blanche M, Brakebusch C, Fässler R, Thiery JP, Dufour S. Lack of beta1 integrins in enteric neural crest cells leads to a Hirschsprung-like phenotype. Dev Camb Engl. 2006;133:1725–1734. doi: 10.1242/dev.02346. Cited: in: : PMID: 16571628.

172. Tanyel FC, Müftuoglu SF, Dağdeviren A, Unsal I, Büyükpamukcu N, Hiçsonmez A. Expression of beta-1 integrins in ganglionic and aganglionic segments of patients with Hirschsprung's disease. Eur J Pediatr Surg Off J Austrian Assoc Pediatr Surg Al Z Kinderchir. 1997;7:16–20. doi: 10.1055/s-2008-1071042. Cited: in: : PMID: 9085803.

173. Selfridge J, Song L, Brownstein DG, Melton DW. Mice with DNA repair gene Ercc1 deficiency in a neural crest lineage are a model for late-onset Hirschsprung disease. DNA Repair. 2010;9:653–660. doi: 10.1016/j.dnarep.2010.02.018. Cited: in: : PMID: 20362516.

174. Akbareian SE, Nagy N, Steiger CE, Mably JD, Miller SA, Hotta R, Molnar D, Goldstein AM. Enteric neural crest-derived cells promote their migration by modifying their microenvironment through tenascin-C production. Dev Biol. 2013;382:446–456. doi: 10.1016/j.ydbio.2013.08.006.

175. Breau MA, Dahmani A, Broders-Bondon F, Thiery J-P, Dufour S. Beta1 integrins are required for the invasion of the caecum and proximal hindgut by enteric neural crest cells. Dev Camb Engl. 2009;136:2791–2801. doi: 10.1242/dev.031419. Cited: in: : PMID: 19633172.

176. Nagy N, Goldstein AM. Endothelin-3 regulates neural crest cell proliferation and differentiation in the hindgut enteric nervous system. Dev Biol. 2006;293:203–217. doi: 10.1016/j.ydbio.2006.01.032. Cited: in: : PMID: 16519884.

177. Parikh DH, Tam PK, Van Velzen D, Edgar D. The extracellular matrix components, tenascin and fibronectin, in Hirschsprung's disease: an immunohistochemical study. J Pediatr Surg. 1994;29:1302–1306. doi: 10.1016/0022-3468(94)90101-5. Cited: in: : PMID: 7528797.

178. Parikh DH, Leibl M, Tam PK, Edgar D. Abnormal expression and distribution of nidogen in Hirschsprung's disease. J Pediatr Surg. 1995;30:1687–1693. doi: 10.1016/0022-3468(95)90453-0. Cited: in: : PMID: 8749925.

179. Wright CM, Schneider S, Smith-Edwards KM, Mafra F, Leembruggen AJL, Gonzalez MV, Kothakapa DR, Anderson JB, Maguire BA, Gao T, et al. scRNA-Seq Reveals New Enteric Nervous System Roles for GDNF, NRTN, and TBX3. Cell Mol Gastroenterol Hepatol. 2021;11:1548-1592.e1. doi: 10.1016/j.jcmgh.2020.12.014. Cited: in: : PMID: 33444816.

180. Gunn M. A study of the enteric plexuses in some amphibians. Q J Microsc Sci. 1951;92:55–77. Cited: in: : PMID: 24540538.

181. Lamanna C, Costagliola A, Vittoria A, Mayer B, Assisi L, Botte V, Cecio A. NADPH-diaphorase and NOS enzymatic activities in some neurons of reptilian gut and their relationships with two neuropeptides. Anat Embryol (Berl). 1999;199:397–405. doi: 10.1007/s004290050238. Cited: in: : PMID: 10221451.

182. Baker PA, Meyer MD, Tsang A, Uribe RA. Immunohistochemical and ultrastructural analysis of the maturing larval zebrafish enteric nervous system reveals the formation of a neuropil pattern. Sci Rep. 2019;9:6941. doi: 10.1038/s41598-019-43497-9. Cited: in: : PMID: 31061452.

183. Nagy N, Burns AJ, Goldstein AM. Immunophenotypic characterization of enteric neural crest cells in the developing avian colorectum. Dev Dyn Off Publ Am Assoc Anat. 2012;241:842–851. doi: 10.1002/dvdy.23767. Cited: in: : PMID: 22411589.

184. Burt DW. Chicken genome: current status and future opportunities. Genome Res. 2005;15:1692–1698. doi: 10.1101/gr.4141805. Cited: in: : PMID: 16339367.

185. Gerstein MB, Rozowsky J, Yan K-K, Wang D, Cheng C, Brown JB, Davis CA, Hillier L, Sisu C, Li JJ, et al. Comparative analysis of the transcriptome across distant species. Nature. 2014;512:445–448. doi: 10.1038/nature13424. Cited: in: : PMID: 25164755.

186. International Chicken Genome Sequencing Consortium. Sequence and comparative analysis of the chicken genome provide unique perspectives on vertebrate evolution. Nature. 2004;432:695–716. doi: 10.1038/nature03154. Cited: in: : PMID: 15592404.

187. Bódi I, Nagy N, Sinka L, Igyártó B-Z, Oláh I. Novel monoclonal antibodies recognise guinea fowl thrombocytes. Acta Vet Hung. 2009;57:239–246. doi: 10.1556/AVet.57.2009.2.5. Cited: in: : PMID: 19584037.

188. Fejszák N, Kocsis K, Halasy V, Szőcs E, Soós Á, Roche D von L, Härtle S, Nagy N. Characterization and functional properties of a novel monoclonal antibody which identifies a B cell subpopulation in bursa of Fabricius. Poult Sci. 2022;101:101711. doi: 10.1016/j.psj.2022.101711. Cited: in: : PMID: 35151935.

189. Gumati MK, Magyar A, Nagy N, Kurucz E, Felföldi B, Oláh I. Extracellular matrix of different composition supports the various splenic compartments of guinea fowl (Numida meleagris). Cell Tissue Res. 2003;312:333–343. doi: 10.1007/s00441-003-0736-y. Cited: in: : PMID: 12756528.

190. Nagy N, Magyar A, Oláh I. A novel monoclonal antibody identifies all avian embryonic myogenic cells and adult smooth muscle cells. Anat Embryol (Berl). 2001;204:123–134. doi: 10.1007/s004290100192. Cited: in: : PMID: 11556528.

191. Oláh I, Gumati KH, Nagy N, Magyar A, Kaspers B, Lillehoj H. Diverse expression of the K-1 antigen by cortico-medullary and reticular epithelial cells of the bursa of Fabricius in chicken and guinea fowl. Dev Comp Immunol. 2002;26:481–488. doi: 10.1016/s0145-305x(01)00094-5. Cited: in: : PMID: 11906727.

192. Mortell A, Montedonico S, Puri P. Animal models in pediatric surgery. Pediatr Surg Int. 2006;22:111–128. doi: 10.1007/s00383-005-1593-4. Cited: in: : PMID: 16331525.

193. Meijers JH, Tibboel D, van der Kamp AW, van Haperen-Heuts IC, Molenaar JC. A model for aganglionosis in the chicken embryo. J Pediatr Surg. 1989;24:557–561. doi: 10.1016/s0022-3468(89)80505-6. Cited: in: : PMID: 2738823.

194. Payette RF, Tennyson VM, Pomeranz HD, Pham TD, Rothman TP, Gershon MD. Accumulation of components of basal laminae: association with the failure of neural crest cells to colonize the presumptive aganglionic bowel of ls/ls mutant mice. Dev Biol. 1988;125:341–360. doi: 10.1016/0012-1606(88)90217-5. Cited: in: : PMID: 3338619.

195. Rothman TP, Le Douarin NM, Fontaine-Pérus JC, Gershon MD. Developmental potential of neural crest-derived cells migrating from segments of developing quail bowel back-grafted into younger chick host embryos. Dev Camb Engl. 1990;109:411–423. doi: 10.1242/dev.109.2.411. Cited: in: : PMID: 2401204.

196. Thiery JP, Duband JL, Delouvée A. Pathways and mechanisms of avian trunk neural crest cell migration and localization. Dev Biol. 1982;93:324–343. doi: 10.1016/0012-1606(82)90121-x. Cited: in: : PMID: 7141101.

197. Natsikas NB, Sbarounis CN. Adult Hirschsprung's disease. An experience with the Duhamel-Martin procedure with special reference to obstructed patients. Dis Colon Rectum. 1987;30:204–206. doi: 10.1007/BF02554342. Cited: in: : PMID: 3829865.

198. Druckenbrod NR, Epstein ML. The pattern of neural crest advance in the cecum and colon. Dev Biol. 2005;287:125–133. doi: 10.1016/j.ydbio.2005.08.040. Cited: in: : PMID: 16197939.

199. Shin MK, Levorse JM, Ingram RS, Tilghman SM. The temporal requirement for endothelin receptor-B signalling during neural crest development. Nature. 1999;402:496–501. doi: 10.1038/990040. Cited: in: : PMID: 10591209.

200. Woodward MN, Sidebotham EL, Connell MG, Kenny SE, Vaillant CR, Lloyd DA, Edgar DH. Analysis of the effects of endothelin-3 on the development of neural crest cells in the embryonic mouse gut. J Pediatr Surg. 2003;38:1322–1328. doi: 10.1016/s0022-3468(03)00389-0. Cited: in: : PMID: 14523813.

201. Kruger GM, Mosher JT, Tsai Y-H, Yeager KJ, Iwashita T, Gariepy CE, Morrison SJ. Temporally distinct requirements for endothelin receptor B in the generation and migration of gut neural crest stem cells. Neuron. 2003;40:917–929. doi: 10.1016/s0896-6273(03)00727-x. Cited: in: : PMID: 14659091.

202. Chalazonitis A, D'Autréaux F, Guha U, Pham TD, Faure C, Chen JJ, Roman D, Kan L, Rothman TP, Kessler JA, et al. Bone Morphogenetic Protein-2 and -4 Limit the Number of Enteric Neurons But Promote Development of a TrkC-Expressing Neurotrophin-3-Dependent Subset. J Neurosci. 2004;24:4266–4282. doi: 10.1523/JNEUROSCI.3688-03.2004. Cited: in: : PMID: 15115823.

203. Goldstein AM, Brewer KC, Doyle AM, Nagy N, Roberts DJ. BMP signaling is necessary for neural crest cell migration and ganglion formation in the enteric nervous system. Mech Dev. 2005;122:821–833. doi: 10.1016/j.mod.2005.03.003. Cited: in: : PMID: 15905074.

204. Huycke TR, Miller BM, Gill HK, Nerurkar NL, Sprinzak D, Mahadevan L, Tabin CJ. Genetic and Mechanical Regulation of Intestinal Smooth Muscle Development. Cell. 2019;179:90-105.e21. doi: 10.1016/j.cell.2019.08.041. Cited: in: : PMID: 31539501.

205. De Santa Barbara P, Williams J, Goldstein AM, Doyle AM, Nielsen C, Winfield S, Faure S, Roberts DJ. Bone morphogenetic protein signaling pathway plays multiple roles during gastrointestinal tract development. Dev Dyn Off Publ Am Assoc Anat. 2005;234:312–322. doi: 10.1002/dvdy.20554. Cited: in: : PMID: 16110505.

206. Roberts DJ. Molecular mechanisms of development of the gastrointestinal tract. Dev Dyn Off Publ Am Assoc Anat. 2000;219:109–120. doi: 10.1002/1097-0177(2000)9999:9999<::aid-dvdy1047>3.3.co;2-y. Cited: in: : PMID: 11002332.

207. Jiang Y, Liu M, Gershon MD. Netrins and DCC in the guidance of migrating neural crest-derived cells in the developing bowel and pancreas. Dev Biol. 2003;258:364–384. doi: 10.1016/s0012-1606(03)00136-2. Cited: in: : PMID: 12798294.

208. Nagy N, Barad C, Graham HK, Hotta R, Cheng LS, Fejszak N, Goldstein AM. Sonic hedgehog controls enteric nervous system development by patterning the extracellular matrix. Development. 2016;143:264–275. doi: 10.1242/dev.128132.

209. Fu M, Vohra BPS, Wind D, Heuckeroth RO. BMP signaling regulates murine enteric nervous system precursor migration, neurite fasciculation and patterning via altered Ncam1 polysialic acid addition. Dev Biol. 2006;299:137–150. doi: 10.1016/j.ydbio.2006.07.016. Cited: in: : PMID: 16952347.

210. Chalazonitis A, Pham TD, Li Z, Roman D, Guha U, Gomes W, Kan L, Kessler JA, Gershon MD. Bone morphogenetic protein regulation of enteric neuronal phenotypic diversity: relationship to timing of cell cycle exit. J Comp Neurol. 2008;509:474–492. doi: 10.1002/cne.21770. Cited: in: : PMID: 18537141.

211. Chalazonitis A, D'Autréaux F, Pham TD, Kessler JA, Gershon MD. Bone Morphogenetic Proteins Regulate Enteric Gliogenesis by Modulating ErbB3 Signaling. Dev Biol. 2011;350:64–79. doi: 10.1016/j.ydbio.2010.11.017. Cited: in: : PMID: 21094638.

212. Faure C, Chalazonitis A, Rhéaume C, Bouchard G, Sampathkumar S-G, Yarema KJ, Gershon MD. Gangliogenesis in the enteric nervous system: roles of the polysialylation of the neural cell adhesion molecule and its regulation by bone morphogenetic protein-4. Dev Dyn Off Publ Am Assoc Anat. 2007;236:44–59. doi: 10.1002/dvdy.20943. Cited: in: : PMID: 16958105.

213. Pisano JM, Colón-Hastings F, Birren SJ. Postmigratory enteric and sympathetic neural precursors share common, developmentally regulated, responses to BMP2. Dev Biol. 2000;227:1–11. doi: 10.1006/dbio.2000.9876. Cited: in: : PMID: 11076672.

214. Thang SH, Kobayashi M, Matsuoka I. Regulation of glial cell line-derived neurotrophic factor responsiveness in developing rat sympathetic neurons by retinoic acid and bone morphogenetic protein-2. J Neurosci Off J Soc Neurosci. 2000;20:2917–2925. doi: 10.1523/JNEUROSCI.20-08-02917.2000. Cited: in: : PMID: 10751444.

215. van Grunsven LA, Taelman V, Michiels C, Verstappen G, Souopgui J, Nichane M, Moens E, Opdecamp K, Vanhomwegen J, Kricha S, et al. XSip1 neuralizing activity involves the co-repressor CtBP and occurs through BMP dependent and independent mechanisms. Dev Biol. 2007;306:34–49. doi: 10.1016/j.ydbio.2007.02.045. Cited: in: : PMID: 17442301.

216. Wei W, Liu B, Jiang H, Jin K, Xiang M. Requirement of the Mowat-Wilson Syndrome Gene Zeb2 in the Differentiation and Maintenance of Non-photoreceptor Cell Types During Retinal Development. Mol Neurobiol. 2019;56:1719–1736. doi: 10.1007/s12035-018-1186-6. Cited: in: : PMID: 29922981.

217. Wakamatsu N, Yamada Y, Yamada K, Ono T, Nomura N, Taniguchi H, Kitoh H, Mutoh N, Yamanaka T, Mushiake K, et al. Mutations in SIP1, encoding Smad interacting protein-1, cause a form of Hirschsprung disease. Nat Genet. 2001;27:369–370. doi: 10.1038/86860. Cited: in: : PMID: 11279515.

218. Nagaya M, Kato J, Niimi N, Tanaka S, Wakamatsu N. Clinical features of a form of Hirschsprung's disease caused by a novel genetic abnormality. J Pediatr Surg. 2002;37:1117–1122. doi: 10.1053/jpsu.2002.34455. Cited: in: : PMID: 12149685.

219. McGrew MJ, Sherman A, Ellard FM, Lillico SG, Gilhooley HJ, Kingsman AJ, Mitrophanous KA, Sang H. Efficient production of germline transgenic chickens using lentiviral vectors. EMBO Rep. 2004;5:728–733. doi: 10.1038/sj.embor.7400171. Cited: in: : PMID: 15192698.

220. Hamburger V, Hamilton HL. A series of normal stages in the development of the chick embryo. J Morphol. 1951;88:49–92. doi: 10.1002/jmor.1050880104.

221. Hamburger V, Hamilton HL. A series of normal stages in the development of the chick embryo. Dev Dyn. 1992;195:231–272. doi: 10.1002/aja.1001950404.

222. Southwell BR. Staging of intestinal development in the chick embryo. Anat Rec A Discov Mol Cell Evol Biol. 2006;288A:909–920. doi: 10.1002/ar.a.20349.

223. Moniot B, Biau S, Faure S, Nielsen CM, Berta P, Roberts DJ, de Santa Barbara P. SOX9 specifies the pyloric sphincter epithelium through mesenchymal-epithelial signals. Development. 2004;131:3795–3804. doi: 10.1242/dev.01259.

224. Le Guen L, Notarnicola C, de Santa Barbara P. Intermuscular tendons are essential for the development of vertebrate stomach. Dev Camb Engl. 2009;136:791–801. doi: 10.1242/dev.029942. Cited: in: : PMID: 19176584.

225. Dealy CN, Roth A, Ferrari D, Brown AMC, Kosher RA. Wnt-5a and Wnt-7a are expressed in the developing chick limb bud in a manner suggesting roles in pattern formation along the proximodistal and dorsoventral axes. Mech Dev. 1993;43:175–186. doi: 10.1016/0925-4773(93)90034-U.

226. Marcelle C, Stark MR, Bronner-Fraser M. Coordinate actions of BMPs, Wnts, Shh and noggin mediate patterning of the dorsal somite. Dev Camb Engl. 1997;124:3955–3963. doi: 10.1242/dev.124.20.3955. Cited: in: : PMID: 9374393.

227. Chapman SC, Brown R, Lees L, Schoenwolf GC, Lumsden A. Expression analysis of chick Wnt and frizzled genes and selected inhibitors in early chick patterning. Dev Dyn. 2004;229:668–676. doi: 10.1002/dvdy.10491.

228. Roberts DJ, Johnson RL, Burke AC, Nelson CE, Morgan BA, Tabin C. Sonic hedgehog is an endodermal signal inducing Bmp-4 and Hox genes during induction and regionalization of the chick hindgut. Development. 1995;121:3163–3174. doi: 10.1242/dev.121.10.3163.

229. Zou H, Niswander L. Requirement for BMP Signaling in Interdigital Apoptosis and Scale Formation. Science. 1996;272:738–741. doi: 10.1126/science.272.5262.738.

230. Acloque H, Wilkinson DG, Nieto MA. In situ hybridization analysis of chick embryos in whole-mount and tissue sections. Methods Cell Biol. 2008;87:169–185. doi: 10.1016/S0091-679X(08)00209-4. Cited: in: : PMID: 18485297.

231. Faure S, Georges M, McKey J, Sagnol S, de Santa Barbara P. Expression pattern of the homeotic gene Bapx1 during early chick gastrointestinal tract development. Gene Expr Patterns. 2013;13:287–292. doi: 10.1016/j.gep.2013.05.005.

232. Nielsen C, Murtaugh LC, Chyung JC, Lassar A, Roberts DJ. Gizzard formation and the role of Bapx1. Dev Biol. 2001;231:164–174. doi: 10.1006/dbio.2000.0151. Cited: in: : PMID: 11180960.

233. Riddle RD, Johnson RL, Laufer E, Tabin C. Sonic hedgehog mediates the polarizing activity of the ZPA. Cell. 1993;75:1401–1416. doi: 10.1016/0092-8674(93)90626-2. Cited: in: : PMID: 8269518.

234. Smith DM, Nielsen C, Tabin CJ, Roberts DJ. Roles of BMP signaling and Nkx2.5 in patterning at the chick midgut-foregut boundary. Dev Camb Engl. 2000;127:3671–3681. doi: 10.1242/dev.127.17.3671. Cited: in: : PMID: 10934012.

235. Hearn CJ, Young HM, Ciampoli D, Lomax AE, Newgreen D. Catenary cultures of embryonic gastrointestinal tract support organ morphogenesis, motility, neural crest cell migration, and cell differentiation. Dev Dyn Off Publ Am Assoc Anat. 1999;214:239–247. doi: 10.1002/(SICI)1097-0177(199903)214:3<239::AID-AJA7>3.0.CO;2-O. Cited: in: : PMID: 10090150.

236. Hao MM, Bergner AJ, Newgreen DF, Enomoto H, Young HM. Technologies for Live Imaging of Enteric Neural Crest-Derived Cells. Methods Mol Biol Clifton NJ. 2019;1976:97–105. doi: 10.1007/978-1-4939-9412-0_8. Cited: in: : PMID: 30977068.

237. Potts WM, Olsen M, Boettiger D, Vogt VM. Epitope mapping of monoclonal antibodies to gag protein p19 of avian sarcoma and leukaemia viruses. J Gen Virol. 1987;68 (Pt 12):3177–3182. doi: 10.1099/0022-1317-68-12-3177. Cited: in: : PMID: 2447226.

238. Nagy N, Goldstein AM. Intestinal coelomic transplants: a novel method for studying enteric nervous system development. Cell Tissue Res. 2006;326:43–55. doi: 10.1007/s00441-006-0207-3. Cited: in: : PMID: 16736197.

239. Dobin A, Davis CA, Schlesinger F, Drenkow J, Zaleski C, Jha S, Batut P, Chaisson M, Gingeras TR. STAR: ultrafast universal RNA-seq aligner. Bioinforma Oxf Engl. 2013;29:15–21. doi: 10.1093/bioinformatics/bts635. Cited: in: : PMID: 23104886.

240. Anders S, Pyl PT, Huber W. HTSeq--a Python framework to work with high-throughput sequencing data. Bioinforma Oxf Engl. 2015;31:166–169. doi: 10.1093/bioinformatics/btu638. Cited: in: : PMID: 25260700.

241. Robinson MD, McCarthy DJ, Smyth GK. edgeR: a Bioconductor package for differential expression analysis of digital gene expression data. Bioinformatics. 2010;26:139–140. doi: 10.1093/bioinformatics/btp616. Cited: in: : PMID: 19910308.

242. Benjamini Y, Hochberg Y. Controlling the False Discovery Rate: A Practical and Powerful Approach to Multiple Testing. J R Stat Soc Ser B Methodol. 1995;57:289–300. doi: 10.1111/j.2517-6161.1995.tb02031.x.

243. Ashburner M, Ball CA, Blake JA, Botstein D, Butler H, Cherry JM, Davis AP, Dolinski K, Dwight SS, Eppig JT, et al. Gene ontology: tool for the unification of biology. The Gene Ontology Consortium. Nat Genet. 2000;25:25–29. doi: 10.1038/75556. Cited: in: : PMID: 10802651.

244. Mi H, Muruganujan A, Casagrande JT, Thomas PD. Large-scale gene function analysis with the PANTHER classification system. Nat Protoc. 2013;8:1551–1566. doi: 10.1038/nprot.2013.092. Cited: in: : PMID: 23868073.

245. Supek F, Bošnjak M, Škunca N, Šmuc T. REVIGO summarizes and visualizes long lists of gene ontology terms. PloS One. 2011;6:e21800. doi: 10.1371/journal.pone.0021800. Cited: in: : PMID: 21789182.

246. Metsalu T, Vilo J. ClustVis: a web tool for visualizing clustering of multivariate data using Principal Component Analysis and heatmap. Nucleic Acids Res. 2015;43:W566-570. doi: 10.1093/nar/gkv468. Cited: in: : PMID: 25969447.

247. Zhou G, Soufan O, Ewald J, Hancock REW, Basu N, Xia J. NetworkAnalyst 3.0: a visual analytics platform for comprehensive gene expression profiling and meta-analysis. Nucleic Acids Res. 2019;47:W234–W241. doi: 10.1093/nar/gkz240. Cited: in: : PMID: 30931480.

248. Karim A, Tang CS-M, Tam PK-H. The Emerging Genetic Landscape of Hirschsprung Disease and Its Potential Clinical Applications. Front Pediatr. 2021;9:638093. doi: 10.3389/fped.2021.638093. Cited: in: : PMID: 34422713.

249. Sukegawa A, Narita T, Kameda T, Saitoh K, Nohno T, Iba H, Yasugi S, Fukuda K. The concentric structure of the developing gut is regulated by Sonic hedgehog derived from endodermal epithelium. Dev Camb Engl. 2000;127:1971–1980. doi: 10.1242/dev.127.9.1971. Cited: in: : PMID: 10751185.

250. McLelland J. Anatomy of the avian cecum. J Exp Zool Suppl Publ Auspices Am Soc Zool Div Comp Physiol Biochem. 1989;3:2–9. doi: 10.1002/jez.1402520503. Cited: in: : PMID: 2575123.

251. Annison EF, Hill KJ, Kenworthy R. Volatile fatty acids in the digestive tract of the fowl. Br J Nutr. 1968;22:207–216. doi: 10.1079/bjn19680026. Cited: in: : PMID: 5673541.

252. Mead GC. Microbes of the avian cecum: types present and substrates utilized. J Exp Zool Suppl Publ Auspices Am Soc Zool Div Comp Physiol Biochem. 1989;3:48–54. doi: 10.1002/jez.1402520508. Cited: in: : PMID: 2575127.

253. Maisonnier S, Gomez J, Chagneau AM, Carré B. Analysis of variability in nutrient digestibilities in broiler chickens. Br Poult Sci. 2001;42:70–76. doi: 10.1080/00071660020035082. Cited: in: : PMID: 11337971.

254. Thomas DH. Salt and water excretion by birds: the lower intestine as an integrator of renal and intestinal excretion. Comp Biochem Physiol A. 1982;71:527–535. doi: 10.1016/0300-9629(82)90201-8. Cited: in: : PMID: 6124341.

255. Bienenstock J, Gauldie J, Perey DY. Synthesis of IgG, IgA, IgM by chicken tissues: immunofluorescent and 14C amino acid incorporation studies. J Immunol Baltim Md 1950. 1973;111:1112–1118. Cited: in: : PMID: 4199556.

256. Yildiz M, Aydemir I, Kum S, Eren U. Histological and immunohistochemical studies of the proximal caecum and caecal tonsils of quail (Coturnix coturnix japonica). Anat Histol Embryol. 2019;48:476–485. doi: 10.1111/ahe.12469. Cited: in: : PMID: 31305954.

257. Randal Bollinger R, Barbas AS, Bush EL, Lin SS, Parker W. Biofilms in the large bowel suggest an apparent function of the human vermiform appendix. J Theor Biol. 2007;249:826–831. doi: 10.1016/j.jtbi.2007.08.032. Cited: in: : PMID: 17936308.

258. Laurin M, Everett ML, Parker W. The cecal appendix: one more immune component with a function disturbed by post-industrial culture. Anat Rec Hoboken NJ 2007. 2011;294:567–579. doi: 10.1002/ar.21357. Cited: in: : PMID: 21370495.

259. Smith HF, Parker W, Kotzé SH, Laurin M. Morphological evolution of the mammalian cecum and cecal appendix. Comptes Rendus Palevol. 2017;16:39–57. doi: 10.1016/j.crpv.2016.06.001.

260. Barlow AJ, Wallace AS, Thapar N, Burns AJ. Critical numbers of neural crest cells are required in the pathways from the neural tube to the foregut to ensure complete enteric nervous system formation. Development. 2008;135:1681–1691. doi: 10.1242/dev.017418.

261. Simpson MJ, Zhang DC, Mariani M, Landman KA, Newgreen DF. Cell proliferation drives neural crest cell invasion of the intestine. Dev Biol. 2007;302:553–568. doi: 10.1016/j.ydbio.2006.10.017.

262. Ji Y, Hao H, Reynolds K, McMahon M, Zhou CJ. Wnt Signaling in Neural Crest Ontogenesis and Oncogenesis. Cells. 2019;8:1173. doi: 10.3390/cells8101173. Cited: in: : PMID: 31569501.

263. Theodosiou NA, Tabin CJ. Wnt signaling during development of the gastrointestinal tract. Dev Biol. 2003;259:258–271. doi: 10.1016/s0012-1606(03)00185-4. Cited: in: : PMID: 12871700.

264. McBride HJ, Fatke B, Fraser SE. Wnt signaling components in the chicken intestinal tract. Dev Biol. 2003;256:18–33. doi: 10.1016/s0012-1606(02)00118-5. Cited: in: : PMID: 12654289.

265. Carreira-Barbosa F, Concha ML, Takeuchi M, Ueno N, Wilson SW, Tada M. Prickle 1 regulates cell movements during gastrulation and neuronal migration in zebrafish. Development. 2003;130:4037–4046. doi: 10.1242/dev.00567.

266. Medina A, Reintsch W, Steinbeisser H. Xenopus frizzled 7 can act in canonical and non-canonical Wnt signaling pathways: implications on early patterning and morphogenesis. Mech Dev. 2000;92:227–237. doi: 10.1016/s0925-4773(00)00240-9. Cited: in: : PMID: 10727861.

267. Sumanas S, Ekker SC. Xenopus frizzled-7 morphant displays defects in dorsoventral patterning and convergent extension movements during gastrulation. Genes N Y N 2000. 2001;30:119–122. doi: 10.1002/gene.1044. Cited: in: : PMID: 11477687.

268. Winklbauer R, Medina A, Swain RK, Steinbeisser H. Frizzled-7 signalling controls tissue separation during Xenopus gastrulation. Nature. 2001;413:856–860. doi: 10.1038/35101621. Cited: in: : PMID: 11677610.

269. De Calisto J, Araya C, Marchant L, Riaz CF, Mayor R. Essential role of non-canonical Wnt signalling in neural crest migration. Development. 2005;132:2587–2597. doi: 10.1242/dev.01857.

270. Stewart AL, Young HM, Popoff M, Anderson RB. Effects of pharmacological inhibition of small GTPases on axon extension and migration of enteric neural crest-derived cells. Dev Biol. 2007;307:92–104. doi: 10.1016/j.ydbio.2007.04.024. Cited: in: : PMID: 17524389.

271. Marlow F, Topczewski J, Sepich D, Solnica-Krezel L. Zebrafish Rho kinase 2 acts downstream of Wnt11 to mediate cell polarity and effective convergence and extension movements. Curr Biol CB. 2002;12:876–884. doi: 10.1016/s0960-9822(02)00864-3. Cited: in: : PMID: 12062050.

272. Rodriguez-Hernandez I, Maiques O, Kohlhammer L, Cantelli G, Perdrix-Rosell A, Monger J, Fanshawe B, Bridgeman VL, Karagiannis SN, Penin RM, et al. WNT11-FZD7-DAAM1 signalling supports tumour initiating abilities and melanoma amoeboid invasion. Nat Commun. 2020;11:5315. doi: 10.1038/s41467-020-18951-2. Cited: in: : PMID: 33082334.

273. Kispert A, Vainio S, Shen L, Rowitch DH, McMahon AP. Proteoglycans are required for maintenance of Wnt-11 expression in the ureter tips. Dev Camb Engl. 1996;122:3627–3637. doi: 10.1242/dev.122.11.3627. Cited: in: : PMID: 8951078.

274. Majumdar A, Vainio S, Kispert A, McMahon J, McMahon AP. Wnt11 and Ret/Gdnf pathways cooperate in regulating ureteric branching during metanephric kidney development. Dev Camb Engl. 2003;130:3175–3185. doi: 10.1242/dev.00520. Cited: in: : PMID: 12783789.

275. Pepicelli CV, Kispert A, Rowitch DH, McMahon AP. GDNF induces branching and increased cell proliferation in the ureter of the mouse. Dev Biol. 1997;192:193–198. doi: 10.1006/dbio.1997.8745. Cited: in: : PMID: 9405108.

276. Takeo M, Lee W, Rabbani P, Sun Q, Hu H, Lim CH, Manga P, Ito M. EdnrB Governs Regenerative Response of Melanocyte Stem Cells by Crosstalk with Wnt Signaling. Cell Rep. 2016;15:1291–1302. doi: 10.1016/j.celrep.2016.04.006. Cited: in: : PMID: 27134165.

277. Chalazonitis A, Kessler JA. Pleiotropic Effects of the Bone Morphogenetic Proteins on Development of the Enteric Nervous System. Dev Neurobiol. 2012;72:843–856. doi: 10.1002/dneu.22002. Cited: in: : PMID: 22213745.

278. Shyer AE, Huycke TR, Lee C, Mahadevan L, Tabin CJ. Bending gradients: how the intestinal stem cell gets its home. Cell. 2015;161:569–580. doi: 10.1016/j.cell.2015.03.041. Cited: in: : PMID: 25865482.

279. Nerurkar NL, Mahadevan L, Tabin CJ. BMP signaling controls buckling forces to modulate looping morphogenesis of the gut. Proc Natl Acad Sci U S A. 2017;114:2277–2282. doi: 10.1073/pnas.1700307114. Cited: in: : PMID: 28193855.

280. Fu M, Tam PKH, Sham MH, Lui VCH. Embryonic development of the ganglion plexuses and the concentric layer structure of human gut: a topographical study. Anat Embryol (Berl). 2004;208:33–41. doi: 10.1007/s00429-003-0371-0. Cited: in: : PMID: 14991401.

281. Young HM, Turner KN, Bergner AJ. The location and phenotype of proliferating neural-crest-derived cells in the developing mouse gut. Cell Tissue Res. 2005;320:1–9. doi: 10.1007/s00441-004-1057-5. Cited: in: : PMID: 15714282.

282. Almond S, Lindley RM, Kenny SE, Connell MG, Edgar DH. Characterisation and transplantation of enteric nervous system progenitor cells. Gut. 2006;56:489. doi: 10.1136/gut.2006.094565. Cited: in: : PMID: 16973717.

283. Lindley RM, Hawcutt DB, Connell MG, Almond SN, Vannucchi M-G, Faussone-Pellegrini MS, Edgar DH, Kenny SE. Human and Mouse Enteric Nervous System Neurosphere Transplants Regulate the Function of Aganglionic Embryonic Distal Colon. Gastroenterology. 2008;135:205-216.e6. doi: 10.1053/j.gastro.2008.03.035. Cited: in: : PMID: 18515088.

284. Rauch U, Hänsgen A, Hagl C, Holland-Cunz S, Schäfer K-H. Isolation and cultivation of neuronal precursor cells from the developing human enteric nervous system as a tool for cell therapy in dysganglionosis. Int J Colorectal Dis. 2006;21:554–559. doi: 10.1007/s00384-005-0051-z.

285. Metzger M, Bareiss PM, Danker T, Wagner S, Hennenlotter J, Guenther E, Obermayr F, Stenzl A, Koenigsrainer A, Skutella T, et al. Expansion and Differentiation of Neural Progenitors Derived From the Human Adult Enteric Nervous System. Gastroenterology. 2009;137:2063-2073.e4. doi: 10.1053/j.gastro.2009.06.038. Cited: in: : PMID: 19549531.

286. Cheng LS, Graham HK, Pan WH, Nagy N, Carreon-Rodriguez A, Goldstein AM, Hotta R. Optimizing neurogenic potential of enteric neurospheres for treatment of neurointestinal diseases. J Surg Res. 2016;206:451. doi: 10.1016/j.jss.2016.08.035. Cited: in: : PMID: 27884342.

287. Metzger M, Caldwell C, Barlow AJ, Burns AJ, Thapar N. Enteric nervous system stem cells derived from human gut mucosa for the treatment of aganglionic gut disorders. Gastroenterology. 2009;136:2214-2225.e1-3. doi: 10.1053/j.gastro.2009.02.048. Cited: in: : PMID: 19505425.

288. Cheng LS, Hotta R, Graham HK, Belkind-Gerson J, Nagy N, Goldstein AM. Postnatal human enteric neuronal progenitors can migrate, differentiate, and proliferate in embryonic and postnatal aganglionic gut environments. Pediatr Res. 2017;81:838–846. doi: 10.1038/pr.2017.4. Cited: in: : PMID: 28060794.

289. Cheng LS, Hotta R, Graham HK, Nagy N, Goldstein AM, Belkind-Gerson J. Endoscopic delivery of enteric neural stem cells to treat Hirschsprung disease. Neurogastroenterol Motil Off J Eur Gastrointest Motil Soc. 2015;27:1509. doi: 10.1111/nmo.12635. Cited: in: : PMID: 26190543.

290. Lindley RM, Hawcutt DB, Connell MG, Edgar DH, Kenny SE. Properties of secondary and tertiary human enteric nervous system neurospheres. J Pediatr Surg. 2009;44:1249–1256. doi: 10.1016/j.jpedsurg.2009.02.048. Cited: in: : PMID: 19524749.

291. Hetz S, Acikgoez A, Voss U, Nieber K, Holland H, Hegewald C, Till H, Metzger R, Metzger M. In vivo transplantation of neurosphere-like bodies derived from the human postnatal and adult enteric nervous system: a pilot study. PloS One. 2014;9:e93605. doi: 10.1371/journal.pone.0093605. Cited: in: : PMID: 24699866.

292. Bondurand N, Natarajan D, Thapar N, Atkins C, Pachnis V. Neuron and glia generating progenitors of the mammalian enteric nervous system isolated from foetal and postnatal gut cultures. Development. 2003;130:6387–6400. doi: 10.1242/dev.00857.

293. Hotta R, Cheng LS, Graham HK, Nagy N, Belkind-Gerson J, Mattheolabakis G, Amiji MM, Goldstein AM. Delivery of enteric neural progenitors with 5-HT4 agonist-loaded nanoparticles and thermosensitive hydrogel enhances cell proliferation and

differentiation following transplantation *in vivo*. Biomaterials. 2016;88:1–11. doi: 10.1016/j.biomaterials.2016.02.016.

294. Hotta R, Cheng LS, Graham HK, Pan W, Nagy N, Belkind-Gerson J, Goldstein AM. Isogenic enteric neural progenitor cells can replace missing neurons and glia in mice with Hirschsprung disease. Neurogastroenterol Motil. 2016;28:498–512. doi: 10.1111/nmo.12744. Cited: in: : PMID: 26685978.

295. Mueller JL, Stavely R, Guyer RA, Soos Á, Bhave S, Han C, Hotta R, Nagy N, Goldstein AM. Agrin Inhibition in Enteric Neural Stem Cells Enhances Their Migration Following Colonic Transplantation. Stem Cells Transl Med. 2024;13:490–504. doi: 10.1093/stcltm/szae013.

296. McKeown SJ, Mohsenipour M, Bergner AJ, Young HM, Stamp LA. Exposure to GDNF Enhances the Ability of Enteric Neural Progenitors to Generate an Enteric Nervous System. Stem Cell Rep. 2017;8:476–488. doi: 10.1016/j.stemcr.2016.12.013. Cited: in: : PMID: 28089669.

297. Fattahi F, Steinbeck JA, Kriks S, Tchieu J, Zimmer B, Kishinevsky S, Zeltner N, Mica Y, El-Nachef W, Zhao H, et al. Deriving human ENS lineages for cell therapy and drug discovery in Hirschsprung disease. Nature. 2016;531:105–109. doi: 10.1038/nature16951. Cited: in: : PMID: 26863197.

298. Li Z, Ngan ES-W. New insights empowered by single-cell sequencing: From neural crest to enteric nervous system. Comput Struct Biotechnol J. 2022;20:2464–2472. doi: 10.1016/j.csbj.2022.05.025. Cited: in: : PMID: 35664232.

299. Zhou B, Feng C, Sun S, Chen X, Zhuansun D, Wang D, Yu X, Meng X, Xiao J, Wu L, et al. Identification of signaling pathways that specify a subset of migrating enteric neural crest cells at the wavefront in mouse embryos. Dev Cell. 2024;59:1689-1706.e8. doi: 10.1016/j.devcel.2024.03.034. Cited: in: : PMID: 38636517.

300. Tarapcsak S, Huang X, Qiao Y, Farrell A, Mammen L, Lovichik A, Khanderao GD, Musci T, Moos PJ, Firpo MA, et al. Single-cell RNA sequencing in Hirschsprung's disease tissues reveals lack of neuronal differentiation in the aganglionic colon segment. bioRxiv. 2025;2025.07.01.662516. doi: 10.1101/2025.07.01.662516. Cited: in: : PMID: 40631286.

Bibliography of the candidate's publications

8.1. List of own publications related to the PhD thesis

Nagy, N.*, **Kovacs, T.***, Stavely, R., Halasy, V., Soos, A., Szocs, E., Hotta, R., Graham, H., & Goldstein, A. M. (2021). Avian ceca are indispensable for hindgut enteric nervous system development. *Development (Cambridge, England)*, *148*(22), dev199825. https://doi.org/10.1242/dev.199825

IF: 6.862

Kovács, T.*, Halasy, V.*, Pethő, C., Szőcs, E., Soós, Á., Dóra, D., de Santa Barbara, P., Faure, S., Stavely, R., Goldstein, A. M., & Nagy, N. (2023). Essential Role of BMP4 Signaling in the Avian Ceca in Colorectal Enteric Nervous System Development. *International journal of molecular sciences*, *24*(21), 15664. https://doi.org/10.3390/ijms242115664

IF: 4.900

8.2. List of own publications not related to the PhD thesis

Kudlik, G., Matula, Z., **Kovács, T.**, Urbán, S. V., & Uher, F. (2015). A pluri- és multipotencia határán: a ganglionléc őssejtjei [At the border of pluri- and multipotency: the neural crest stem cells]. *Orvosi hetilap*, *156*(42), 1683–1694. https://doi.org/10.1556/650.2015.30271
IF: 0.291

Dülk, M., Kudlik, G., Fekete, A., Ernszt, D., Kvell, K., Pongrácz, J. E., Merő, B. L., Szeder, B., Radnai, L., Geiszt, M., Csécsy, D. E., **Kovács, T.**, Uher, F., Lányi, Á., Vas, V., & Buday, L. (2016). The scaffold protein Tks4 is required for the differentiation of mesenchymal stromal cells (MSCs) into adipogenic and osteogenic lineages. *Scientific reports*, *6*, 34280. https://doi.org/10.1038/srep34280
IF: 4.259

Vas, V., **Kovács, T.**, Körmendi, S., Bródy, A., Kudlik, G., Szeder, B., Mező, D., Kállai, D., Koprivanacz, K., Merő, B. L., Dülk, M., Tóvári, J., Vajdovich, P., Şenel, Ş. N., Özcan, I., Helyes, Z., Dobó-Nagy, C., & Buday, L. (2019). Significance of the Tks4 scaffold protein in bone tissue homeostasis. *Scientific reports*, *9*(1), 5781. https://doi.org/10.1038/s41598-019-42250-6
IF: 3.998

Dora, D., Arciero, E., Hotta, R., Barad, C., Bhave, S., **Kovacs, T.**, Balic, A., Goldstein, A. M., & Nagy, N. (2018). Intraganglionic macrophages: a new population of cells in the enteric ganglia. *Journal of anatomy*, *233*(4), 401–410. https://doi.org/10.1111/joa.12863
IF: 2.638

Nagy, N., Guyer, R. A., Hotta, R., Zhang, D., Newgreen, D. F., Halasy, V., **Kovacs, T.**, & Goldstein, A. M. (2020). RET overactivation leads to concurrent Hirschsprung disease and intestinal ganglioneuromas. *Development (Cambridge, England)*, *147*(21), dev190900. https://doi.org/10.1242/dev.190900
IF: 6.862

Dóra, D., **Kovács, T.**, & Nagy, N. (2020). Az intestinalis macrophagok és az enteralis idegrendszer szerepe a bél neuroimmunológiai kapcsolataiban. Alapkutatás és klinikai vonatkozások [The role of intestinal macrophages and the enteric nervous system in gut neuroimmunology. Basic science and clinical implications]. *Orvosi hetilap*, *161*(19), 771–779. https://doi.org/10.1556/650.2020.31685
IF: 0.540

Mogor, F., **Kovács, T.**, Lohinai, Z., & Dora, D. (2021). The Enteric Nervous System and the Microenvironment of the Gut: The Translational Aspects of the Microbiome-Gut-Brain Axis. *Applied Sciences*, *11*(24), 12000. https://doi.org/10.3390/app112412000
IF: 2.838

Dora, D., Ferenczi, S., Stavely, R., Toth, V. E., Varga, Z. V., **Kovacs, T.**, Bodi, I., Hotta, R., Kovacs, K. J., Goldstein, A. M., & Nagy, N. (2021). Evidence of a Myenteric Plexus Barrier and Its Macrophage-Dependent Degradation During Murine Colitis: Implications in Enteric Neuroinflammation. *Cellular and molecular gastroenterology and hepatology*, *12*(5), 1617–1641. https://doi.org/10.1016/j.jcmgh.2021.07.003
IF: 8.797

Onódi, Z., Visnovitz, T., Kiss, B., Hambalkó, S., Koncz, A., Ágg, B., Váradi, B., Tóth, V. É., Nagy, R. N., Gergely, T. G., Gergő, D., Makkos, A., Pelyhe, C., Varga, N., Reé, D., Apáti, Á., Leszek, P., **Kovács, T.**, Nagy, N., Ferdinandy, P., … Varga, Z. V. (2022). Systematic transcriptomic and phenotypic characterization of human and murine cardiac myocyte cell lines and primary cardiomyocytes reveals serious limitations and low resemblances to adult cardiac phenotype. *Journal of molecular and cellular cardiology*, *165*, 19–30. https://doi.org/10.1016/j.yjmcc.2021.12.007
IF: 5.000

Oláh, I., Felföldi, B., Benyeda, Z., **Kovács, T.**, Nagy, N., & Magyar, A. (2022). The bursal secretory dendritic cell (BSDC) and the enigmatic chB6^{+} macrophage-like cell (Mal). *Poultry science*, *101*(4), 101727. https://doi.org/10.1016/j.psj.2022.101727
IF: 4.400

Matula, Z., Mikala, G., Lukácsi, S., Matkó, J., **Kovács, T.**, Monostori, É., Uher, F., & Vályi-Nagy, I. (2021). Stromal Cells Serve Drug Resistance for Multiple Myeloma via Mitochondrial Transfer: A Study on Primary Myeloma and Stromal Cells. *Cancers*, *13*(14), 3461. https://doi.org/10.3390/cancers13143461
IF: 6.575

Oláh, I., Felföldi, B., Benyeda, Z., Nagy, N., & **Kovács, T.** (2022). The morphology and differentiation of stromal cells in the cortex of follicles in the bursa of Fabricius of the chicken. *Anatomical record (Hoboken, N.J.: 2007)*, *305*(11), 3297–3306. https://doi.org/10.1002/ar.24893
IF: 2.00

Felföldi, B., Benyeda, Z., **Kovács, T.**, Nagy, N., Magyar, A., & Oláh, I. (2022). Glycoprotein Production by Bursal Secretory Dendritic Cells in Normal, Vaccinated, and Infectious Bursal Disease Virus (IBDV)-Infected Chickens. *Viruses*, *14*(8), 1689. https://doi.org/10.3390/v14081689
IF: 4.700

Gergely, T. G., Kucsera, D., Tóth, V. E., **Kovács, T.**, Sayour, N. V., Drobni, Z. D., Ruppert, M., Petrovich, B., Ágg, B., Onódi, Z., Fekete, N., Pállinger, É., Buzás, E. I., Yousif, L. I., Meijers, W. C., Radovits, T., Merkely, B., Ferdinandy, P., & Varga, Z. V. (2023). Characterization of immune checkpoint inhibitor-induced cardiotoxicity reveals interleukin-17A as a driver of cardiac dysfunction after anti-PD-1 treatment. *British journal of pharmacology*, *180*(6), 740–761. https://doi.org/10.1111/bph.15984
IF: 6.800

Kucsera, D., Tóth, V. E., Sayour, N. V., **Kovács, T.**, Gergely, T. G., Ruppert, M., Radovits, T., Fábián, A., Kovács, A., Merkely, B., Ferdinandy, P., & Varga, Z. V. (2023). IL-1β neutralization prevents diastolic dysfunction development, but lacks hepatoprotective effect in an aged mouse model of NASH. *Scientific reports*, *13*(1), 356. https://doi.org/10.1038/s41598-022-26896-3
IF: 3.800

Halasy, V., Szőcs, E., Soós, Á., **Kovács, T.**, Pecsenye-Fejszák, N., Hotta, R., Goldstein, A. M., & Nagy, N. (2023). CXCR4 and CXCL12 signaling regulates the development of extrinsic innervation to the colorectum. *Development (Cambridge, England)*, *150*(8), dev201289. https://doi.org/10.1242/dev.201289
IF: 3.700

Dora, D., Ligeti, B., **Kovacs, T.**, Revisnyei, P., Galffy, G., Dulka, E., Krizsán, D., Kalcsevszki, R., Megyesfalvi, Z., Dome, B., Weiss, G. J., & Lohinai, Z. (2023). Non-small cell lung cancer patients treated with Anti-PD1 immunotherapy show distinct microbial signatures and metabolic pathways according to progression-free survival and PD-L1 status. *Oncoimmunology*, *12*(1), 2204746.
https://doi.org/10.1080/2162402X.2023.2204746
IF: 6.500

Ferenczi, S., Mogor, F., Takacs, P., **Kovacs, T.**, Toth, V. E., Varga, Z. V., Kovács, K., Lohinai, Z., Vass, K. C., Nagy, N., & Dora, D. (2023). Depletion of muscularis macrophages ameliorates inflammation-driven dysmotility in murine colitis model. Scientific reports, 13(1), 22451. https://doi.org/10.1038/s41598-023-50059-7
IF: 3.800

Kucsera, D., Ruppert, M., Sayour, N. V., Tóth, V. E., **Kovács, T.**, Hegedűs, Z. I., Onódi, Z., Fábián, A., Kovács, A., Radovits, T., Merkely, B., Pacher, P., Ferdinandy, P., & Varga, Z. V. (2024). NASH triggers cardiometabolic HFpEF in aging mice. GeroScience, 10.1007/s11357-024-01153-9.
IF: 5.400

Chen, Y. H., **Kovács, T.**, Ferdinandy, P., & Varga, Z. V. (2024). Treatment options for immune-related adverse events associated with immune checkpoint inhibitors. British journal of pharmacology, 10.1111/bph.16405. Advance online publication. https://doi.org/10.1111/bph.16405
IF: 7.700

Sayour, N. V., Gergely, T. G., Váradi, B., Tóth, V. É., Ágg, B., **Kovács, T.**, Kucsera, D., Kovácsházi, C., Brenner, G. B., Giricz, Z., Ferdinandy, P., & Varga, Z. V. (2024). Comparison of mouse models of heart failure with reduced ejection fraction. *ESC heart failure*, 10.1002/ehf2.15031. https://doi.org/10.1002/ehf2.15031
IF: 3.700

Gergely, T. G., **Kovács, T.**, Kovács, A., Tóth, V. E., Sayour, N. V., Mórotz, G. M., Kovácsházi, C., Brenner, G. B., Onódi, Z., Enyedi, B., Máthé, D., Leszek, P., Giricz, Z., Ferdinandy, P., & Varga, Z. V. (2024). CardiLect: A combined cross-species lectin histochemistry protocol for the automated analysis of cardiac remodelling. ESC heart failure, 10.1002/ehf2.15155. https://doi.org/10.1002/ehf2.15155
IF: 3.700

Sayour, N. V., Kucsera, D., Alhaddad, A. R., Tóth, V. É., Gergely, T. G., **Kovács, T.**, Hegedűs, Z. I., Jakab, M. E., Ferdinandy, P., & Varga, Z. V. (2024). Effects of sex and obesity on immune checkpoint inhibition-related cardiac systolic dysfunction in aged mice. *Basic research in cardiology*, 10.1007/s00395-024-01088-4. https://doi.org/10.1007/s00395-024-01088-4
IF: 8.000

Kovács, S. A., **Kovács, T.**, Lánczky, A., Paál, Á., Hegedűs, Z. I., Sayour, N. V., Szabó, L., Kovács, A., Bianchini, G., Ferdinandy, P., Ocana, A., Varga, Z. V., Fekete, J. T., & Győrffy, B. (2025). Unlocking the power of immune checkpoint inhibitors: Targeting YAP1 reduces anti-PD1 resistance in skin cutaneous melanoma. *British journal of pharmacology*, 10.1111/bph.70052. Advance online publication. https://doi.org/10.1111/bph.70052
IF: 7.700

Hegedűs, Z. I., Jakab, M. E., Gergely, T. G., Sayour, N. V., Kovács, A., Antal, S., **Kovács, T.**, Ferdinandy, P., Varga, Z. V., & Tóth, V. E. (2025). Tirzepatide, a dual GIP/GLP1-receptor co-agonist preserves cardiac function and improves survival in angiotensin II-induced heart failure model in mice: comparison to liraglutide. *Cardiovascular diabetology*, *24*(1), 253. https://doi.org/10.1186/s12933-025-02806-5

IF: 10.600

9. Acknowledgements

I would like to thank all those without whom my doctoral thesis would not have been possible. First of all, I would like to thank my supervisor, Prof. Nándor Nagy for his professional guidance, patience and indispensable advice, which has enabled me to progress in my research career.

I am very grateful for the whole staff of the Department of Anatomy, Histology and Embryology, Semmelweis University. Especially, I would like to thank Prof. Ágoston Szél, former and Prof. Dr. Alán Alpár, current director for making it possible to do my PhD studies at the Institute. Prof. Alán Alpár also guided me not just professionally but personally as a mentor under the umbrella of Kerpel-Fronius Ödön Talent Development Program. Every current and former member of the Laboratory of Stem Cell and Experimental Embryology Laboratory helped me during this effort; I am happy to have worked with them.

I am especially thankful to our collaborators, Allan M. Goldstein, Ryo Hotta, Rhian Stavely and Hannah Graham from Harvard Medical School and Massachusetts General Hospital, Boston, USA for the RNA sequencing work and bioinformatic analysis. I am very grateful for the opportunity that I could spend nearly a month abroad in another lab and learn wholemount in situ hybridization technique from Pascal de Santa Barbara and Sandrine Faure in the PhyMedExp, University of Montpellier, INSERM in France.

I am grateful to my current workplace, the Department of Pharmacology and Pharmacotherapy, Center for Pharmacology and Drug Research & Development, HCEMM-SU Cardiometabolic Immunology Research Group and MTA-SE Momentum Cardio-Oncology and Cardioimmunology Research Group for providing time for dissertation writing and opening new horizons in my professional career.

Last, but not least I would like to address my gratitude to my family and to my other-half, Katalin Vincze for being patient, supportive, understanding all the time throughout this journey. Without them both of my professional and personal life would not be so happy and successful. Without them, this work would not have been possible.